NASA CONTRACTOR REPORT

NASA CR-2779

NASA CR-2779

FINITE STATE MODELING OF AEROELASTIC SYSTEMS

Ranjan Vepa

Prepared by
STANFORD UNIVERSITY
Stanford, Calif. 94305
for Langley Research Center

NATIONAL AERONAUTICS AND SPACE ADMINISTRATION • WASHINGTON, D. C. • FEBRUARY 1977

1. Report No.	2. Government Accession No.	3. Recipient's Catalog No.
NASA CR-2779		

4. Title and Subtitle	5. Report Date
FINITE STATE MODELING OF AEROELASTIC SYSTEMS	February 1977
	6. Performing Organization Code

7. Author(s)	8. Performing Organization Report No.
Ranjan Vepa	
	10. Work Unit No.

9. Performing Organization Name and Address	11. Contract or Grant No.
Stanford University Stanford, California 94305	NGL 05-020-243
	13. Type of Report and Period Covered
12. Sponsoring Agency Name and Address	Contractor Report
National Aeronautics and Space Administration Washington, DC 20546	14. Sponsoring Agency Code

15. Supplementary Notes

Adapted from Ph.D. Dissertation, May 1975
Langley technical monitor: Robert V. Doggett, Jr. Topical report.

16. Abstract

A general theory of finite state modeling of aerodynamic loads on thin airfoils and lifting surfaces performing completely arbitrary, small, time-dependent motions in an airstream is systematically developed and presented. In particular, the nature of the behavior of the unsteady airloads in the frequency domain is explained. This scheme employs as raw materials any of the unsteady linearized theories that have been mechanized for simple harmonic oscillations. Each desired aerodynamic transfer function is approximated by means of an appropriate Padé approximant, that is, a rational function of finite degree polynomials in the Laplace transform variable.

The modeling technique is applied to several two-dimensional and three-dimensional airfoils. Circular, elliptic, rectangular and tapered planforms are considered as examples. Identical functions are also obtained for control surfaces for two- and three-dimensional airfoils.

17. Key Words (Suggested by Author(s))	18. Distribution Statement
Unsteady aerodynamics Aeroelasticity Active controls	Unclassified-Unlimited Subject Category 39

19. Security Classif. (of this report)	20. Security Classif. (of this page)	21. No. of Pages	22. Price*
Unclassified	Unclassified	188	$7.00

* For sale by the National Technical Information Service, Springfield, Virginia 22161

CONTENTS

TABLES

Number Page

ILLUSTRATIONS

FINITE STATE MODELING OF AEROELASTIC SYSTEMS

Ranjan Vepa
Stanford University

SUMMARY

A general theory of finite state modeling of aerodynamic loads on thin airfoils and lifting surfaces performing completely arbitrary, small, time-dependent motions in an airstream is systematically developed and presented. In particular, the nature of the behavior of the unsteady airloads in the frequency domain is explained. This scheme employs as raw materials any of the unsteady linearized theories that have been mechanized for simple harmonic oscillations. Each desired aerodynamic transfer function is approximated by means of an appropriate Padé approximant, that is, a rational function of finite degree polynomials in the Laplace transform variable.

The modeling technique is applied to several two-dimensional and three-dimensional airfoils. Circular, elliptic, rectangular and tapered planforms are considered as examples. Identical functions are also obtained for control surfaces for two- and three-dimensional airfoils.

INTRODUCTION

In the last decade rapid advances have taken place in the area of automatic control of practical engineering systems. The vast technological developments in autopilot design and in the design of aircraft take-off and landing systems has led to the possibility of applying this technology to control the vibration modes of aircraft wing structures and the elimination of aeroelastic instabilities in the flight envelope

of the aircraft. Although the mathematical theory of distributed parameter systems has made rapid advances recently, it seems more expedient, from a practical point of view, to approximate aeroelastic systems, mainly aircraft wings and control surfaces, by finite state models. The techniques of approximating aircraft wing structures by finite state models which make use of finite elements and other structural idealizations are well known. No systematic techniques exist, however, for approximating the aerodynamic loads on these structures by compatible finite state models for aeroelastic purposes. Thus a systematic theory for approximating aerodynamic loads on aircraft wings by finite state models used along with well-known techniques of structural idealization could be tremendously useful not only for understanding aeroelastic instabilities but also in the development of control systems for suppressing aeroelastic instabilities. Such theories can also prove helpful in the minimum weight design of aircraft structures.

This paper is concerned with the finite state modeling of aeroelastic systems. The well-known theories of modeling of aircraft wing structures are briefly presented. A general theory is then developed for the modeling of unsteady aerodynamic loads on wings and airfoils. These aerodynamic models may be used in conjunction with structural models for aeroelastic purposes.

General Description of the Problem

The general techniques of calculating unsteady aerodynamic loads for simple harmonically oscillating airfoils and lifting surfaces are outlined in [1], [2] and [3]. With these techniques it is possible to calculate the unsteady aerodynamic loads for different modes of oscillation at a given frequency of oscillation. Little is known about the analytical behavior of these loads in the frequency domain. Thus it is

first essential to identify the behavior in the frequency domain of the aerodynamic loads on airfoils and lifting surfaces.

The next step is to approximate this behavior in a manner that will permit the construction of aerodynamic models, which may be used along with structural models for aeroelastic purposes. Also, for the work described in this paper existing techniques of calculating aerodynamic loads for airfoils and lifting surfaces were utilized whenever possible.

Review of Pertinent Literature

The theory of finite state modeling of structures for dynamic analysis is well known. The various methods of weighted residuals [4], finite element techniques [5] and variational techniques [4] have all proved extremely useful for analytical modeling purposes. Recently system identification techniques [6] have been formulated for approximating structures by finite state models from experimental data.

The author is not aware of any systematic modeling procedures in unsteady aerodynamics. However, there were several related developments in the past fifty years. In 1925, Wagner [1,3] first studied the growth of lift on a two dimensional airfoil in incompressible flow due to an impulsive change in the vertical velocity of the airfoil. Garrick [7], later showed the relationship between Wagner's solution and Theodorsen's solution [8] for the lift on an oscillating airfoil. Sears [9] showed the relationship between solutions for a sharp edge gust and a sinusodial gust. R. T. Jones [10] first considered the aerodynamic forces on finite wings of elliptic planform in non-uniform motion in incompressible flow. W. P. Jones [11] calculated the lift on rectangular and tapered wings for impulsive motion in incompressible flow. Lomax, et al., [12] solved the problem of obtaining the lift and moment for impulsive motion,

exactly, at the starting instant using a useful analogy with with supersonic steady flow over three dimensional lifting surfaces. Nazelsky and Drischler [13] and Drischler [14] used the Fourier transform relationship for oscillatory and impulsive motions developed by Bisplinghoff, and obtained approximations to the indicial lift and moment in plunging and pitching in compressible flow, over two-dimensional airfoils. Miles [15,16] considered the transient loading on wide delta wings and rectangular wings at supersonic speeds.

Recently Djojodihardjo and Widnall [17] and Hess [18] developed a numerical technique for arbitrarily moving airfoils and lifting surfaces based on Green's representation theorem in potential theory.

While the theory to be presented in this paper has some common features with each one of the above techniques, one does not get from them any insight into the general behavior of the aerodynamic loads and pressure distributions in the frequency domain. The differences in the behavior of incompressible and compressible flows have not been fully explained.

Several techniques have been presented in the past for the calculation of aerodynamic loads for simple harmonically oscillating airfoils and lifting surfaces. These techniques have been reviewed by Ashley, Widnall and Landahl [19], Landahl and Stark [20], Woodward [21] and Ashley [22]. Recent methods now widely in use are the kernel function techniques of Cunningham [23], Rowe [24] and Laschka [25], and the doublet-lattice technique of Albano and Rodden [26]. The latter seems to be an extremely useful and practical tool for aeroelastic purposes. Some of these methods and their extensions are briefly described in Appendix C.

In this paper the theory of finite state modeling of structures is

first outlined. Then a systematic procedure is presented for the modeling of unsteady aerodynamic loads. Some contributions are also made towards extending and modifying methods for calculating aerodynamic loads for oscillating airfoils and lifting surfaces.

Summary of Contributions

(1) A general theory is presented to describe the behavior of the aerodynamic pressure and loads in the frequency domain.

(2) A numerical technique has been developed for modeling the aerodynamic loads in the frequency domain.

(3) A numerical technique is developed for calculating the aerodynamic loads on two dimensional airfoils with trailing and leading edge flaps, for a fairly large frequency bandwidth. For three dimensional lifting surfaces the bandwidth, for which the doublet lattice method leads to reasonable results, is improved.

(4) Indicial functions have been obtained for various types of impulsive motions for wings of different planform.

a distance of elastic axis from the center of gravity.

b reference semi-chord of wing.

c speed of sound in the free stream.

c_i distance of flap hingeline from the center of gravity.

$C(k)$ Theodorsen's function.

C_p non-dimensional pressure coefficient $= \Delta p/q$.

$C_{zz}(x,\xi)$ bending influence function.

$C_{\theta\theta}(x,\xi)$ torsional influence function.

EI flexural rigidity.

GJ torsional rigidity.

$h(x,t)$ vertical displacement of wing elastic axis.

$H_i^{(2)}(\cdot)$ Hankel functions.

I unit matrix.

I_θ moment of inertia of wing.

I_{β_i} moments of inertia of flaps.

$I_i(\cdot)$ modified Bessel functions of the first kind.

k reduced frequency $\frac{\omega b}{V}$.

K_h wing root stiffness in shear

K_R wing root stiffness in lateral rotation.

K_T wing root stiffness in torsion.

$\mathbf{K}(t)$ Wagner's indicial function.

$\mathbf{K}_0, \mathbf{K}_1$ stiffness matrices.

$K_2(X,s)$ Kernel function for two dimensional aerofoils.

$K_{20}(X,s)$ Kernel function for two dimensional aerofoils in incompressible flow.

$K_3(X,Y,s)$ Kernel function for three dimensional lifting surfaces.

$K_{\beta i}$ Control surface stiffness constant.

ℓ_i defined in figure 1.

ℓ_w semi-span of wing.

L_h lift in the plunging mode.

$m(x)$ mass per unit length.

M_0, M_1 Mass matricies

M Mach number

M_θ aerodynamic pitching moment.

M_{β_i} aerodynamic flap moment.

NB number of collocation points.

NF number of flaps

p Laplace transform variable.

$p(x,s)$, $p(x,y,s)$ pressure distribution.

$\Delta p(x,s)$, $\Delta p(x,y,s)$	pressure jump across the wing.
q	dynamic pressure = $1/2\ \rho V^2$.
q_{0_1}	nodal displacement vector.
q_1	modal displacement vector.
$\bar{q}_0, \bar{q}_1$	Laplace transform of q_0, q_1.
$q_{ij}(s,M)$	i, j^{th} element of $Q(s,M)$.
$Q(s,M)$	aerodynamic load matrix.
$R_1 = \sqrt{x^2 + \beta^2 Y^2}$	
$s = \frac{pb}{V}$	
$S_\theta(x)$	unbalance of entire wing.
S_{β_i}	unbalance of i^{th} flap.
t	time
$T_{c\beta i}$	control torque on i^{th} flap.
U	gust velocity.
$U(n,a,t)$	Kummer functions.
V	free stream velocity.
$w(x,y,t)$	downwash velocity.

$\bar{w}(x,y,p)$	Laplace transform of $w(x, y, t)$.
x,y,z	Cartesian coordinates.
$X = x - \xi$	
$Y = y - \eta$	
$Z = z - \zeta$	
$Z^j(x,y)$	displacement of the j^{th} mode.
α	angle of attack
β	$\sqrt{1 - M^2}$ for $M < 1$, $\sqrt{M^2 - 1}$ for $M > 1$.
$\beta_i(t)$	flap rotation of i^{th} flap
$\theta(x,t)$	torsional rotation
$\varphi(s)$	Laplace transform of Wagner s function.
$\psi(s) = s\varphi(s)$.	
$\tau = \frac{Vt}{b}$ or $\frac{Vt}{\ell_w}$	
ξ, η, ζ	Cartesian coordinate system

Finite Element Models

The finite element method is often regarded as generating a discrete model of a physical system. The method may also be viewed as a variational technique, where an attempt is made to minimize the demand for ingenuity in the construction of trial functions. This discrete matrix technique for the formulation and solution of linear dynamic problems in engineering mechanics has been widely discussed in the literature [5]. This approach has proved useful in obtaining approximate analyses of complex structural configurations that are difficult to handle by exact mathematical formulations. The bookkeeping required for solving the large number of linear simultaneous equations involved is readily handled by matrix algebra techniques and the resulting analytical formulations are tremendously simplified. Thus concurrent development or revision of different sections of large digital computer programs to perform the analysis is feasible. This feature has led to its use and acceptance as a basic tool for dynamic structural response calculations. The aim of this section is to briefly describe how the technique can be useful for finite state modeling of wing structures.

The efficient utilization of the discrete element influence-coefficient approach in a digital computer would provide for construction of a stiffness matrix and a mass matrix for the entire wing

structure by simple superposition of each matrix, from corresponding matricies for the discrete elements that model the wing in detail. A stiffness and mass matrix generator program (SAMGEN) was written for this purpose. Several different types of elements were incorporated in the program. This program was found to be extremely useful in structural optimization work [27].

Idealization as a Beam-Rod

The swept wing structure shown in Figure 1 is considered. The wing is connected structurally to the fuselage, so that the root is not completely rigid. Further it is assumed to have a finite number of trailing edge flaps, NF in number, which provide for the control torques. The flaps are assumed to function as rigid bodies which are good approximations for most control flaps. The wing is assumed to have a large aspect ratio, at least, for structural purposes. This permits the wing to be modeled as a beam-rod. The actual root is replaced by an effective root normal to the elastic axis of the wing. Rotational inertia, shear deformations and sectional bending are neglected.

Let $h(x, t)$, $\theta(x, t)$, $\beta_i(t)$ $i = 1, 2, 3, \ldots$ NF, be the vertical displacement of the wing along the elastic axis, the torsional displacement of the wing along the elastic axis and the angular displacements of the flaps respectively. The kinetic energy of the wing/flap system may be written as

$$= \frac{1}{2}\int_0^{\ell_w} (m(x)(\frac{\partial}{\partial t}h(x,t))^2 + I_0(x)(\frac{\partial}{\partial t}\theta(x,t))^2 - S_0(x)\frac{\partial}{\partial t}\theta(x,t)\frac{\partial}{\partial t}h(x,t)$$

$$+ \sum_{i=1}^{NF} I_{\beta_i}(\frac{\partial}{\partial t}\beta_i(t))^2 + 2(I_{\beta_i} + b(a_i - a)S_{\beta_i})\frac{\partial}{\partial t}\beta_i(t)\frac{\partial}{\partial t}\theta(x,t)$$

$$+ \int_{\beta_i} S_{\beta_i}\frac{\partial}{\partial t}\beta_i(t)\frac{\partial}{\partial t}h(x,t)\,dx \qquad (2.1)$$

where $\beta_i(t)$ is assumed to be equal to zero in the regions where the i^{th} flap does not exist. The potential energy of the system may be written as,

$$= \frac{1}{2}\int_0^{\ell_w} (EI(x)(\frac{\partial^2 h(x,t)}{\partial x^2})^2 + GJ(x)(\frac{\partial\theta(x,t)}{\partial x})^2)dx$$

$$+ \frac{1}{2}K_h h^2(0,t) + \frac{1}{2}K_R(\frac{\partial}{\partial x}(0,t))^2 + \frac{1}{2}K_\theta\theta^2(0,t) + \frac{1}{2}\sum_{i=1}^{NF} K_{\beta_i}\beta_i^2(t) \qquad (2.2)$$

A prime (') will be used to represent $\frac{\partial}{\partial x}$ and a dot (˙) to represent $\frac{\partial}{\partial t}$.

The aerodynamic forces and control torques may be viewed as non-conservative forces.

Using the Lagrangian technique, we have the following equations of motion and boundary conditions.

$$m(x)\ddot{h}(x,t) - S_\theta(x)\ddot{\theta}(x,t) - \left(\sum_{i=1}^{NF} S_{\beta_i}\ddot{\beta}_i(t)\right) + (EI(x)h''(x,t))'' = L_h(x) \quad (2.3a)$$

$$-S_\theta(x)\ddot{h}(x,t) + I_\theta(x)\ddot{\theta}(x,t) + \left(\sum_{i=1}^{NF} (I_{\beta_i} + b(c_i - a)S_{\beta_i})\ddot{\beta}_i(t)\right) - (GJ(x)\theta'(x,t))' = M_\theta(x) \quad (2.3b)$$

$$-S_{\beta_i}\ddot{h}(x,t) + (I_{\beta_i} + b(c_i - a)S_{\beta_i})\ddot{\theta}(x,t) + I_{\beta_i}\ddot{\beta}_i(t) + \frac{K_{\beta_i}\beta_i(t)}{\ell_i - \ell_{i-1}} = M_{\beta_i}(x) + Tc_{\beta_i}, \quad i = 1,2,3,\ldots NF \quad (2.3c)$$

where $L_h(x)$, $M_\theta(x)$ and $M_{\beta_i}(x)$, $i = 1, 2, 3, \ldots NF$, are the aerodynamic forces and moments and Tc_{β_i}, $i = 1, 2, 3, \ldots NF$, the control torques on the flaps.

The boundary conditions at $x = 0$ are given by,

$$(EI(x)h''(x,t))' - K_h h(x\ t) = 0 \quad (2.4a)$$

$$EI(x)h''(x,t) + K_R h'(x,t) = 0 \quad (2.4b)$$

$$GJ(x)\theta'(x,t) + K_T\theta(x,t) = 0 \quad (2.4c)$$

The boundary conditions at the wing tip $x = \ell w$ are

$$EI(x)h''(x,t) = 0 \quad (2.5a)$$

$$(EI(x)h''(x,t))' = 0 \quad (2.5b)$$

$$GJ(x)\theta'(x,t) = 0 \tag{2.5c}$$

If $EI(x)$ and $GJ(x)$, the flexural and torsional rigidities are zero at the wing tip, the boundary conditions are,

$$EI'(x)h''(x,t) = 0 \tag{2.6a}$$

$$2EI'(x)h'''(x,t) + EI''(x)h''(x,t) = 0 \tag{2.6b}$$

$$- GJ'(x)\theta'(x,t) = 0 \tag{2.6c}$$

In the above equations the inertia and aerodynamic loads are also assumed to be zero at the wing tip .

Since the properties of a practical wing are not uniform it is difficult to solve the above boundary value problem even in the absence of external loads. Hence these differential equations are reduced to integral equations and then discretized.

The influence functions $C_{zz}(x, \xi)$, the static deflections at station x due to a unit load at station ξ along the elastic axis, and $C_{\theta\theta}(x, \xi)$, the state torsional deflection at station x due to a unit moment at station ξ along the elastic axis, for a wing with a flexible root, are given in Appendix A.

The inertial properties are assumed to be lumped at NB collocation points, x_i, along the elastic axis. Then following standard techniques it is possible to rewrite the equations of motion, in the absence of

external loads, in the form,

$$[I]\{q_o\} = -[K_o]^{-1}[M_o]\{\ddot{q}_o\} \tag{2.7}$$

where

$[I]$ is the unit matrix,

$\{q_o\}$ is the vector of nodal displacements, torsional rotations and flap rotations,

$[K_o]^{-1}$ is the influence coefficient matrix, and $[M_o]$ is the inertia matrix.

$$\text{Defining } [U_c]^T = [Tc_{\beta_1}, Tc_{\beta_2}, \ldots Tc_{\beta_{NF}}] \tag{2.8}$$

$$\text{and } [B_o]^T = \begin{bmatrix} \overset{NF \times NB}{0} & \vdots & \overset{NF \times NB}{0} & \vdots & \overset{NF \times NF}{I} \end{bmatrix} \tag{2.9}$$

we may rewrite the entire equations of motion as

$$[K_1]q_1 + [M_1]\ddot{q}_1 = F_o(t) + BU_c \tag{2.10}$$

where $F_o(t)$ is the aerodynamic load vector, U_c is the vector of control torques, B the control torque distribution matrix, and q_1 the vector of modal displacements. It is also assumed it is possible to measure modal displacements and rates and these measurements can be written as,

$$Z_m = H_1 q_1 + H_2 \dot{q}_1$$

If a linear aerodynamic theory is assumed, the Laplace transform of this load vector, $\bar{F}_0(p)$, where p is the Laplace transform variable, is specified as,

$$\bar{F}_0(p) = \frac{1}{2}\rho_\infty V^2 A_w \cdot b \cdot [Q(s,M)]\{\bar{q}_1(p)\}$$

where $Q(s,M) = \{q_{ij}(s,M)\}$ is an aerodynamic load matrix, defined by the relations,

$$q_{ij}(s,M) \overset{\Delta}{=} \frac{1}{A_w}\iint_{A_w} \frac{Z^i(x,y)}{b} \frac{\Delta p^j(x,y,s,M)}{\frac{1}{2}\rho_\infty V^2} \, dx \, dy$$

where A_w is the area of the lifting surface for a three dimensional lifting surface and equal to the chord for two dimensional aerofoils, $z^i(x,y)$ is the modal deflection surface in the i^{th} mode and $\Delta p^j(x,y,s,M)$, is the Laplace transform of the pressure difference in the j^{th} mode. The modal deflection surfaces may be obtained by solving the free vibration problem given by equation 2.7 .

A general theory for approximating the aerodynamic loads $q_{ij}(s,M)$ in the frequency domain, will be presented in the next chapter. This theory will permit the entire aeroelastic system to be replaced by a finite state modal.

In this section, a general method of approximating the aerodynamic loads in the frequency domain is presented for wings in two and three dimensional flow.

Two Dimensional Airfoils

The Padé approximant method is applied to obtain the solution to the pressure distribution on wings performing arbitrary oscillations in two dimensional incompressible flow. The method is then generalized and applied to two dimensional compressible flow problems.

Incompressible flow. - Aerodynamic loads on arbitrarily oscillating rigid wings in two-dimensional incompressible flow can be synthesized from Wagner's solution for the lift on a wing due to a sudden stepwise change in the downwach as described in Ref. 1. R. T. Jones [10] has obtained an approximate Laplace transform of Wagner's indicial function. It can be shown that equations for the pressure distribution and aerodynamic loads may be obtained for converging or diverging oscillations by replacing C(k) by $\psi(s) \quad s\phi(s)$ where $\varphi(s)$ is the Laplace transform of Wagner's indicial function. Thus equations of motion of a wing with a trailing edge flap [ ] or a wing with an aileron and a flap [,] may be obtained by using the corresponding equations for oscillatory motion. For converging oscillations the wake is assumed to be finite and dependent on initial conditions.

In this section, Theodorsen's circulation lag function is analytically continued for converging motion of an airfoil with no

oscillating components in two dimensional incompressible flow, and the physical significance of the results explained. By representing Theodorsen's function as a series of Kummer functions, an asymptotic expression for Wagner's indicial function is obtained. The first two terms of this approximation are identical to the approximation for Wagner's function obtained by Garrick. By applying the Padé approximant theory, it is shown that Theodorsen's function may be represented by a sequence of rational functions which converge uniformly. This method of approximating Theodorsen's function is generalized so one can construct rational function approximations not only to Theodorsen's function, but to gust response problems also. These rational function approximations may be easily inverted, using Laplace inversion, to obtain good approximations to various indicial functions.

The lift and moment about the elastic axis on a rigid thin airfoil, performing vertical translational or torsional oscillations can be easily obtained by integrating the pressure and its moments (given in Appendix B).

These expressions are,

$$\begin{bmatrix} Lb \\ M_\alpha \end{bmatrix} = 2\pi q b^2 \left[\begin{array}{c|c} s^2 + 2s\psi(s) & s - as^2 + 2\psi(s)\left(1+\left(\frac{1}{2}-a\right)s\right) \\ \hline as^2 + 2\left(a+\frac{1}{2}\right)\psi(s)\cdot s & s\left(a-\frac{1}{2}\right) - \left(\frac{1}{8}+a^2\right)s^2 + \left(a+\frac{1}{2}\right)2\cdot\psi(s)\left(1+\left(\frac{1}{2}-a\right)s\right) \end{array}\right]$$

$$\times \begin{bmatrix} h/b \\ \alpha \end{bmatrix}$$

These equations may be written also as,

$$\begin{bmatrix} Lb \\ M_\alpha \end{bmatrix} = 2\pi qb^2 \left\{ \begin{bmatrix} s^2 & s - as^2 \\ as^2 & s(a-1/2)-(1/8 + a^2)s^2 \end{bmatrix} + \begin{bmatrix} 2 \\ 2a + 1 \end{bmatrix} \psi(s)[s_1(1+(\frac{1}{2} - a)s)] \right\} \begin{bmatrix} \frac{h}{b} \\ \alpha \end{bmatrix}$$

Thus the circulatory part of the aerodynamic matrix can be decomposed into the product of two vectors. As a consequence we have,

$$\begin{bmatrix} Lb \\ M_\alpha \end{bmatrix} = 2\pi qb^2 \begin{bmatrix} s^2 & s - as^2 \\ as^2 & s(a - \frac{1}{2})-(\frac{1}{8} + a^2)s^2 \end{bmatrix} \begin{bmatrix} \frac{h}{b} \\ \alpha \end{bmatrix} + 2\pi qb^2 \begin{bmatrix} 2 \\ 2a + 1 \end{bmatrix} y(s)$$

$$y(s) = \psi(s)[s,(1 +(\frac{1}{2} - a)s)] \begin{bmatrix} \frac{h}{b} \\ \alpha \end{bmatrix}$$

Thus it is sufficient to construct a finite state model of $\psi(s)$ (shown in Figures 2 and 3) in order to obtain finite state models of the generalized aerodynamic forces. An application of this approach to flutter suppression studies is presented in Ref. 30.

In general, if the influence of compressibility and finite span are included, it is impossible to decompose the matrix in the above manner. In two dimensional incompressible flow, the circulatory aerodynamic forces are dependent only on the downwash velocity at one point (the 3/4 chord point for a rigid airfoil). In compressible flow or for three dimensional lifting surfaces, the aerodynamic forces are dependent on the downwash at a finite number of collocation stations. Further the contribution of the downwash at each of the collocation point, to different generalized forces, is different. Thus one cannot assume apriori that a decomposition of the form discussed above is possible. Thus, the above approach is not useful in compressible flow or for three dimensional lifting surfaces.

Garrick has shown that Wagner's indicial function and Theodorsen's function are related by the Fourier transform relationships. Thus,

$$K_1(t) = 1 + \frac{1}{2\pi} \int_{-\infty}^{\infty} \frac{C(k)-1}{ik} e^{ikt}\, dk \qquad \text{for } t \geq 0$$

$$= 0 \qquad \text{for } t < 0.$$

This may be written in the form

$$Wg(t) = K_1(t + T) - 1 = \int_{-\infty}^{\infty} C_f(f) e^{i2\pi ft}\, df$$

where $C_f\left(\frac{k}{2\pi}\right) = \frac{C(k)-1}{ik} e^{ikT}$

This equation suggests that numerical quadrature may be used to compute $K(t)$ for $T \leq t \leq 2T$ for any given T. An equivalent possibility is the use of discrete Fourier transforms like the fast Fourier transforms [31]. In order to show the disadvantages of this technique a brief discussion of the method is presented.

To observe the effect of sampling both in the frequency and time domain, at finite but equal intervals, the above equation is evaluated at the points,

$$t_j = j \cdot \Delta t, \quad j = 0, \pm 1, \pm 2, \ldots, \pm (N-1) \qquad \text{and}$$

$$f_n = n \cdot \Delta f, \quad n = 0, \pm 1, \pm 2, \ldots, \pm (N-1)$$

where $N = TF$, with $F = 1/\Delta t$ and $T = 1/\Delta f$. Δt_j is chosen small enough for the highest frequency present to be sampled at least twice during each cycle. With the assumption that the indicial function and the spectrum $C_f(f)$ are periodic with period T we have,

$$W_g(j \cdot \Delta t) = \frac{1}{T} \sum_{n=0}^{N-1} C_f(n \cdot \Delta t) e^{+2\pi i \, n \cdot j/N}$$

$$C_f(n \cdot \Delta f) = \frac{T}{N} \sum_{n=0}^{N-1} W_g(j \cdot \Delta t) e^{-2\pi i \, n \cdot j/N}$$

Let $A_n \triangleq C_f(n, \Delta f)$, $X_j \triangleq TW_g(j, \Delta t)$ and $\bar{w} = e^{2\pi i/N}$

We then have the discrete transform pair,

$$X_j = \sum_{n=0}^{N-1} A_n \bar{w}^{+n \cdot j} \{x_j\} = [\Omega]\{A_n\} .$$

$$A_n = \frac{1}{N} \sum_{j=0}^{N-1} X_j \, \bar{w}^{-nj}, \qquad \{A_n\} = [\Omega]^{-1}\{X_j\}$$

From the orthogonality properties and the properties of the exponential function it is possible to factor [Ω] in such a manner that the number of computations involved for inversions are reduced from N^2 to $\frac{N}{2}\log_2 N$ (provided $N = 2^m$). This decomposition technique is the Fast Fourier transform. Thus it is possible to obtain numerical values for $W_g(t_j)$ for various values of t_j by using different sampling periods T to any desired degree of accuracy. Also errors due to the assumption of periodicity can be corrected for, using Window Techniques. However this does not lead to a finite state model. From the numerical data generated for the indicial functions, $K_1(t)$, it is essential to fit the data with a finite number of exponentials (2 or 3). This is usually a non-linear technique [32]. The Laplace transform of such an approximation would then lead to a finite state model in the frequency domain. This whole procedure is undoubtedly extremely tedious and involves several computational steps. Conceptually the procedure involves approximating a distributed parameter system by a discrete time system which is then approximated again by a continuous system in the time domain. Thus a direct procedure of finite state modelling from known values of the response at $f = f_n$, with the correct initial and steady state behavior is desirable. In order to develop such a technique, Theodorsen's function is analyzed in detail.

Analytic continuation of Theodorsen's function: The function $\psi(s)$ will now be evaluated in the left half of the 's' plane along the real axis and the physical significance of the results will be explained. In this case, $\psi(s)$ may be written as

$$\psi(s) = 1 - \frac{1}{1 + \underset{\lambda\to\infty}{Lt} \dfrac{\int_0^\lambda e^{-s\cosh v} \cosh v \, dv}{\int_0^\lambda e^{-s\cosh v} \, dv}}$$

The integrands of the two integrals are monotonically increasing in the domain of v. Further they are both divergent. Hence the limit may be evaluated by using L'Hospitals rule, which immediately leads to

$$\psi(s) = 1 \qquad \text{for Re } (s) < 0, \qquad \text{Im}(s) = 0 \ .$$

This result is of fundamental importance. It was assumed that at time t = 0, the wing was stationary and unperturbed. Clearly, converging motion with no oscillatory components from an unperturbed state is not possible. This implies that on the negative real axis of the 's' plane the 'motion' remains unperturbed. As $\psi(s) = 1$, is the solution for the case of steady translation of the wing, the quasi-steady solution for the pressure distribution is the exact solution on the negative real axis of the 's' plane.

Asymptotic expansions of Wagner's indicial function: In terms of Krummer functions we have

$$\psi(s) = \frac{1}{1 + \frac{1}{2}\dfrac{U(\frac{1}{2}, 1, 2s)}{sU(1\frac{1}{2}, 3, 2s)}} \qquad \text{Re}(s) \geq 0$$

The Kummer functions U(a, n, z) are a class of confluent hypergeometric functions that are multiple valued with the principal branch defined for $-\pi < \arg(z) \leq \pi$. The order of the singularities for large

and small values of z are determined by a and n respectively.

As a consequence of the properties of Kummer functions $\Psi(s)$ may be represented as an asymptotic series for large s as,

$$\Psi(s) = 1 - \frac{1}{2}(4sU(1,1,4s) + \sum_{i=1}^{N+4} B_i(C_i s)U(1,1,C_i s) + O(\frac{1}{s})^{2(N+4)}$$

$$N = 0, 1, 2, \ldots, \infty .$$

where B_i and C_i are constants. Apart from being asymptotic for large s the expression also satisfies the condition,

$$\lim_{s \to 0} \Psi(s) = 1 .$$

Further, the inverse Laplace transform of the asymptotic series can be easily found. Hence it is also possible to find an asymptotic expression for Wagner's indicial function. In particular, for N = 0,

$$K(t) = 1 - \frac{2}{\tau + 4} + \frac{\tau^3}{768\ P(\tau)}$$

where $P(\tau) = 1 + 0.875\tau + 1.28435\tau^2 + 1.84283\tau^3 + 4.09134\tau^4$.

The first two terms are identical to the indicial function given by Garrick. In general the correction to Garrick's approximation may be written as,

$$K(t) - 1 + \frac{2}{\tau + 4} = \frac{\tau^3}{768} \frac{(\text{Polynomial of degree N in } \tau)}{(\text{Polynomial of degree N+4 in } \tau)}$$

The rational function in the brackets is usually referred to as a [N + 4, N] Padé approximant. Baker [33] has discussed the methods of

construction and the properties of Padé approximants.

Padé approximants of Theodorsen's function: For small values of s, W. P. Jones [34] gives the following series for $\psi(s)$:

$$\psi(s) = 1 + ys + y^2 s + s^3\left(\frac{y-1}{4} - \frac{y^2}{2} + y^3 + \frac{y\gamma}{2}\right)$$

where $y = \log(s/2) + \gamma$. The correct asymptotic series for small values of s is given by,

$$\psi(s) = 1 + ys + y^2 s^2 + s^3\left[\frac{y-1}{4} - \frac{y^2}{2} + y^3 + \frac{y}{4}\right] + s^4\left(y^4 - y^3 + y^2 - \frac{y}{2}\right)$$

$$+ s^5\left(y^5 - \frac{3}{2}y^4 + \frac{3}{2}y^3 - \frac{19}{16}y^2 + \frac{11}{32}y - \frac{11}{128}\right)$$

$$+ s^6\left(y^6 - 2y^5 + \frac{11}{4}y^4 - \frac{19}{8}y^3 + \frac{19}{16}y^2 - \frac{27}{64}y + \frac{77}{1152}\right) + O(s^7),$$

$$\mathrm{Re}(s) \geq 0 .$$

Obviously it is quite difficult to construct a Padé approximant from this series. However for large values of s, we have the asymptotic expansion,

$$\psi(s) = \frac{1}{2}\left(1 + \frac{1}{4s} - \frac{1}{8s^2} + \frac{7}{64s^3} - \frac{19}{128s^4} + \frac{143}{512s^5} - \frac{629}{1024s^6} + \frac{8273081}{4194304s^7} + O\left(\frac{1}{s^8}\right)\right)$$

$$\mathrm{Re}(s) \geq 0 .$$

The fact that the lag function has a value of 0.5 for $s = \infty$ and 1 for $s = 0$, suggests that it may be approximated by an [N,N] Padé

approximant quite accurately. To demonstrate this, the first four Padé approximants are constructed from the asymtotic series for large s. They are asymptotic to the lag function up to the first, third, fifth and seventh orders in $\frac{1}{s}$ respectively. They are given by

$$\frac{s + 0.5}{2s + 0.5} \quad , \qquad \frac{s^2 + 1.5s + 0.375}{2s^2 + 2.5s + 0.375} \quad ,$$

$$\frac{s^3 + 3.5s^2 + 2.7125s + 0.46875}{2s^3 + 6.5s^2 + 4.25s + 0.46875} \qquad \text{and}$$

$$\frac{s^4 + 4.64696s^3 + 9.33371s^2 + 5.51735s + 0.49334}{2s^4 + 8.79392s^3 + 16.71894s^2 + 7.67296s + 0.49334} \quad , \ \mathrm{Re}(s) \geq 0 \ ,$$

These expressions are found to converge rapidly over the entire right half of the 's' plane. However the above approximations are not very good for small values of s as they are obtained from the asymptotic series for large s.

This method of approximating Theodoresen's function and evaluating the Wagner indicial function approximately is similar in principle to the method suggested by Luke [35] for evaluating the Randall function in the theory for the unsteady aerodynamics of oscillating cylindrical shells in supersonic flow.

The method of construction of the Padé approximants may be generalized. Since the lag function is known exactly along the imaginary axis s = ik, the Padé approximant may be constructed by a suitable least squares technique. If $C(k) = N(ik)(D(ik))^{-1}$, where N(s) and D(s) are polynomials in s, the coefficients of tne polynomials may be determined by minimizing

$$\sum_{j=1}^{m} (D(ik_j)C(k_j) - N(ik_j))^2$$

where k_j, $j = 1, 2, 3, \ldots, m$ are the values of k at n different points. This technique needs only the values of C(k) at a finite number of points in the frequency domain, and hence may be generalized to other cases, where the aerodynamic loads can be calculated numerically only. This problem may then be reduced to the solution of an over determined linear system for the coefficients of the polynomials N(s) and D(s). This procedure results in

$$\psi(s) \doteq \frac{s^4 + 0.761036s^3 + 0.102058s^2 + 0.00255067s + 9.55732 \times 10^{-6}}{2s^4 + 1.063996s^3 + 0.113928s^2 + 0.00261680s + 9.55732 \times 10^{-6}}$$

$$\mathrm{Re}(s) \geq 0.$$

Clearly Wagner's indicial function may be approximated using the formula,

$$K(t) = \mathcal{L}^{-1} \frac{\psi(s)}{s} = 1 - \sum_{i=1}^{4} A_i e^{-\beta_i \tau}$$

where β_i are the roots of the denominator polynomial where

i	A_i	β_i
1	0.011285763	0.0044482234
2	0.043280564	0.027697193
3	0.21639860	0.096054968
4	0.22903508	0.40379780

By taking the Laplace transform of the approximation for Wagner's function obtained by R. T. Jones [10], we have

$$\psi(s) = \frac{s^2 + 0.5615s + 0.0273}{2s^2 + 0.6910s + 0.0273}, \qquad \mathrm{Re}(s) \geq 0$$

The [4,4] Padé approximant obtained by least squares and the corresponding indicial function are compared to the exact values and the results of R. T. Jones (Figures 4 - 8).

This approximation is very good both in the frequency and the time domain. The simplicity of this method compared to the one given by R. T. Jones is quite obvious. The main advantage of this method is that it can be generalized to three dimensional lifting surfaces.

It is also interesting to note that the poles of the six approximations for the lag function are negative real values. This indicates that the transient pressure response to a downwash input is asymptotically stable. Further since the negative real axis is a branch cut of the exact expression for the lag function it represents a continuous distribution of poles.

Application to gust response problems: In applying the above theory to gust response problems, a certain amount of caution is essential. It must be emphasized that only the Laplace transform of the temporal portion of the circulatory pressure distribution can be approximated by a sequence of [N,N] Padé approximants. This does not hold for sinusodially convected gusts.

Sears [9] considers a gust velocity of the form,

$$W_G = W_0 e^{i\omega(t-x/V)}$$

and shows that lift to be equal to

$$L(k) = 4\pi\, q\cdot b\cdot \frac{W_0}{V}\, e^{i\omega t}\, S(k)$$

where $S(k) = (J_0(k) - iJ_1(k))C(k) + iJ_1(k)$.

Küssner's indicial function is related to $S(k)e^{-ik}$ in the same manner as Wagner's indicial function is related to $C(k)$. However to obtain an exponential approximation of Küssner's function one should construct a [N,N-1] sequence of Padé approximants of $S(k)e^{-ik}$. In fact, using the least squares smoothing technique developed above and taking the inverse Laplace transform we obtain the following expression for Küssner's indicial function $K_2(t)$,

$$K_2(t) = 1 - \sum_{i=1}^{4} A_i e^{-\beta_i \tau}$$

where

i	A_i	β_i
1	0.012994467	0.0049896174
2	0.062319920	0.034931400
3	0.40920539	0.13796713
4	0.51548022	1.1645811

In order to show the relationship between the temporal and spatial portions of the gust response, it is essential to consider a gust of form,

$$W_G = W_O \, e^{i\omega t - i\gamma x/V}$$

Kemp [36] shows the lift to be of the form

$$L(k,\lambda) = 4\pi q \frac{W_o}{V} b \, e^{i\omega t} \, K(k,\lambda)$$

where $K(k,\lambda) = ((J_0(\lambda) - iJ_1(\lambda))C(k) + \frac{ik}{\lambda} J_1(\lambda))$

and $\lambda = \frac{\gamma b}{V}$.

The first term in the function $K(k,\lambda)$ is the circulatory part while the second is the virtual inertia effect. Clearly it is now sufficient to approximate $C(k)$ by an [N,N] Padé approximant to obtain the indicial function corresponding to a downwash of the form

$$W_G = W_O e^{-i\gamma x/V} \, H(t)$$

where $H(t)$ is a step function.

A sinusoidally convected chordwise gust past an airfoil at a steady angle of attack α, of the form, $U_G = U_O e^{i\omega(t-x/V)}$, is known to produce a lift equal to [37],

$$L(k) = 4\pi q \frac{U_O}{V} \alpha b \, e^{i\omega t} \, T(k)$$

where $T(k) = C(k)(J_0(k) - iJ_1(k)) + J_0(k) + i2J_1(k)$.

From this result we may obtain the indicial function for a sharp edged chordinse gust striking the leading edge of the aerofoil at t = 0

$$U_G = \begin{cases} U & X > Vt - b \\ U_0 & X < Vt - b \end{cases}$$

The indicial lift is given by

$$L(t) = 4\pi q \frac{U_0}{V} \alpha b K_3(t)$$

where $K_3(t)$ may be found in the same manner as Küssner's function. In fact $K_3(t)$ is approximately given by

$$K_3(t) = 2 - \sum_{i=1}^{4} A_i e^{-\beta_i \tau}$$

i	A_i	β_i
1	0.026965564	0.0023690134
2	0.044268810	0.040647302
3	0.45282297	0.14614369
4	1.4759427	1.7305802

Separating the spatial and temporal portions of the gusts into

$$U_g = U_0 e^{i\omega t - i\gamma x/V}$$

we may show the lift to be

$$L = 4\pi q \frac{U_0}{V} \alpha b e^{i\omega t} V(k,\lambda)$$

where $V(k,\lambda) = C(k)(J_0(\lambda) - iJ_1(\lambda)) + J_0(\lambda) + iJ_1(\lambda) + \frac{ikJ_1(\lambda)}{\lambda}$

Sharp edge gusts moving with respect to inertial observers are considered; i.e., gusts of the form

$$W_G = \begin{cases} 0 & X > Ut - b \\ W_0 & X < Ut - b \end{cases}$$

and

$$U_G = \begin{cases} 0 & X > Ut - b \\ U_0 & X < Ut - b \end{cases}$$

where U is different from the free stream velocity V. U_0 is assumed to be very small compared to U so only first order effects need be considered. The corresponding indicial functions are related to $K(k,\alpha k)e^{-i\alpha k}$ and $V(k,\alpha k)e^{-i\alpha k}$, where $\alpha = V/U$, in the same manner as Küssner's function is related to $S(k)e^{-ik}$ and hence may be written as,

$$K_T = 1 - \sum_{J=1}^{4} A_j^T e^{-\beta_j^T \tau}$$

$$K_C = 2 - \sum_{J=1}^{4} A_j^C e^{-\beta_j^C \tau}$$

These indicial functions are shown graphically in Figure 9 and Figure 10.

Before going into the nature of the solution of the pressure distribution in two dimensional compressible flow it may be instructive to

review the effects of thickness and viscosity on $\psi(s)$. Hewson-Browne [38] has investigated the oscillation of a thick airfoil in an incompressible flow and obtain a general expression for $\Psi(s)$ (which he evaluates only for simple harmonic motion!) including thickness effects. The generalization is different in the expressions for lift and moment. This would destroy the decomposition property of the circulatory portion of the aerodynamic matrix discussed earlier. The singularity in the derivative of $\Psi(s)$ continues to exist. Woods [39] has presented a new approach for the calculation of the unsteady two dimensional flow about aerofoils performing arbitrary motion in an incompressible fluid. While the flow is assumed inviscid, the potential flow boundary conditions are modified semi-empirically to make some allowance for viscous effects. The method is applicable to thick airfoils, the only limitation being that the velocities and displacments of the unsteady perturbation about the mean motion be small. Results are obtained for the lift and moment by an application of Blasius theorem. However these results, while being very impressive mathematically, seem to be practically useless as most of the integrals cannot be evaluated for general motion. Provided the Reynolds number is sufficiently large for boundary layer theory to be applicable, viscosity has three main effects on the theoretical potential flow. These are, 1) the Kutta condition is modified in that the position of the rear stagnation point is independent of incidence 2) the velocity distribution of the mean steady flow particularly near the rear trailing edge is modified 3) viscosity contributes to the damping that is independent of the velocity but does not effect the inertial loading. Woods accounts for 1) and 2) but not 3). The results indicate that the reduction in the wake velocity due

to the thickness and viscous effects, changes the flat plate derivatives by an amount which is quite large for k large but negligible for small values of k. Chen and Wirtz [40] have included second order wake effects, but it appears that the singularities they obtain are no different from those of the first order solution.

It seems probable that the nonlinear and viscous effects in the wake may reduce the wake velocity and distort the wake which may be significant especially for low values of k and large values of $|s|$. So far there is no theoritical justification of this. The above considerations are important if experimental verifications of Wagner's solution are sought.

Subsonic flow. - In Appendix C, the behavior of the pressure differential across the airfoil in subsonic flow was shown to be essentially like incompressible flow for low values of reduced frequency and mach number. However for large values of reduced frequency, unlike incompressible flow, the force required to generate impulsive motion may be expected to remain bounded for all time and finally reach a steady state value. In particular, the work required to generate impulsive motion is not entirely recoverable, so that the process is irreversible, and some part of the starting force must be regarded as "damping". It is well known, that for large values of reduced frequency the pressure is given by Piston theory [1] for all mach numbers, M, greater than zero.

$$\text{i.e.,} \qquad \frac{\Delta p}{q} = \frac{4}{M}\frac{\partial z}{\partial t}$$

where z is the displacement of the airfoil.

Another curious fact, that has not received the attention of any previous investigators in unsteady aerodynamics, is that the steady state aerodynamic load on an airfoil in steady subsonic flow or supersonic flow is always finite as long as the mode shapes are bounded. This indicates that the aerodynamic system by itself is a completely stable system, in subsonic or supersonic flow, in spite of being a circulatory system. This physical fact fully explains the reason for all the poles, of each one of the Padé approximants of $\psi(s)$, being in the left half of the 's' plane. The stability problem is especially significant in transonic shock free flows and hence is discussed in greater detail in the next section.

In Appendix B, it was shown that the integral equation for the pressure distribution can be reduced to a Fredholm integral equation of the second kind with a completely continuous kernel. The significance of complete continuity will be discussed in 3.2. In Appendix D, it was shown that for an equation of this type, the solution has the form of a [N, N+J] Padé approximant. Clearly, comparing this result, with the Piston theory result for large s, we conclude that the loads must be of the form,

$$q_{ij}(s,M) = \underset{N\to\infty}{\mathcal{L}t} \quad \frac{a_0 s^{N+1} + a_1 s^{N} + \cdots a_{N+1}}{M s^{N} + b_2 s^{N-1} \cdots b_{N+1}}$$

where the coefficients a_i and b_i are functions of Mach number alone. Clearly as $s \to \infty$, $q_{ij} = a_0 s/M$ and a_0 can be obtained from piston theory. In the limit as $s \to 0$, $q_{ij}(0,M) = a_{N+1}/b_{N+1} = q_{ij}^{0}(M)$ and equals the steady state value. As the mach number approaches zero,

one of the poles of the denominator moves to negative infinity in the 's' plane. This clearly indicates that in incompressible flow an impulsive force is needed to generate impulsive motion. Hence for large values of s, q_{ij} behaves like an inertial force in incompressible flow. In compressible flow, unlike incompressible flow, the coefficients b_i are different for different types of loads and mode shapes.

This difference in behavior may be easily explained physically. In incompressible flow there is a lag in the development of the circulation around the aerofoil, while the pressure variations are propogated with an infinite speed. In compressible flow in addition to this lag the pressure variations caused by the motion of the aerofoil are propogated by a finite speed. This introduces an additional lag in the loads. On the other hand as the speed of the airfoil increases, it is clear that the pressure variations move upstream more and more slowly in relation to the aerofoil. If the airfoil moves faster than the speed of sound, it cannot make its presence known to the fluid ahead of it and the mechanism for bending the streamlines ahead of the airfoil no longer exists. Eventually for very high speeds, the influence of the pressure variations is only local. At this stage the airfoil behaves like a one dimensional piston and piston theory leads to the exact pressure on the aerofoil for all values of s.

Thus

$$q_{ij}(s,M) = \frac{a_0 s}{M} \qquad \text{for} \qquad M \to \infty$$

It was also shown in Appendix D that the sequence of rational functions for increasing values of N converge and hence can be truncated and assumed to be of the form

$$q_{ij}(s,M) = \frac{a_0 s^{N+1} + a_1 s^N \ldots + a_N s + q_{ij}^0(M) b_{N+1}}{M s^N + b_2 s^{N-1} \ldots + b_{N+1}} \qquad (3.1)$$

for some fixed N.

Further, in view of the aerodynamic system being completely stable, we may conclude that all the poles of $q_{ij}(s,M)$ lie in the left half of the 's' plane. This is an important and useful property, as it can check on the validity of the rational function approximants after they have been constructed.

The exact solution for subsonic flows, can be obtained by Mathieu functions [1]. However the actual computation of the solutions is extremely tedious. Furthermore, the solutions are not closed form solutions and hence are only approximate. Thus it is difficult to obtain series expansions in frequency of the aerodynamic loads, in order to analytically construct the Padé approximants.

Hence a numerical technique used often in the area of system identification and for digital filter synthesis [41] is proposed and applied to various cases. The problem of computing the approximants is reduced to a least squares minimization problem. This is then transformed to a overdetermined linear system for the coefficients of the Padé approximants and the solution obtained by QR decomposition.

Now $q_{ij}(s,M)$ may be easily calculated by the numerical method outlined in Appendix C for a given mach number, and for various real values of reduced frequency.

$$k = k_m = -is_m \qquad m = 1, 2, 3, \ldots, m_0 .$$

Also a_0 can be obtained from piston theory and $q^0_{ij}(M)$ from steady state calculations. Thus the above equation may be written as,

$$a_1 s_m^{-1} + s_m^{-2} a_2 + \cdots s_m^{-N} a_N - q_{ij}(s_m,M)(b_2 s_m^{-2} + \cdots b_N s_m^{-N})$$

$$+ s_m^{-(N+1)}(q^0_{ij}(M) - q_{ij}(s_m,M))b_{N+1} = s_m^{-1} M q_{ij}(s_m,M) - a_0$$

$$m = 1, 2, 3, \cdots m_0 \qquad (3.2)$$

Hence these equations are a system of m_0 complex equations in the 2N real unknowns a_1, a_2, $\cdots$ a_N and b_2, b_3 $\cdots$ b_{N+1}. If m_0, is chosen larger than N, this system of equations may be solved by the linear least squares technique.

Numerical experience indicates that a large number of values must be chosen for k_m, in the low and high frequency regions. In the low frequency regions the coefficient of b_{N+1} could be a small complex quantity while at high frequencies the right side of equation (3.2) would be a small complex quantity. Hence a large number of values must be chosen for k_m, in the low and high frequency regions, in order that the approximation be sufficiently accurate in these frequency regions.

These approximants for nondimensional generalized forces in (1) plunging, (2) pitching and (3) flapping mode and tabulated in Tables 1 - 5. The flap hinge is assumed to be at the rear quarter chord point. In most of these cases N was chosen equal to 2. In these cases it was

found that more accurate results could be obtained with N = 4. However these results are not tabulated.

It was assumed that it is possible to calculate the aerodynamic loads $q_{ij}(s,M)$ accurately for all values of k and M in the subsonic regime. This assumption is generally true in two dimensional subsonic flow, provided a fairly large number of collocation and integration points are used in the method described in Appendix C. The method is very accurate even in the presence of control surfaces, provided collocation points are not chosen too close to the hinge line.

The influence of compressibility which is well known in steady flow is different for the steady and unsteady components of the loads. For low mach numbers ($0.1 < M \leq 0.3$) it was found that higher order Padé approximants were required to model the pitching moments, where the poles of the approximants have a tendency to move towards the imaginary axis of the s plane. This could be due to the higher order of the approximants without any physical significance.

For high subsonic mach numbers ($0.7 \leq M \leq 0.9$) the loads were less stable even with lower order Padé approximants. On the other hand it is well known [42, 43 and Section 9.2, 1] that oscillations of a two dimensional aerofoil about a pitching axis may become unstable for low values of reduced frequency and high mach numbers, if the axis lies in a certain region, ahead of the quarter chord axis and if the moment of inertia about this axis is sufficiently large. This has been attributed to the fact that the logarithmic term in frequency in the kernel function is stronger at high mach numbers for two-dimensional aerofoils than for three dimensional lifting surfaces.

By taking the Lapalce inverse transform of $q_{ij}(s,M)/s$, it is possible to obtain the indicial response in the i^{th} mode due to a time-

wise step change in displacement of the j^{th} mode at time t = 0. These results are shown in Figures 11 to 19, and have been obtained from [4, 5] Padé approximants in all cases except in the case of q_{11} at M = 0.7. From these figures it is quite clear the loads corresponding to the same pressure mode have the same general behavior in the time domain. Also the loads corresponding to the flap mode take much longer to reach the steady state value, than the loads due to plunging and pitching.

The influence of compressibility on Wagner's indicial function may be studied. In this case, the lift q_{11}, due to a rigid plunging mode is calculated at several Mach numbers and the corresponding indicial function is obtained by taking the Laplace inverse of q_{11}/s^2. This result is shown in Figure 20. These curves are compared with that of Mazelsky and Drischler [13] for Mach number = 0.5, in which case the error was found to be the highest.

Supersonic and transonic flow. - In supersonic flow the expressions for the lift, moment and partial moment for an aerofoil with a flap are given in [44] and for an aerofoil with both trailing and leading edge flaps in [45]. The Padé approximants for the exact expressions for the lift and moment of a rigid aerofoil in plunging and pitching may be obtained. The lift coefficient for an airfoil in pure plunging motion is,

$$\frac{L_h}{qb} \doteq 4\left(\frac{s^2 + as + b}{Ms^2 + cs + \beta b}\right)\frac{\dot{h}}{V} \quad \text{or}$$

$$4\left(\frac{s + \beta M - \beta^2}{Ms + \beta^2 M - \beta^3}\right)\frac{\dot{h}}{V}$$

where

$$a = \frac{3M\beta}{\Delta}\left[5M\beta + 3 + 3M^3(\beta - M) - M^2\right], \qquad \Delta = M^2(7M^2 - 3)$$

$$b = \frac{3\beta}{\Delta}\left(4M^2\beta^2(\beta - M) + 3\beta^2 M\right), \qquad c = \frac{3\beta^2M^2}{\Delta}\left((3M^2 + 1)(\beta - M) + 4M\right)$$

The moment coefficient in pure plunging motion is,

$$\frac{M_h}{qb^2} = 4\left(\frac{a_1 s}{Ms^2 + c_1 s + b_1}\right)\frac{\dot{h}}{V}, \text{ where } a_1 = \frac{-5\beta}{3M(11M^2 - 3)},$$

$$b_1 = \frac{5\beta^4}{M(11M^2 - 3)}, \quad \text{and} \quad c_1 = \frac{10M\beta^2}{11M^2 - 3}.$$

The lift coefficient in pitching is given by,

$$\frac{L_\alpha}{qb} = 4\left(\frac{a_2 s + b_2}{Ms + \beta b_2}\right)\alpha, \quad \text{where} \quad a_2 = \frac{M}{\beta}\left(\frac{3M^2 - 2}{3M^2 + 1}\right), \; b_2 = \frac{3M\beta}{3M^2 + 1}$$

The moment coefficient in pitching is given by,

$$\frac{M_\alpha}{qb^2} = 4\left(\frac{s^2 + a_3 s}{3Ms + b_3}\right)\alpha, \quad a_3 = \frac{M^2 - 2}{\beta^2} b_3, \quad b_3 = \frac{3(2 - M^2)M\beta^2 + 3\beta^5}{2M^2}$$

All four approximants have the correct asymptotic behavior in the limit $s \to 0$ and the piston theory limit was enforced for $s = \infty$. Also the poles of all four of the approximants satisfy the stability criterion discussed in the last section. The approximants are good

approximations for the loads for $M > 2.0$. Though not extremely accurate these approximations are certainly better than piston theory or quasi-steady theory.

It was observed that for higher order Padé approximants, the poles behaved in an erratic manner especially for low supersonic mach numbers, moving often into the right half of the 's' plane. In transonic flow, it is well known from the exact solution for the pressure [46], that the linear aerodynamic theory leads to infinite aerodynamic loads in the steady state as the loads have a pole of the form $\sqrt{s}$. This was probably the reason for one of the poles of the approximants moving towards the origin for low mach numbers in the supersonic regime and high mach numbers (≥ 0.8) in the subsonic regime. For the reason indicated above it seems appropriate that in transonic flow, the aerodynamic loads may be written as a [N,N+2] Padé approximant in $\sqrt{s}$ with a pole at $\sqrt{s} = 0$. However this result has no practical value, as the linear theory is known to be invalid in steady transonic flow.

The physical interpretation of this result is that two dimensional shock-free transonic flows are unstable on the basis of linear theory. One of the arguments against the physical existence of shock-free transonic flows was based on the supposed instability of these flows with respect to upstream moving disturbance waves [47]. The argument was that these waves when superposed on a steady shock-free basic flow could move upstream as long as the local steady flow speed was subsonic, but as they entered a region of supersonic flow they would come to a standstill and coalesce to form a steady shock wave.

However Pearcey [48] showed using laborious experimental techniques, that the disturbance waves moving upstream can penetrate the supersonic region, and that in fact, shock-free transonic flow could be experimentally realized. This is attributed to the non-linear turning effect of the waves moving upstream into the supersonic region, which was not theoretically accounted for earlier [49]. Then based on geometrical acoustics one may show that disturbance waves moving upstream can penetrate the supersonic region. The problem of shock-free transonic flow is too complex at present for a strict mathematical treatment.

The numerical technique developed in the last section is also applicable to supersonic flow. The results are tabulated as in the subsonic case for N = 2 in Tables 6 - 8. It may be noted that the derivatives of the indicial response functions to time-wise step changes in the downwash in plunging and pitching [12] are not continuous, since the period of influence of an impulsive source is finite. The above technique approximates these derivatives by continuous exponential functions (Figure 21). Thus higher order Padé approximants are essential to approximate the derivatives of the above indicial functions.

It was found that for Mach numbers less than 1.5 second order Padé approximants were insufficient for modelling the loads. The possible reason for this has already been discussed. On the other hand for Mach numbers greater than 2, a first order Padé approximant was sufficient

for the lift and moment in plunging and pitching in the frequency domain. This is to be expected as for a wide range of frequencies. In fact Piston theory may be considered as a zeroth order Padé approximant for high mach numbers.

Three Dimensional Lifting Surfaces

In this section a systematic method of obtaining Padé approximants of the aerodynamic pressure loads is presented. Though the method is actually quite difficult to apply in practice, it will prove the existence of Padé approximants and the form of the solution. The method is also applicable for two dimensional airfoils.

First it must be noted that Piston theory is also valid for three dimensional lifting surfaces for high frequencies and that any solution for the pressure distribution must converge to this limit for high frequencies.

In subsonic flow for two-dimensional airfoils, it is well known that the non-dimensional pressure $\overline{C_p}(\xi, \eta, ik)$ may be written as,

$$\overline{C_p} = p_{20}^{0} + ik\, p_{20}^{1} + ik \log ik\, p_{21}^{0} + O(k^2) + O(k^2 \log ik) \qquad (3.3)$$

For three-dimensional lifting surfaces it is given by

$$\overline{C_p} = \sum_{n=0}^{\infty} p_{30}^{n}(ik)^n + (ik)^2 \log ik\, p_{31}^{n}(ik)^n \qquad (3.4)$$

where p_{30}^{n} and p_{31}^{n} are independent of frequency. Assuming the downwash to be $w_{00} + ik\, w_{01}$ and using the kernel function expansion in Appendix

B, for low frequency (equation B18), we have

$$\frac{8\pi(w_{10} + ik\, w_{01})}{V} = \iint_A \Big[\sum_{n=0}^{\infty} a_n (ik)^n + (ik)^2 \log ik\, b_n (ik)^n \Big] \overline{C_p}(\xi, \eta, ik)\, d\xi\, d\eta$$

Hence we have the infinite system of equations,

$$\frac{w_{00}}{V} = -\frac{1}{8\pi} \iint_A a_0 p_{30}^0 \, d\xi \, d\eta$$

$$\frac{w_{01}}{V} = -\frac{1}{8\pi} \iint (a_1 p_{30}^0 + a_0 p_{30}^1) d\xi \, d\eta$$

$$0 = \iint_A (b_0 p_{30}^0 + a_0 p_{31}^0) d\xi \, d\eta$$

$$0 = \iint_A (a_2 p_{30}^0 + a_1 p_{30}^1 + a_0 p_{30}^2) d\xi \, d\eta$$

The first equation in this infinite set, involves the calculation of the pressure distribution by application of steady state lifting surface theory. After having determined the steady state pressure the second term is also determined from steady state lifting surface theory since p_{30}^0 is known and p_{30}^1 occurs in combination with the steady state kernel a_0. Thus the coefficients may be obtained numerically by a procedure like the kernel function technique. In this manner it is possible to obtain all the coefficients p_{30}^i and p_{31}^i. One special case of importance is when $w_{00} = 0$. In this case $p_{30}^0 = 0$ and $p_{31}^0 = 0$. Hence in this case,

$$\overline{C_p} = p_{30}^1 ik - p_{30}^2 k^2 + O(k^3) + O(k^3 \log ik)$$

Thus the existence of a solution of the form given by (3.2) is established.

Next we note that

$$s \log(s_0(s/s_0)) = s \sum_{i=1}^{\infty} (-1)^{i+1} \frac{(\frac{s}{s_0} - 1)^i}{i} + s \log s_0 \quad 0 \leq s \leq 2s_0.$$

From (3.2) we have

$$\overline{C_p} = \sum_{n=0}^{\infty} p_{30}^n (ik)^n + \left[ik^2 \sum_{n=1}^{\infty} (-1)^{j+1} \frac{(\frac{k}{k_0} - 1)^j}{j} p_{31}^n (ik)^n + (ik)^2 \log ik_0 \right]$$

This can be rearranged in the form,

$$\overline{C_p} = \sum_{n=0}^{2N-2} C_n (ik)^n \tag{3.5}$$

The coefficients C_n are functions of the number of terms included in the series for the logarithm. However the coefficients converge. Further the first two coefficients are unaffected. We may now construct a [N, N+1] Padé approximant such that Piston theory is satisfied in the limit $s \to \infty$. The coefficients of [N, N+1] Padé approximants may be obtained in terms of C_n by solving a linear system. Thus one may construct a sequence of [N, N+1] Padé approximants. These would have the same asymptotic behavior as equation (3.5) for small values of frequency and the correct limit for high frequency.

It is now essential to establish the convergence of this sequence of Padé approximants.

In Appendix D, a similar problem was considered. First the Neumann series solution of the problem was established. It was then shown that convergence of the Padé approximants is assured if the kernel function is a completely continuous kernel.

Symbollically we may denote the lifting surface problem as,

$$w = Lp = [L_0 + ikL_1 + (ik)^2 L_2 \ldots + (ik)^2 \log ik(M_0 + ik\, M_1 \ldots)]\, p$$

where L_i and M_i are integral operators. The solution to the steady state problem is

$$p_{steady} = L_0^{-1}\, w \ .$$

The iterative method described can be symbolically written as,

$$p = L_0^{-1} w - L_0^{-1} [ikL_1 + (ik)^2 L_2 + \ldots + (ik)^2 \log(ik)(M_0 + ik\, M_1 \ldots)]\, p$$

The above is a Fredholm integral equation of the second kind of the type considered in Appendix D. Complete continuity of the kernel function in the above equation can be assumed in view of the uniform numerical convergence of the kernel function method. As explained in Appendix D the condition of boundedness of the kernel function is not related to the condition of boundedness of the operator or complete continuity. Complete continuity ensures that the integral equation may be reduced to an algebraic system and that the solution converges uniformly. If

it is so, L may be thought of as a matrix and

$$p = L^{-1}w = \frac{[ADJ(L)]}{det(L)}\, w$$

If the elements of L are rational functions or polynomials of a parameter s, then elements of $\frac{[ADJ(L)]}{Det(L)}$ are ratios of polynomials. It is from this fact that we are able to conclude that there exists a sequence of Padé approximants if the kernel function is completely continuous. Hence the theory developed in Appendix D may be applied to the above system and it could be concluded that there exists a sequence of [N,N+1] Padé approximants that converge to the exact pressure distribution as $N \to \infty$. The same conclusions hold for the aerodynamic loads.

Thus we may write $q_{ij}(s,M)$ approximately as,

$$q_{ij}(s,M) \doteq \frac{a_o s^{N+1} + a_1 s^N \cdots a_{N+1}}{M s^N + b_2 s^{N-1} \cdots b_{N+1}}$$

In compressible flow a_0 may be calculated exactly from piston theory. In the case of M = 0, we can easily verify from the equation that the loads are given by a sequence of [N,N+2] Padé approximants. In the limit $M \to 0$ and $s \to \infty$ we have the integral equation for virtual inertia given by

$$s^2 \frac{z(x,y)}{b} = -\frac{1}{8\pi} \iint_A d\xi\, d\eta \overline{(C_p}(\xi,\eta,s) \frac{1}{(X^2 + Y^2)^{3/2}})$$

This is a self adjoint integral equation and can be solved by a kernel function technique. Unlike compressible flow the pressure distribution has no singularities along the boundaries. It is important to realize that virtual inertia and Piston theory loads are independent of the direction of flight. However as circulation begins to develop the Kutta condition is of importance and the classical theory of motion of a body through an ideal fluid is not valid. W. P. Jones [50] has proposed a simple method for solving the above equation for rectangular wings. Two dimensional broadside configurations such as circles and ellipse with symmetrically placed fins have been treated by Bryson [51, 52, 53] with a view to analyzing the stabilizing effect of control surfaces on aircraft.

For a circular wing of radius r_0, in incompressible flow it could easily be shown (Appendix C) using the same technique as van Spiegel's [54] solution for low frequencies, that for large frequencies

$$\Delta C_p(r,\theta) = O(k^2)$$

The actual computation of the Padé approximants, though possible in principle, was not carried out. Exact Padé approximants could also be computed in compressible flow. However the amount of computations involved to get meaningful results is enormous, as it is essential to expand several special functions and their products in power series. Also circular and elliptic wings are not used often in practice. The numerical technique outlined in the previous sections with some modifications for three dimensional lifting surfaces is more useful.

For three dimensional lifting surfaces the aerodynamic loads may be written as

$$q_{ij}(s,M) = q_{ij}^{0}(M) + sq_{ij}^{1}(M)$$

$$+ \frac{c_0 s^{N+1} + c_1 s^{N} + \cdots c_{N-1} s^{2}}{s^{N} + b_2 s^{N-1} \cdots b_{N+1}}$$

where $q_{ij}^{0}(M) + sq_{ij}^{1}(M)$ are the exact loads in the limit $s \to 0$ and $c_0 = a_0 - q_{ij}^{1}(M) \cdot M$. $q_{ij}^{0}(M)$ and $q_{ij}^{1}(M)$ may be calculated from p_{30}^{0} and p_{30}^{1}.

If $[A_0 + ikA_1]$ is the influence coefficient matrix for small values of k and $\{w_j\} = \{w_{j0} + ikw_{j1}\}$, the downwash vector, the pressure coefficients for small k are given by

$$p_j = [A_0]^{-1}[\{w_j\} - ik A_1 [A_0]^{-1} w_{j0}]$$

$[A_0]$ may be calculated exactly as in steady flow. $[A_1]$ is calculated from the coefficient of ik in the expansion for the kernel function given by equation B18, using either the doublet-lattice or kernel function technique. Integrating the pressure with appropriate displacement mode shapes leads to $q_{ij}^{0}(M)$ and $q_{ij}^{1}(M)$.

The numerical evaluation of the coefficients b_i and c_i in compressible flow is similar to the two dimensional case. In incompressible flow since the numerical technique for the calculation of the virtual inertia loads for arbitrarily shaped wings was not completed, a_0 was assumed to be unknown and b_2 euqal to unity.

After some numerical experiment N was chosen to be equal to 2. This leads to a first order rational function in incompressible flow. A simple lag is sufficient to model the circulatory effects in this case. In compressible flow two lags are essential, for large aspect ratio wings at low mach numbers, one to account for the lag due to compressibility effects at high frequencies and the other to model the lag due to circulatory effects at low frequencies. For moderately low aspect ratios at high subsonic mach numbers the lag due to compressibility effects may be modelled by a single lag. For low aspect ratio wings ($AR < 1$) there exists no physical reason for aerodynamic lag and hence no lags are required at all Mach numbers. Some examples are presented.

(1) Circular Planforms: A circular wing is considered in incompressible flow. For circular wings the exact results of Van Spiegel and Benthem and Wouters [55] for simple harmonic motion in plunging, pitching, chordwise bending and spanwise bending modes are used. Rational function approximations to these loads are given in Table (9). The error in the virtual inertia lift in plunging is about 30% . This high value is due to the lack of any data points for $k > 1$. The growth of lift and moment for a timewise step change in the downwash in the plunging and the spanwise bending modes are shown in Figures 22 to 25. No other results were available for comparisons. The corresponding indicial functions and the indicial functions for the lift and moment due to a time wise step change in the displacement in different modes are tabulated in Tables 10 and 12. The lift and moment in the spanwise bending mode reached the steady state value much faster than the chordwise bending mode. This is to be expected as in the first case, the major contribution

to the load is from the pressure at the wing tips where it does not change aprreciably with time.

(2) Elliptic Planform: An elliptic wing, AR = 6, is considered in incompressible flow. R. T. Jones considered elliptic wings of aspect ratio 6 and 3 and computed the indicial response for the lift due to plunging. In the limiting case for high frequencies, he obtains approximately,

$$q_{11}(s) = \pi\left(\frac{1}{E\left(\sqrt{1-\left(\frac{4}{\pi AR}\right)^2}\right)}\right)\frac{h}{b}\left(s^2 + s\left(1+O\left(\frac{1}{AR}\right)\right)+O(s^0)\right)$$

where $E(\cdot)$ is the complete elliptic function of the second kind and represents the ratio of the semi-perimenter to the span. The first term represents virtual inertia. It may be noted that it is independent of the direction of flight and hence is minimum for circular planforms.

For low reduced frequencies, we may compute the asymptotic value of q_{11} by the iterative technique described, using the kernel function method to solve the integral equations. Fifteen spanwise integration points, three chordwise collocation points and ten chordwise integration points were used for the calculation. Thus for small s we have,

$$q_{11}(s) = sq_{11}^1 + s^2 q_{11}^2 + O(s^3) + O(s^3 \log s)$$

q_{11}^1 is identically equal to the stability derivative C_{ℓ_α} may be approximated by the formula,

$$C_{\ell_\alpha} = \frac{2\pi}{\beta}\left(\frac{(\beta AR)^2 + 1.7372(\beta AR)}{(\beta AR)^2 + 3.7680(\beta AR) + 6.9439}\right)$$

The corresponding formula for rectangular wings is,

$$C_{\ell_\alpha} = \frac{2\pi}{\beta} \left(\frac{(\beta AR)^2 + 0.7881(\beta AR)}{(\beta AR)^2 + 3.5760(\beta AR) + 3.1526} \right)$$

Both the above formulae have the correct limiting solutions for AR $\rightarrow \infty$ and 0.

$q_{11}^2 \left(= V \cdot \frac{C_{\ell_\alpha}}{2\pi b}\right)$ is also computed for elliptic and rectangular wings for increasing values of AR and shown in Figure 26. The curves indicate a maxima for circular and square lifting surfaces. For lower aspect ratios, low aspect ratio wing theory is a good approximation.

For a circular wing q_{11}^1 and q_{11}^2 may be obtained from the exact calculations of Van Spiegel. The errors in the numerically calculated values, using the method described above, were found to be 0.16% and 0.9% respectively.

From these asymptotic values it is possible to construct exact [1, 3] Padé approximants. Taking the Lapalce inverse transform we obtain the indicial response to a impulsive displacement. These results are compared to those R. T. Jones in Figure (27). Though the difference in the two results is not too large for high frequencies (!) it is considerable in steady flow.

Next the lift due to an elliptic wing, performing simple harmonic oscillations in the plunging mode was calculated at ten frequency points using Laschka's collocation technique with fifteen spanwise integration points, eleven chordwise integration points and three chordwise collocation points. The least squares technique for computing Padé approximants described earlier was used and the indicial function was computed for an AR = 6 lifting surface. This is compared to the results of R. T. Jones

in Figure 28. This result compares very well with the corresponding indicial function, obtained by using only the asymptotic values. This is quite significant for as it clearly indicates that with only the calculation of the asymptotes and the aerodynamic loads for one frequency of oscillation, it is possible to predict aerodynamic loads for all types of arbitrary motion.

(3) Rectangular Planform: Rectangular planforms of aspect ratio 4 and 6, in incompressible as well as compressible flow, are considered. The aerodynamic loads for simple harmonic motion are obtained using Laschka's method with fifteen spanwise collocation points, three chordwise collocation points and eleven chordwise integration points. The optimum number of chordwise integration points is the integer value of $[n(m + 0.5)]$, $n = 1, 3, 5, 7, \ldots$, m = number of chordwise collocation points. It has been shown by Rowe [24] that not using the optimum number of integration points could lead to considerable amount of oscillations in the predicted values of the loads as compared to the exact values. The numerical technique is used to calculate Padé approximants and indicial functions. The indicial functions for plunging are compared with those of W. P. Jones [11] for AR = 6.0 and 4.0 in incompressible flow (figures 29, 30, and 31, Table 11). In [56] the result for AR = 6.0 is compared to the one obtained by a potential flow technique. The fact that the virtual inertia for an AR = 6 wing is slightly lower than the case AR = 4.0 cannot be attributed to any physical reason. In fact it can be argued that the virtual inertia must be a minimum for a square lifting surface (AR = 1) and have the same value as a two dimensional airfoil AR = 0.

When compressibility effects are included (Figure 32) the influence of finite aspect ratio is to reduce the steady state lift while the starting value given by Piston theory is unaffected. Sweeping the lifting surface backwards, with the planform area a constant, further reduces the steady state lift without effecting the starting value.

In Figure (33) and Table 13 is shown a comparison of the generalized aerodynamic loads due to plunging (1) and pitching (2) for an aspect ratio 6 wing. This indicates that the basic behavior of the loads due to the pressure in any one of the modes is about the same. Thus this raises the possibility of approximating all the loads due to the pressure in any one mode, by the same combination of exponentials with different magnitudes. Also one may conclude that the exponential rise times in all the loads due to the pressure in the same mode are interelated. This fact led to a simplified scheme of approximating the aerodynamic load matrices for purposes of flutter analysis. This scheme is briefly discussed in the next chapter.

In Figure (34) the influence of compressibility on the indicial response in the plunging mode for a finite aspect ratio wing (AR = 6.0) is shown. This again is similar to its two dimensional counterpart shown earlier. The steady state lift is considerably reduced due to induction effects.

The indicial rolling moment for an impulsively rolling wing is shown (Figure 35) for a straight and swept wing of AR = 6. Here the influence of sweep is to reduce the lift uniformly for all value of time.

(4) Tapered Planform: A tapered planform of AR = 5.84 and a taper ratio of 0.524 was considered. The indicial lift for plunging

was compared with that of W. P. Jones in Figure 36, and indicates good agreement. The influence of taper is to raise the magnitude of the indicial lift quite uniformly for all time. This is to be expected as the pressure falls to zero, near the wing tips and hence does not contribute much to the total lift. Hence the influence of tapering with AR and planform area fixed would be to increase the total lift, both in steady and unsteady flow.

(5) Swept Wing ($\Lambda = 45^{\circ}$) with a control surface (AR = 4.16): This wing (Figure 37) was studied extensively using the improved version of the doublet-lattice method described in the appendix to calculate the aerodynamic loads on the wing for simple harmonic oscillations.

The wing was modelled as a beam-rod and its mode shapes (first bending and first torsion) were calculated by curve fitting discrete mode shapes (Table 14). These two polynomial mode shapes and a rigid control surface mode were used to calculate the aerodynamic loads on the wing.

First the convergence of the doublet lattice method in the limits of small and large reduced frequencies was investigated. For low reduced frequencies, the method was applied with 1) 6 chordwise boxes (NCB) and 5 spanwise boxes (NSB) 2) NCB = 6, NSB = 10 and 3) NCB = 9, NSB = 5 (Table 15).

This indicated that increasing the number of spanwise boxes (from 5 to 7, 8, and 10) resulted in a converging result. However changing the number of chordwise boxes did not alter the results significantly.

To verify the usefulness of the box integration scheme at high frequencies it was assumed that the pressure at the sending point (quarter chord point) of each box is given by 4/M times the downwash at the receiving point (three quarter chord point) of each box. In this manner the generalized forces are computed in each of the three cases given above and compared with the exact piston theory results. This did indicate convergence with increasing number of chordwise boxes. These results are shown in Table 16.

Finally the method was used to calculate the loads at a number of frequencies starting from small values of frequencies to high reduced frequencies (up to 5 based on semi-chord).

The generalized forces due to the pressure in the bending and control surface modes did converge slowly to the piston theory result. However the generalized forces, associated with the torsion mode did not converge to the results of piston theory. Hence using the results of the first case and the numerical method for calculating Padé approximants, it was found that the poles of the approximants were unstable in the loads associated with the torsion mode. In the second case (Table 17) the results did improve considerably at low frequencies but not at high frequencies. It was not possible to construct a stable first order Padé approximant for the generalized force in the second mode due to the pressure in the first. Also the rise times for the loads (Figures 38 - 46) associated with the torsion mode were small when compared to the first bending and control surface modes. The partial moment on the partial span flap has the same behavior as the corresponding indicial function for two dimensional

aerofoils. Also since the results for simple harmonic motion did converge to the piston theory limit in this case the indicial function seems quite accurate. However there is no check on the accuracy of the results as no comparisons are available.

From equations (3.3) and (3.4) we may conclude that the influence of finite aspect ratio would be to push the poles of the approximants further into the left half of the 's' plane. For this reason also, it is important to calculate the aerodynamic loads for higher reduced frequencies in order to get accurate representations of the loads than would be necessary in the two dimensional case. An efficieint and fast method for calculating unsteady aerodynamic loads at all frequencies is therefore essential.

On the other hand for aeroelastic purposes, it may not be necessary to enforce the piston theory limit for low aspect ratio wings. However extensive flutter calculations are essential for any conclusive results.

The doublet lattice method does not converge uniformly for all frequencies. The reason for this appears to be the lattice integration scheme. Hence the doublet lattice method is not too useful for finite state modelling of aeroelastic systems.

SUGGESTIONS FOR FUTURE RESEARCH

Generally for purposes of flutter analysis, it is sufficient to calculate aerodynamic loads accurately at the frequency and flight velocity at which flutter begins to occur. However for designing control systems for the suppression of flutter, it is not only essential to predict the root locus in the neighborhood of the flutter frequency, with respect to the flight velocity, but also some of the stable roots of the transcendental characteristic equation which influence the unstable locus. Thus aerodynamic models used for flutter suppression studies must be fairly accurate over a range of frequencies. Numerical techniques must converge uniformly over a large bandwidth. Collocation techniques discussed earlier for the calculation of aerodynamic forces generally satisfy these convergence requirements.

The aerodynamic modeling theory presented in this report suggests the possibility of representing the aerodynamic load matrices, Q_x, in a certain modal coordinate system X, as

$$Q_x = \{q_{xij}\} = \{p_{xij}(s)/r_{xj}(s)\} = P_x R_x^{-1}$$

where R_x is diagonal. Transforming to the actual modal coordinate system Z = TX

$$Q = T^{-1}Q_x T = T^{-1}P_x T \left[T^{-1}R_x T\right]^{-1} = P(s)R(s)^{-1}.$$

where R(s) is not diagonal. Hence in general

$$P(s) = \sum_{n=0}^{N} P_n s^n + P_{N+1} s^{N+1} \qquad (4.1)$$

and

$$R(s) = \sum_{n=0}^{N-1} R_n s^n + MIs^N$$

The interpretation of this approximation is based on the fact that the loads due to the pressure in any mode may be approximated by the same combination of exponentials with different magnitudes. If M = 0, this reduces to a [N + 1, N - 1] matrix Padé approximant. The coefficients P_n, R_n may be obtained numerically using a combination of Lagrangian interpolation and least squares technique. This has already been verified for two-dimensional aerofoils and in certain special cases in three dimensional wings. In these cases, however, the Piston theory limit was not enforced and N = 0 and N = 1 were sufficient in the range of frequencies for which the phenomenon of flutter becomes a possibility.

The above approximation of the aerodynamic load matrix has several advantages over the method of approximation already discussed. The matrix approximants lead to only $M_n \cdot N$ ($M_n(N-1)$ in compressible flow) states, in addition to states required to define the structural system, where M_n is the number of vibration modes considered for modelling the structure. Approximating every individual element of the aerodynamic matrix by a Padé approximant leads to $M_n^2 \cdot N$ ($M_n^2(N-1)$ in incompressible flow) additional states.

The equations of motion of the entire system can be written as

$$M_1\ddot{q}_1 + K_1 q_1 - \beta_v P(s,M)R^{-1}(s,M)q_1 = BU_c \tag{4.2}$$

$$Z_m = H_0 q_1 + H_1 \ddot{q}_1$$

$$\beta_v = q\, A_w b$$

The equation reduces to,

$$[M_1 R(s,M)\frac{s^2V^2}{b^2} + K_1 R(s,M) - \beta_v P(s,M)]R^{-1}(s,M)q_1 = BU_c \tag{4.3}$$

The flutter speed is determined by

$$\det[M_1 R(s,M)\frac{s^2V^2}{b^2} + K_1 R(s,M) - \beta_v P(s,M)] = 0 \tag{4.4}$$

The equations of motion can be reduced to the form

$$\dot{X} = FX + GU \tag{4.5a}$$

$$Z_m = HX \tag{4.5b}$$

where X is the vector of states $\{y\}\{\dot{y}\}$ etc. and U are the control torques on the aerodynamic control surfaces. There are several criteria when such a realization would lead to a system which is controllable and observable [57]. These are generalizations of the criteria for scalar transfer functions. The survey article by Silverman [58] presents an excellent description of the realization problem.

The model is useful for synthesizing control laws for active flutter suppression. Control laws may be written in terms of the state vector [X] as

$$U = - \hat{C} X$$

$\hat{C}$ may be obtained by arbitrary pole placement. The characteristic polynomial of the open loop system is assumed to be

$$\chi(F) = s^n + \sum_{i=1}^{N} a_i s^{n-i}$$

and that of the desired closed loop system,

$$\chi(F - G\hat{C}) = s^n + \sum_{i=1}^{N} p_i s^{n-i} \quad .$$

The coefficients a_i are related to F by the relations,

$$a_k = \frac{1}{k} \sum_{j=0}^{k} a_j \, S_{k+1-j} \quad , \quad k = 1, 2, 3, \ldots N$$

where S_ℓ = trace (F^ℓ) and $a_0 = 1$. Similar relationships hold for $(F - G\hat{C})$ and p_i. Using the notation,

$$p^T \triangleq [p_1, p_2, \cdots p_n]$$

$$a^T \triangleq [a_1, a_2, \cdots a_n]$$

and

$$\bar{A} \triangleq \begin{bmatrix} 1 & 0 & 0 & \cdots & 0 & 0 \\ a_1 & 1 & 0 & \cdots & 0 & 0 \\ \vdots & \vdots & \vdots & \vdots & \vdots & \vdots \\ a_{n-1} & a_{n-2} & & \cdots & 1 & 0 \\ a_n & a_{n-1} & & \cdots & a_1 & 1 \end{bmatrix}$$

it is possible to obtain a relationship between the control gains $\hat{C}$ and [p]-[a]. It may be noted that A^{-1} always exists and can be evaluated easily. In [59] it is shown that provided F is cyclic (if not an initial gain $\hat{C}_i$ may be chosen such that $[F - G\hat{C}_i]$ is cyclic)

$$\begin{bmatrix} \text{trace } G\hat{C} \\ \text{trace } FG\hat{C} \\ \vdots\vdots \\ \text{trace } F^{n-1}G\hat{C} \end{bmatrix} = \bar{A}^{-1}(p-a)$$

This is a linear system of equations in terms of the unknowns in $\hat{C}$ and may be easily solved. Preliminary results are extremely encouraging. A detailed discussion of the modeling procedure and numerical results is beyond the scope of this paper. A simple scheme for control law synthesis is shown in Figure 47. This technique is outlined by Lyons, et al. [60]. Optimal laws based on quadratic synthesis may be obtained by the eigenvector decomposition technique as applied in Ref. 61. An offshoot of this technique would be a new method of flutter analysis which would be useful in structural optimization [62].

CONCLUDING REMARKS

A general theory of finite state modeling of the aerodynamic loads on oscillating airfoils and lifting surfaces has been systematically developed and presented. In particular, the nature of the behavior of the unsteady aerodynamic loads in the frequency domain is now well understood. The analytical reasons for the difference in the behavior of these loads at high frequencies in incompressible and compressible flows are explained. Extensive studies need to be carried out for supersonic lifting surfaces, where it is expected that higher order Padé approximants would be necessary for an accurate prediction of the aerodynamic loads for arbitrary motion. The theory presented has several useful applications, especially in the control of the vibration modes of aircraft wing structures and in the active suppression of aeroelastic instabilities.

This study suggests the possibility of approximating aerodynamic loads as Padé approximants in Mach number as well. However, in the transonic regime nonlinearities need to be considered to account for shock waves.

Several other suggestions for improving the results and for applying the theory have also been presented.

APPENDIX A

INFLUENCE COEFFICIENTS FOR A BEAM-ROD WITH A FLEXIBLE ROOT

The influence coefficients for bending of a beam of length ℓ are given by (the deflection at point x due to a unit load at point ξ)

$$C_{zz}(x,\xi) = \int_0^x \frac{(\xi-\lambda)(x-\lambda)}{EI(\lambda)}\,d\lambda + \frac{\xi x}{K_R} + \frac{1}{K_h}, \quad \text{for} \quad \xi \geq x \geq 0$$

$$= \int_0^\xi \frac{(\xi-\lambda)(x-\lambda)}{EI(\lambda)}\,d\lambda + \frac{\xi x}{K_R} + \frac{1}{K_h}, \quad \text{for} \quad \ell \geq x \geq \xi$$

where $EI(\lambda)$ is the flexural rigidity distribution, K_R is the root restraint stiffness constant for rotation in the plane of bending, and K_h is the root stiffness constant in shear. The influence coefficients for torsion of a rod of length ℓ are given by (torsional deflection at point x due to unit moment at point ξ)

$$C_{\theta\theta}(x,\xi) = \int_0^x \frac{d\lambda}{GJ(\lambda)} + \frac{1}{K_\theta} \quad \text{, for} \quad \xi \geq x \geq 0$$

$$= \int_0^\xi \frac{d\lambda}{GJ(\lambda)} + \frac{1}{K_\theta} \quad \text{, for} \quad \ell \geq x \geq \xi$$

where $GJ(\lambda)$ is the torsional rigidity distribution and K_θ is the torsional spring constant at the root. If the root is rigidly fixed, the influence coefficients reduce to those given in [1].

APPENDIX B

INTEGRAL EQUATIONS FOR UNSTEADY AERODYNAMICS

Three Dimensional Lifting Surface

The source solution of the linearized equation for the velocity potential is given by

$$4\pi\Phi = \frac{-H(\tau - r/c)}{r} \tag{B.1}$$

where $H(\cdot)$ is the Heaviside step function, r is the distance between the observation and the source point, τ is the time measured from the instant of the disturbance and c is the speed of sound. The observation point is affected at time τ if the disturbance moving with a velocity c can traverse the distance r in that time; the strength of the disturbance is $-1/4\pi r$.

A coordinate system (ξ, η, ζ, τ) moving with respect to a fixed coordinate system (x_0, y_0, z_0, t_0), along the negative x_0 axis with a velocity v, fixed in the wing, is considered. The fixed and moving coordinate systems are assumed to coincide at time $t_0 = t$. The coordinates of the point (ξ, η, ζ, τ) referred to the fixed axes are $(\xi - v(t_0 - t), \eta, \zeta, t_0)$. A unit acceleration potential source at the point (ξ, η, ζ) in the moving reference frame will produce an acceleration disturbance at the point, (x, y, z), after some time delay; the magnitude of the disturbance is

$$= \left[\frac{1}{H(\tau - r/c)} \phi \right] = - \frac{1}{4\pi r} ,$$

$$r^2 = (x - \xi + v(t_o - t))^2 + (y - \eta)^2 + (z - \zeta)^2, \qquad (B.2)$$

In fixed coordinates, the velocity potential is related to the acceleration potential as

$$\Phi(x,y,z,t) = \int_{t_1}^{t_2} \phi(x,y,z,\bar{t}) d\bar{t}$$

where $[t_1, t_2]$ is the time domain of influence of ϕ, which affects the velocity potential at time t in fixed coordinates, t_2 and t_1 are the last and first instants of time at which the moving source can affect the observation point.

Therefore the velocity potential at (x,y,z,t) due to a moving doublet at (ξ, η, ζ, t_0) of strength $\Delta\phi(\xi, \eta, \zeta, t_0)$ is given by,

$$\Phi(x,y,z,t) = - \frac{1}{4\pi} \frac{\partial}{\partial z} \int_{t_1}^{t_2} \Delta\phi(\xi, \eta, \zeta, t_0) \frac{1}{r} dt_0 \qquad (B.3)$$

The time t_2 satisfies the equation,

$$((x - \xi) + v(t_2 - t))^2 + (y-\eta)^2 + (z-\zeta)^2 = c^2 (t_2 - t)^2 \qquad (B.4)$$

This is the equation for en ellipse and determines the region of integration for equation (B.3). If $X = x - \xi$, $Y = y - \eta$ and $Z = z - \zeta$ and $t_2 - t = T$, we have

$$cT = \frac{MX \pm R}{1 - M^2} \quad \text{or} \quad \pm \frac{R - MX}{M^2 - 1} \tag{B.5}$$

where $R = \sqrt{X^2 + (1 - M^2)(Y^2 + Z^2)}$

For $M < 1$, only one of the solutions is negative. Hence

$$t_2 = t + \frac{1}{c} \frac{MX - R}{1 - M^2} \tag{B.6}$$

If the perturbations in the flow field existed for infinite time in the past then $t_1 = -\infty$. On the other hand if the flow field is unperturbed for time $t \leq 0$, then clearly

$$\left.\begin{aligned} t_2 &= t_0 + \frac{1}{c} \frac{MX - R}{1 - M^2} \\ \text{and} \qquad t_1 &= 0 \quad \text{provided } t > -\frac{1}{c} \frac{MX - R}{1 - M^2} \end{aligned}\right\} \tag{B.7}$$

If $t \leq \frac{1}{c} \frac{MX - R}{1 - M^2}$, $t_1 = t_2 = 0$, as the disturbance has not reached the observation point. For $M > 1$, both solutions for T are negative and the period of influence is the time an advancing spherical wave would take to pass the point of observation. Therefore,

$$\left.\begin{aligned} t_2 &= t + \frac{1}{c} \frac{R - MX}{M^2 - 1} \\ t_1 &= t - \frac{1}{c} \frac{R + MX}{M^2 - 1} \end{aligned}\right\} \tag{B.8}$$

provided, of course, both t_1 and t_2 are positive. For M = 1, (transonic limit), we may let M = 1 + ε or 1 - ε and take the limit as $\varepsilon \to 0$. If we denote $U_i \triangleq X + V(t_i - t)$, i = 0, 1, 2, then in subsonic flow,

$$U_2 = \frac{X - MR}{1 - M^2} \quad , \; U_1 = x - Vt \tag{B.9}$$

provided the flow field is unperturbed for time $t < 0$.

For supersonic flow, t sufficiently large,

$$U_2 = \frac{MR - X}{M^2 - 1} \; , \; U_1 = - \frac{(MR + X)}{M^2 - 1} \tag{B.10}$$

Hence the velocity potential at (x, y, z, t) due to a moving doublet at (ξ, η, ζ, t_0) is equal to

$$\Phi(x,y,z,t) = - \frac{1}{4\pi V} \frac{\partial}{\partial z} \int_{U_1}^{U_2} \frac{\Delta\phi(\xi, \eta, \zeta, t + \frac{U_0 - X}{V})}{\sqrt{U_0^2 + Y^2 + Z^2}} \, dU_0 \tag{B.11}$$

The total velocity potential at (x, y,z,t) due to a distribution of moving doublets on the lifting surface S, at $\zeta = 0$, is given by

$$4\pi\Phi(x,y,z,t) = - \frac{1}{V} \iint_S d\xi \, d\eta \, \frac{\partial}{\partial z} \int_{U_1}^{U_2} \frac{\Delta\phi(\xi,\eta,0,t + \frac{U_0 - X}{V})}{\sqrt{U_0^2 + Y^2 + Z^2}} \, dU_0 \tag{B.12}$$

The downwash on the surface is given by

$$4\pi \, w(x,y,t) = - \frac{1}{V} \lim_{z \to 0} \frac{\partial}{\partial z} \iint_S d\xi \, dy \, \frac{\partial}{\partial z} \int_{U_1}^{U_2} \frac{\Delta\phi(\xi, \eta, 0, t + \frac{U_o - X}{V}) dU_o}{\sqrt{U_o^2 + Y^2 + Z^2}} \tag{B.13}$$

It can be shown that a discontinuity across a doublet layer exists such that [1]

$$\Delta\phi(x,y,0,t) = \Phi(x,y,0,t) - \Phi(x,y,-0,t) = \frac{\Delta p(x,y,t)}{\rho_\infty} \tag{B.14}$$

where Δp is the pressure differential across the surface.

Substituting (B.14) in (B.13) and performing the differentiation using Liebnitz rule, we have the following integral equation for the downwash in subsonic flow.

$$\frac{w(x,y,t)}{V} = \frac{1}{8\pi q} \iint_S d\xi d\eta \left[\Delta p\left(\xi,\eta,t + \frac{U-X}{V}\right) \frac{M}{R_1} \frac{MX+R_1}{X^2+Y^2} \right.$$

$$+ \int_0^U \Delta p\left(\xi,\eta,t + \frac{U_o-X}{V}\right) \frac{1}{\left(\sqrt{U_o^2+Y^2}\right)^3} \, dU_o$$

$$\left. + \int_0^t \Delta p(\xi,\eta,(t-\tau)) \frac{H(\tau-X/V)}{((X-V\tau)^2+Y^2)} V d\tau \right] \tag{B.15}$$

where $\Delta p(\xi,\eta,t) = 0$ for $t<0$, $U = \dfrac{X-MR_1}{1-M^2}$,

$q = \frac{1}{2}\rho_\infty V^2$, $R_1 = \sqrt{X^2 + (1-M^2)Y^2}$ and $t > \dfrac{1}{c}\dfrac{R_1-MX}{1-M^2}$.

In the limit as $t \to 0$, $U \to X$, $MX \to R_1$ and $X^2 + Y^2 \to 0$, and only the first of the 3 terms remain in the equation B.15. Integrating over a small region around the receiving point (x,y), we have

$$\frac{w(x,y,0)}{V} = -\frac{M}{4} \frac{\Delta p(x,y,0)}{q}$$

which is the familiar piston theory result. At the initial instant, the lifting surface behaves like a piston, and the flow over it is similar to one dimensional compressible flow. It may be noted that a similar equation obtained by Drischler[63] may be reduced to the same form as (B.15) after some algebraic manipulations.

Taking the Laplace transforms of Equation B.15, we may obtain an integral equation relating the Laplace transform of the downwash $\bar{w}(x,y,\frac{pb}{V})$ and the pressure $\Delta p(x,y,\frac{pb}{V})$, where p is the Laplace transform variable.

$$8\pi \frac{\bar{w}(x,y,(pb/v))}{V} = -\frac{1}{q} \iint d\varepsilon\, d\eta\, \overline{\Delta p}(\varepsilon,\eta,\tfrac{pb}{V}) K_3(X,Y,\tfrac{pb}{V})$$

where $K_3(x,Y,\frac{pb}{V}) = \left[e^{\frac{p}{V}\left(\frac{X - MR_1}{1 - M^2} - X\right)} \frac{M}{R_1} \frac{MX + R_1}{X^2 + Y^2} \right.$

$$\left. + \int_0^{\frac{X-MR_1}{1-M^2}} \frac{e^{\frac{p}{V}(U_0 - X)}}{(U_0^2 + Y^2)^{3/2}}\, dU_0 + V\,\mathcal{L}\left\{ \frac{H(t - X/V)}{((x - vt)^2 + y^2)^{3/2}} \right\} \right] \qquad (B.16)$$

$\mathcal{L}(m)$ represents the Laplace transform of m. The third term converges only for real $(s) \geq 0$, and

$$K_3(X,Y,\tfrac{pb}{V}) = e^{-\frac{px}{v}} \left[e^{-\frac{p}{V}\left(\frac{MR_1 - X}{1 - M^2}\right)} \frac{M}{R_1} \frac{MX + R_1}{X^2 + Y^2} + \int_{\frac{MR_1 - X}{1-M^2}}^{0} \frac{e^{-\frac{p\tau}{V}}}{(\tau^2 + Y^2)^{3/2}}\, d\tau \right.$$

$$\left. - \frac{\pi}{Y^2} \left(\frac{p|Y|}{2V}\right) \left[|H|_{-1}\left(\frac{p|Y|}{V}\right) + Y_1\left(\frac{p|Y|}{V}\right) \right] \right]$$

where $|H|_{-1}(\cdot)$ is a Struve function and

$Y(\cdot)$ is a Bessel function of the second kind.

For simple harmonic motion this reduces to the kernel function given by Watkins, et al. (64). For purposes of calculations however it is convenient to write, $K_3(X, Y, \frac{pb}{V})$ as,

$$K_3(x,Y,\frac{pb}{V}) = e^{-\frac{pX}{V}} \left[e^{-\frac{p}{V}\left[\frac{MR_1 - X}{1 - M^2}\right]} \frac{M}{R_1} \frac{MX + R_1}{X^2 + Y^2} \right.$$

$$\left. + \int_{\frac{MR_1 - X}{1 - M^2}}^{\infty} \frac{e^{\frac{-p\tau}{V}} d\tau}{(\tau^2 + Y^2)^{3/2}} \right] \qquad \text{(B.17)}$$

As shown by Landahl [65], the integral is also equal to,

$$\frac{1}{Y^2} \int_{\frac{MY^2 - XR_1}{X^2 + Y^2}}^{1} \text{Exp}\left[\frac{-pY\tau}{V\sqrt{1-\tau^2}} \right] d\tau \ .$$

However equation B.17 is most convenient for calculation purposes. The second term in equation B.17 is a singular integral at Y = 0. Hence the integration over the lifting surface must be done in the sense of Hadamard, as expalined by Mangler [66]. This is indicated in equation B.16 by the symbol $\mathcal{F}$.

For small values of the reduced Laplace transform variable $s = pb/V$, we may write the Kernel function as [67].

$$K_3(X,Y,s) = \sum_{n=0}^{\infty} (a_n s^n + s^2 \ell n(s) \cdot b_n s^n) \qquad (B.18)$$

where $a_0 = \frac{1}{Y^2} \left(1 + \frac{X}{\sqrt{X^2 + \beta^2 Y^2}}\right)$

$$a_1 = -\frac{1}{b} \cdot \frac{1}{Y^2} \left(X + \frac{X^2 + Y^2}{\sqrt{X^2 + \beta^2 Y^2}}\right)$$

$$b_0 = 1/2$$

$$b_1 = -\frac{X}{2b}$$

The coefficients b_n are functions of the spanwise variable Y only (and not of X)

In steady flow, for $s = 0$,

$$K_3(X,Y,0) = \frac{1}{Y^2} \left(1 + \frac{X}{\sqrt{X^2 + \beta^2 Y^2}}\right) \qquad (B.19)$$

and in the limit as $s \to \infty$, from piston theory

$$K_3(X,Y,s)\Big|_{s\to\infty} = 2\pi M \delta(X,Y) \qquad (B.20)$$

In the limit as $M \to 0$, we have,

$$K_3(X,Y,s)\Big|_{M=0} = \int_{-X}^{\infty} \frac{e^{-s\frac{(\tau+X)}{b}}}{(\tau^2+Y^2)^{3/2}}\, d\tau \qquad (B.21)$$

In two dimensional incompressible flow we have,

$$K_2(X,s)\Big|_{M=0} \triangleq K_{20}(X,s) = \int_{-\infty}^{\infty}\int_{-X}^{\infty} \frac{e^{\frac{-s(\tau+X)}{b}}}{(\tau^2+Y^2)^{3/2}}\, d\tau\, dY$$

$$= \frac{2}{X} + \frac{2s}{b} e^{-s\,X/b} E_i(sX/b)$$

$$= \frac{2}{X} - \frac{2s}{b} U(1,1,-\frac{sX}{b}) \qquad (B.22)$$

where $E_i(\frac{sX}{b})$ is the exponential integral and $U(1,1,-sX/b)$ is a Kummer function.

The above Kernel function indicates a distribution of time delays over an infinite time domain. Further they are not valid for Real(s) < 0. However if a solution to the integral equation can be obtained for Real $(s) \geq 0$, the convolution principle may be used to find the solution for any s.

For purposes of calculations, we note that the function $|H|_{-1}(\frac{s|Y|}{b}) - Y_1(\frac{s|Y|}{b})$ in equation B.17 may be approximated by a convergent sequence of rational functions in $\frac{s|Y|}{b}$ or Padé approximants. It follows therefore that $\frac{1}{(\tau^2+1)^{3/2}}$ can be approximated by a finite sum of exponential functions. Two such approximations are known, one due to Laschka [25] and the other due to Runyan and Watkins

[68]. The errors in these approximations are compared in [69]. Laplace transforms of exponentials of the type $e^{-\frac{a\tau}{b}}$ are given by rational functions. Hence, in principle, it is possible to approximate the entire Kernel function by a rational function in s. Further in order that it converge to the piston theory kernel for large S, the approximation must be [N, N] Padé approximant. This point of view has useful consequences, regarding the behavior of the aerodynamic loads in the frequency domain.

In supersonic flow the kernel function may be easily shown to be

$$K_3(x,Y,s) = e^{-\frac{sX}{b}} \left[\int_{\frac{X-MR_1}{M^2-1}}^{\frac{X+MR_1}{M^2-1}} \frac{e^{-\frac{sU}{b}}}{(U^2+Y^2)^{3/2}}\, dU + \frac{M}{R_1}\frac{MX-R_1}{X^2+Y^2} e^{-\frac{s}{b}\frac{X+MR_1}{M^2-1}} + \frac{M}{R_1}\frac{MX+R_1}{X^2+Y^2} e^{-\frac{s}{b}\frac{X-MR_1}{M^2-1}} \right] \quad \text{for} \quad X > \sqrt{M^2-1}\,|Y|$$

$$= 0 \quad \text{for} \quad X < \sqrt{M^2-1}\,|Y| \qquad \text{(B.23)}$$

In this case the kernel function is valid for all s, including the left half of the 's' plane.

In transonic flow though the linearized theory cannot predict shock waves . We may obtain the kernel function by proceeding to the limit as $M \to 1$ from the supersonic case. We have,

$$K_3(X,Y,s) = e^{-\frac{sX}{b}} \left[\int_{\frac{-X}{2}+\frac{Y^2}{2X}}^{\infty} \frac{e^{-\frac{sU}{b}}\, dU}{(U^2+Y^2)^{3/2}} + \frac{2}{X^2+Y^2} e^{+\frac{s}{2b}(X-\frac{Y^2}{2X})} \right]$$

$$X > 0$$

$$= 0 \qquad \text{for } X < 0 \tag{B.24}$$

In this case again the kernel function is only valid for real $(s) \geq 0$.

Two Dimensional Airfoils

In two dimensional flow, the integral equation relating the downwash and the pressure distribution may be obtained by integrating the corresponding three dimensional kernel function with respect to the spanwise coordinate from $-\infty$ to $+\infty$. For the case of arbitrary motion of an airfoil , one can show after some computation, that

$$\frac{8\pi w(x,t)}{V} = -\frac{1}{q} \oint_{x_1}^{x_2} 2d\xi \left[\int_{\frac{-X}{1+M}}^{Vt-X} \Delta p(\xi, t-\frac{X+\tau}{V}) \frac{d\tau}{\tau^2\sqrt{1-\frac{M^2\tau^2}{(\tau+X)^2}}} \right.$$

$$\left. + \int_{\frac{-X}{1-M}}^{\frac{-X}{1+M}} \frac{(1-H(X))d\tau}{\tau^2\sqrt{1-\frac{M^2\tau^2}{(\tau+X)^2}}} \Delta p(\xi, (t-\frac{X+\tau}{V})) \right] \tag{B.25}$$

where $x_1 = x - \frac{Vt(1+M)}{M}$, if $x - Vt\frac{(1+M)}{M} > x_L$

$= x_L$, if $x - Vt\frac{(1+M)}{M} < x_L$

$x_2 = x + \frac{Vt(1-M)}{M}$, if $x + Vt\frac{(1-M)}{M} < x_T$

$= x_T$, if $x + Vt\frac{(1-M)}{M} > x_T$

Equation B.25 is valid for any type of airfoil motion. In incompressible flow we have,

$$\frac{8\pi w(x,t)}{V} = -\frac{1}{q} \fint_{x_L}^{x_T} 2\, d\xi \int_{-X}^{Vt-X} \Delta p\left(\xi,\ t - \frac{(X+\tau)}{V}\right) \frac{d\tau}{\tau^2} \qquad \text{(B.26)}$$

At time $t = 0$, we have

$$\frac{w(x,0)}{V} = -\frac{M}{4}\frac{\Delta p(x,0)}{q} \qquad \text{(B.27)}$$

Non-dimensionalizing the time variable t to $\tau = Vt/b$ and taking the Laplace transforms of the integral equations, we have

$$\frac{8\pi \bar{w}(x,s)}{V} = -\frac{1}{q} \fint_{X_L}^{X_T} K_2(x - \xi,\ s)\ \overline{\Delta p}(\xi,s)\, d\xi \qquad \text{(B.28)}$$

where $\bar{w}(x,s)$ is the Laplace transform of the downwash and $\overline{\Delta p}(x,s)$,

the Laplace transform of the pressure

$$K_2(x,s) = 2s^*\beta\{e^{+s^*M^2X}[(MK_1(Ms^*|X|)+K_0(Ms^*|X|)$$

$$+ e^{-s^*X}\beta\ \ell n(\frac{1+\beta}{M})+ sX\int_0^1 e^{s^*X(\lambda-1)}\ K_0(Ms^*|X|\lambda)d\lambda]\} \qquad (B.29),$$

where $s^* = s/\beta^2$, $K_0(\cdot)$ and $K_1(\cdot)$ being modified Bessel functions of the second kind.

$$\text{Also } K_2(X,s)\Big|_{s-\infty} = + 2M\pi\delta(X) \qquad (B.30)$$

$$\text{and} \qquad K_2(X,s)\Big|_{s-0} = \frac{2\beta}{X} \qquad (B.31)$$

In incompressible flow, equation B.29 reduces to equation B.22. Equation B.22 has a well known inverse given by, (after non-dimensionalizing all distances by the semi-chord).

$$\overline{\Delta p}_0(x,s) = \int_{-1}^{1} G(x,z,s)\overline{w}(z,s)dz \qquad (B.32)$$

$$\text{where} \qquad G(x,z,s) = -\frac{2}{\pi}\left[s\Lambda(x,z) + \sqrt{\frac{1-x}{1+x}}\sqrt{\frac{1+z}{1-z}}\ (\psi(s)- 1 + \frac{1}{z-x}\ )\right] \qquad (B.33)$$

$$\Lambda(x,z) = \frac{1}{2}\log\frac{1 - xz + \sqrt{1-x^2}\ \sqrt{1-z^2}}{1 - xz - \sqrt{1-x^2}\ \sqrt{1-z^2}} \qquad (B.34)$$

$$\psi(s) = \frac{K_1(s)}{K_1(s)+ K_0(s)}\ , \qquad \text{real } (s) \geq 0 \qquad (B.35)$$

continued

$$= \frac{2sU(1\frac{1}{2},\ 3,\ 2s)}{2sU(1\frac{1}{2},\ 3,\ 2s)+\ U(\frac{1}{2},\ 1,\ 2s)}\ ,\ \text{real}\ (s) \geq 0 \qquad \text{(B.35) continued}$$

$$= s\cdot\mathcal{L}\left[1 - \int_0^{\infty} \{(K_0(x)- K_1(x))^2+ \pi^2(I_0(x)+ I_1(x))^2\}^{-1} \frac{e^{-xt}}{x^2}\, dx\right]$$

$K_i(\cdot)$ and $I_i(\cdot)$ are modified Bessel functions and U(a,b,z) is a Kummer function.

Equation (B.28) may be reduced to several alternate forms. One method of doing this reduction was given by Fettis [70]. The integral equation may be reduced to a non-singular Fredholm integral equation with a completely continuous kernel function (defined in Appendix D) given by,

$$\bar{\Delta p}(x,s) = \frac{\bar{\Delta p}_o(x,s)}{\beta} - s^*M^2\int_{-1}^{1} K_{cc}(x,\zeta,s)\bar{\Delta p}(\xi,s)d\xi \qquad \text{(B.36)}$$

$$K_{NC}(x,\xi,s) = H(\xi - x) - \frac{\cos^{-1}x}{\pi} - \frac{(\psi(s)-1)}{\pi}\sqrt{\frac{1-x}{1+x}}$$

$$- \frac{1}{4\pi}\frac{\beta}{sM^2}\int_{-1}^{1} G(x,z,s)\bar{K}(s(z-\xi))dz.$$

$H(\xi - x)$ is the unit step function and

$$\bar{K}(s(z-\xi) = K_2(z - \xi,s) - \frac{K_{20}(z - \xi,s)}{\beta} + \frac{2}{z-\xi}\frac{M^2}{\beta^2}\ .$$

Another important representation of the integral equation may be obtained. The kernel function $K_2(X,s)$ may be written as,

$$K_2(X,s) = e^{+M^2 X s^*}\,\beta\{K_{20}(X,s^*) - \frac{M^2}{2}[K_{20}(X,s^*) - K_{20}^{s}(X,s^*)]$$

$$+ \frac{M^2}{2}\cdot s^*\cdot\left[\frac{4\beta}{M^2}\ln\frac{2}{2+\beta} - 2\ln s^* - 4\,\frac{(1-\beta)}{M^2}\ln\frac{M}{2} - 2\gamma\right]$$

$$- \frac{M^2}{2}\,s^{*2}\left[\frac{4}{M^2}\,\beta\ln\frac{2}{1+\beta} - 1 - \frac{4}{M^2}\ln\frac{M}{2}(1-\beta-\frac{M^2}{2})\right]X$$

$$+ O(M^4)\cdot O(X^2 + aX\log X)\} \qquad (B.37)$$

$$= e^{+s^* X M^2}\,\beta\{K_{20}(X,s^*) - \frac{M^2}{2}[K_{20}(X,s^*) - K_{20}^{s}(X,s^*)]$$

$$+ \frac{M^2 s^*}{2}\,(1-2[\ln(\tfrac{1}{2}Ms^*) + \gamma]) + M^4 K_V(X,s^*)\} \qquad (B.38)$$

where $$K_{20}^{s}(X,s^*) = 2(\frac{1}{X} + s^*\ln X) \qquad (B.39)$$

$$K_V(X,s^*) = O(M^0 + a\ln M) \qquad (B.40)$$

Using equation B.38 we may invert equation B.28 using the well known solution for incompressible flow. Thus we have

$$\frac{\Delta p(x,s)}{q} = \frac{\bar{\Delta}p_{OV}(x,s^*)}{V}\,e^{M^2 s^* x} - \frac{M^2}{2\pi}\,e^{M^2 s^* x}\Big[\sum_{i=0}^{1} A_i(s^*,x)J_i(s^*,-1)$$

$$+ B_i(s^*,x)J_i(s^*,x)\Big] - \frac{M^4}{8\pi}\,e^{M^2 s^* x}\int_{-1}^{1}\int_{-1}^{1} G(x,z,s^*)K_V(z-\xi,s)e^{-M^2 s^*\xi}\cdot\frac{\bar{\Delta}p(\xi,s)}{q}$$

$$\cdot\, d\xi\, dz \qquad (B.41)$$

where

$$\frac{\bar{\Delta p}_{OV}(x,s^*)}{q} = \frac{1}{\beta}\int_{-1}^{1} G(x,z,s^*)\bar{w}(z,s)e^{-M^2 sz}\,dz \qquad (B.42)$$

$$J_i(s^*,x) = \int_x^1 \xi^i \frac{\bar{\Delta p}(\xi,s)}{q} e^{-M^2 s^*\xi}\,d\xi\,.$$

$$A_0(s^*,x) = \ln^{-1}x(2s^* - s^{*2}x) + \frac{1-x}{1+x}(s^*\psi(s^*)\ln 2 - (\psi(s^*)-1)$$

$$+ \frac{s^*\alpha}{2}(\psi(s^*)+s^*(1+x))+s^{*2}(1+\ln 2)(1+x)).$$

$$B_0(s^*,x) = -(2 - s^*x)\pi s^*$$

$$A_1(s^*,x) = s^{*2}\ln^{-1}x + s^*(\psi(s^*)-1)\sqrt{\frac{1-x}{1+x}}$$

$$B_1(s^*,x) = -\pi s^{*2}$$

$$\alpha = [1 - 2(\ln(\tfrac{1}{2}Ms^*) + \gamma)]$$

Thus for sufficiently small M we have for $\bar{\Delta p}$,

$$\frac{\bar{\Delta p}(x,s)}{q} = \frac{\bar{\Delta p}_{OV}(x,s^*)}{q} e^{M^2 s^* x}$$

$$- \frac{M^2}{2\pi} e^{M^2 s^* x}[\sum_{i=0}^{1} A_i(s^*,x)J_i^0(s^*,-1) + B_i(s^*,x)J_i^0(s^*,x)]$$

$$+ O(M^4 s^{*4}(a + b\ln M)) \qquad (B.43)$$

where $J_i^0(s^*,x) = \int_x^1 \xi^i \frac{\bar{\Delta p}_{OV(\xi,s)}}{q} d\xi$.

This solution is exact to $O(M^2 s^*)$. The first term is identical to Osborne's thin airfoil theory [71]. The usefulness of this representation will be briefly discussed in Appendix C.

APPENDIX C

CALCULATION OF AERODYNAMIC LOADS FOR SIMPLE HARMONICALLY OSCILLATING AIRFOILS AND LIFTING SURFACES

In this appendix some of the existing methods and their extensions for the calculation of aerodynamic loads on wings with and without control surfaces will be briefly discussed.

Two Dimensional Airfoils

Analytical methods. - In incompressible flow Theodorsen's solution is well known for calculating pressure distributions and airloads on two dimensional aerofoils. For a downwash $\frac{w}{V} = W_n x^n$, we have,

$$\frac{\Delta p}{q} = C_p = -4\sqrt{\frac{1-x}{1+x}}\, W_n \left[x^n + \left(\sum_{\ell=0}^{n-1} \frac{x^{n-\ell-1} 2^{-\ell} \ell!}{I(\ell)} \right) + \frac{ik(1+x)}{n+1} \cdot \right.$$

$$\left. \left(\sum_{\ell=0,2,4,\ldots}^{n} \frac{x^{n-\ell} 2^{-\ell} \ell!}{I(\ell)} \right) + (C(k)-1)\, \frac{2^{-\eta} \eta!}{I(n)} \right] \qquad (C.1)$$

where $I(n) = \left(\frac{n}{2}!\right)^2$ for n even

$= \frac{n+1}{2}! \; \frac{n-1}{2}!$ for n odd.

For a downwash given by $\frac{w}{V} = w_N (x - x_c)^n$ for $x > x_c$

$= 0$ for $x < x_c$

$$\Delta p = \frac{4}{\pi}\sqrt{\frac{1-x}{1+x}}\ w_n \left[\sum_{r=0}^{n-1} {}_nC_r \left\{ \sum_{k=0}^{n-r-1} (-1)^{k-1}\ {}_{n-r-1}C_k x^k (J_{n-r-1-k} + J_{n-r-k}) \right\} \cdot \right.$$

$$\cdot (x - x_c)^r$$

$$-(x-x_c)^n \cos^{-1} x_c + ik\frac{(1+x)}{n+1} \sum_{r=0}^{n} {}_{n+1}C_r \left(\sum_{k=0}^{n-r} (-1)^{k-1} x^k\ {}_{n-r}C_k J_{n-r-k} \right) \cdot (x-x_c)^r$$

$$\left. + (1 - C(k)) \sum_{r=0}^{n} {}_nC_r (-x_c)^r (J_{n-r} + J_{n-r+1}) \right]$$

$$-\frac{4}{\pi} W_n \left\{ (x - x_c)^n + \frac{ik(x-x_c)^{n+1}}{n+1} \right\} \log \left| \frac{1 - x_c x + \sqrt{1-x_c^2}\sqrt{1-x^2}}{(x - x_c)} \right| \qquad (C.2)$$

where $J_{2\ell} = \frac{\sqrt{1-x_c^2}}{2\ell} \left(x_c^{2\ell-1} + \sum_{k=1}^{\ell-1} \frac{(2\ell-1)(2\ell-3)\cdots(2\ell-2R+1)}{2^{\ell}(\ell-1)(\ell-2)\cdots(\ell-R)} x_c^{2\ell-2k-1} \right)$

$$+ \frac{2\ell!}{2^{2\ell}\ell!\ell!} \cos^{-1} x_c$$

and

$$J_{2\ell+1} = \frac{\sqrt{1-x_c^2}}{2\ell+1} \left\{ x_c^{2\ell} + \sum_{k=0}^{\ell-1} \frac{2^{k+1} \cdot \ell \cdot (\ell-1)(\ell-2)\cdots(\ell-k)}{(2\ell-1)(2\ell-3)\cdots(2\ell-2k+1)} x_c^{2\ell-2k-2} \right\}$$

The expressions for the loads may be easily obtained by integrating the corresponding moments of the pressure distributions.

Equation B.43 extends Theodorsen's solution to subsonic flow for low mach numbers and frequency. The first term of equation B.43 is identical to Osborne's theory. Kemp [72] has provided the closed form

expressions for the lift and moment based on Osbourne's theory. However it was found that this approach is not too attractive for purposes of numerically computing pressure distributions or aerodynamic loads. Further these solutions are not valid for either high subsonic mach numbers or high reduced frequencies, when compressibility effects are not small relative to circulatory effects.

For high frequencies, and Mach numbers $M \neq 0$, the method of acoustic planforms of Lomax, et al. [12] is useful. The two dimensional unsteady problem for compressible flow can be formulated in a coordinate system x',y',z',t' fixed in the undisturbed fluid, by the equation,

$$\varphi_{x'x'} + \varphi_{z'z'} = \frac{1}{c^2} \varphi_{t't'}$$

with the appropriate boundary conditions. For the three dimensional steady supersonic case, in body fixed coordinates, it is

$$\varphi_{yy} + \varphi_{zz} = (M^2 - 1)\varphi_{xx} \ .$$

Hence it is seen that the solution of the unsteady problem can be obtained from the solution for the steady flow about a swept forward wing tip placed in a supersonic flow with Mach number $M = \sqrt{2}$. The angle of sweep is determined by the Mach number of the two dimensional aerofoil from than relation $\Lambda = \tan^{-1} 1/M$. The wake vortices in the unsteady two dimensional problem correspond to the tip vortices in the steady three dimensional problem. The three dimensional steady flow

problem may be solved by Evvard's method [1]. For example the pressure distribution obtained this way, corresponding to an indicial downwash w_0, for $t \geq 0$, is given by,

$$\Delta C_p(\tau,x) = -\frac{4}{M} w_0 \triangleq \Delta C_{p_1}$$

$$\text{for } \tau \leq \min\left(\frac{M}{1+M}, \frac{M}{1-M}(1-x)\right)$$

$$\Delta C_p(\tau,x) = \Delta C_{p_1} + \frac{8}{M}\frac{w_0}{\pi}\left[\tan^{-1}\sqrt{\frac{(1+M)\tau}{M(1+x)} - 1} + \frac{M}{1+M}\sqrt{\frac{(1+M)\tau}{M(1+x)} - 1}\right]$$

$$\text{for } \frac{M}{1+M}(1+x) \leq \tau \leq \frac{M}{1-M}(1-x)$$

$$\Delta C_p(\tau,x) = \Delta C_{p_1} + \frac{8}{M}\frac{w_0}{\pi}\tan^{-1}\sqrt{\frac{(1-M)\tau}{M(1-x)} - 1}$$

$$\text{for } \frac{M}{1-M}(1-x) \leq \tau \leq \frac{M}{1+M}(1+x)$$

where $\tau = \frac{vt}{b}$ and $0 < M \leq 1$

Expanding in the variables (1-x) and (1+x) indicates that for $t > 0$, at the leading edge ($x = -1$)

$$\Delta C_p(\tau,x) \to \infty \text{ as } \frac{1}{\sqrt{1+x}}$$

and at the trailing edge ($x = 1$)

$$\Delta C_p(\tau,x) \to 0 \text{ as } \sqrt{1-x}$$

The indicial aerodynamic load coefficients may be obtained by integrating the pressures over the entire chord of the aerofoil.

Taking the Laplace transforms, and using the asymptotic expansions of the resulting Frenel integrals

$$Fr(R) = \int_0^R \frac{e^{-ih}}{\sqrt{2\pi U}}\,du = \frac{1-i}{2} + \frac{ie^{-iR}}{\sqrt{2\pi R}}\left(1 - \frac{1}{2iR} - \frac{3}{4R^2}\right) + O\left(\frac{1}{R^{7/2}}\right)$$

we may obtain the expressions for the non-dimensional lift and moment coefficients in plunging and pitching for large values of k.

These are

$$\frac{L_h}{2b\cdot q} = -\frac{4ik}{M} + \frac{2}{M^2}(1-M) - \frac{1-i}{M^{5/2}}\sqrt{\frac{2}{\pi k}}\left\{e^{-ik\frac{2M}{1+M}} + (1-M)^2\, e^{-ik\frac{2M}{1-M}}\right\} + O(1/k)$$

$$\frac{M_h}{2b^2q} = -\frac{1-i}{M^{5/2}}\sqrt{\frac{2}{\pi k}}\left\{e^{\frac{-ik2M}{1+M}} - (1-M)^2 e^{-i\frac{2M}{1-M}}\right\} + O(1/k)$$

$$\frac{L_\alpha}{2bq} = -\frac{4}{M} + \frac{1-i}{M^{5/2}}\sqrt{\frac{2}{\pi k}}\left\{e^{-i\frac{k2M}{1+M}} - (1-M)^2 e^{-i\frac{k2M}{1-M}}\right\} + O(1/k)$$

$$\frac{M_\alpha}{2b^2q} = -\frac{4}{3}\frac{ik}{M} + \frac{2(1-M)}{M^2} + \frac{1-i}{\pi M^{5/2}}\sqrt{\frac{2}{\pi k}}\left\{e^{-ik\frac{2M}{1-M}} + (1-M)^2\, e^{-ik\frac{2M}{1-M}}\right\} + O(1/k).$$

It is interesting to note that it is not possible to expand these coefficients in a power series in (1/k). Also they are not valid for M = 0. Thus it is possible to analytically obtain the behavior of the

aerodynamic loads for low and high frequencies. While they contribute to a better understanding of the behavior of the pressure and aerodynamic loads at high and low frequencies, they do not serve any other useful purpose. For this reason and for computational efficiency, it is convenient to resort to numerical techniques which are valid for all values of frequency and mach number.

Numerical methods. - One of the earliest methods to calculate aerodynamic loads on two dimensional aerofoils is due to Dietz (described in Refs. 1, 2, and 3). For wings with trailing or leading edge flaps, Fettis suggests a method that is fairly accurate. From a computational point of view Hsu's method [73] for wings without flaps seems to be simplest. However Hsu's method can be extended for wings with control surfaces. This modification is briefly described below. A pressure loading function of the form,

$$\Delta Cp = \sum_{m=0}^{M} P_m h_m(x) - \frac{2}{\pi}\frac{\delta}{\beta}\sum_{n=0}^{N} a_n (x - x_c)^n \log\left|\frac{1-xx_c+\sqrt{1-x^2}\sqrt{1-x_c^2}}{1-xx_c-\sqrt{1-x^2}\sqrt{1-x_c^2}}\right|$$

is assumed, where $h_m(x)$ are identical to Hsu's chordwise loading functions in compressible flow and are the exact loading functions corresponding to a downwash of x^n in incompressible flow, given by equation C.1. δ is the angular deflection of the trailing edge flap. The above loading function is substituted in the integral equation and integrations of those terms that contribute to discontinuities in the

downwash and its chordwise derivatives are performed analytically. The coefficients a_n can then be found by comparing like terms on both sides of the integral equations. The kernel functions $K_2(x,s)$ may be written as

$$K_2(x,s) \sim \frac{2\beta}{x} - \frac{2s}{\beta} \ln|x| - \left(\frac{s}{\beta}\right)^2(\beta - 3\beta^4)x \ln|x|$$

$$+ \sum_{n=0}^{\infty} \alpha_n x^n + \ln|x| \sum_{n=2}^{\infty} \beta_n x^n.$$

a_0, a_1 and a_2 depend only on the terms outside the summation signs and are given by,

$$a_0 = 1,\ a_1 = \frac{s}{\beta^2}(1 + \beta^2),\ a_2 = \frac{1}{4}\left(\frac{s}{\beta^2}\right)^2(3 - \beta^2)$$

and

$$a_3 = 0\left(\frac{s}{\beta^2}\right)^3 \cdot 0(M)$$

In incompressible flow a_3, a_4, ..., etc., are equal to zero (from equation C.2).

The singular part of the above kernel function and the pressure loading functions are integrated exactly. A computer program is developed that evaluated the Possio kernel by Gaussian and Berthod Zabrowski quadrature, integrates the assumed pressure loading functions and the non-singular portion of the kernel function numerically and then solves for P_i. The program then obtains the corresponding generalized aerodynamic forces for any mode shapes. Results indicate that for M = 0.0 and 0.7, the error in using a ten point collocation

scheme and not including the flap singularity is 20 - 25% of the four point collocation solution with the singularity included. In incompressible flow using the four point collocation scheme results in an error of less than 1%, in the moment about the flap hinge line. The program may be used for values of $0 < k < 10$ and can include trailing and leading edge flaps. For high frequencies a large number of collocation and integration points are required.

In supersonic flow, the expression for the pressure and airloads given in Ref. 1 may be integrated using Gaussian integration with no difficulty as control surfaces do not contribute to any singularities. Results for a rigid airfoil with trailing and leading edge flaps are given in [44] and [45].

Three Dimensional Lifting Surfaces

Analytical techniques. - There are no known analytical techniques available for arbitrarily shaped three dimensional lifting surfaces. However, as pointed out by Miles [74], the solution of the partial differential equations for the velocity potential by separating the variables is possible only in eleven Euclidean coordinate systems. Of these only three define lifting surfaces of practical interest. These are (1) elliptic cylindrical (two dimensional aerofoil) (2) oblate spheroidal (circular planform) and (3) ellipsoidal (elliptic planform).

The circular oscillating lifting surface in incompressible flow was considered by van Spiegel [54]. It is interesting to note that from van Spiegel's general solution, we may extract the solution for the

virtual inertia loading. The orthogonal coordinate system for the circular wing is given by

$$x = \sqrt{1 + \eta^2}\sqrt{1 - \mu^2}\cos\nu \qquad y = \sqrt{1 + \eta^2}\sqrt{1 - \mu^2}\sin\nu ,$$

$z = \mu\eta$ where $0 \leq \eta$, $-1 \leq \mu \leq 1$, $0 \leq \nu < 2\pi$ so that the entire space is covered just once. The wing itself is given by $\eta = 0$, while the part of the x, y - plane outside the surface is given by $\mu = 0$.

The problem is treated by van Spiegel by the method of the acceleration potential. The regular solution is equal to

$$\psi_1 = \sum_{i=1}^{\infty} {\sum_{j=0}^{i-1}}' P_i^j(\mu)Q_i^j(i\eta)\{C_i^j \cos i\nu + S_i^j \sin i\nu\}$$

where P_i^j and Q_i^j are Legendre's associated functions of the first and second kinds. Since ψ_1 should be an odd function of z and μ, the summation sign is restricted to i + j = odd. This is indicated by the prime added to the summation over j in the equation for ψ. The constants C_i^j and S_i^j are determined by the prescribed normal derivatives at the airfoil. By expanding $\psi_{1z} = \psi_{1\eta}/\mu$ in a series of surface harmonics the constants are determined. It is found that,

$$\psi_1(\eta,\mu,\ ) = \int_{-1}^{1}\mu_1 \int_0^{2\pi} \psi_{1z}(\mu_1,\nu_1)G(\eta,\mu,\nu,0,\mu_1,\nu_1)d\nu_1 dy$$

where the Green's function of the second kind is equal to,

$$G(\eta,\mu,\nu;\ 0,\ \mu_1,\nu_1) = \sum_{n=1}^{\infty}\sum_{m=0}^{\infty}{}' \frac{1}{\xi_m}\frac{2n+1}{2\pi}\frac{(n-m)!}{(n+m)!}P_n^m(\mu)P_n^m(\mu_1) \cdot \frac{Q_n^m(i\eta)}{\dfrac{\partial Q_n^m(i0)}{\partial\eta}}\operatorname{Cos} m(\nu-\nu_1)$$

where $\xi_0 = 2, \qquad \xi_1 = \xi_2 = \xi_3 = \ldots = 1.$

The above solution is one that has the exact prescribed acceleration on the aerofoil. Further the solution is not singular at the leading and trailing edges and behaves as $\sqrt{r}$ where r is the distance of the leading edge or trailing edge. The solution that has the exact normal velocity $\bar{w}(\mu,\nu)$, prescribed on the airfoil is

$$\psi^*(\eta,\mu,\nu) = \left(\frac{\partial}{\partial t} + u\frac{\partial}{\partial x}\right)\int_0^{2\pi}\int_{-1}^{1}\mu_1\bar{w}(\mu_1,\nu_1)\cdot$$

$$\cdot G(\eta,\mu,\nu;0,\mu_1,\nu_1)d\nu,\ du\ .$$

This solution leads to a pressure singularity at the trailing and leading edges due to the differentation in x.

Consider now

$$G_\mu(\eta,\mu,\nu;\ 0,\ 0,\ \nu_1) = -\frac{\mu}{\pi^2}\frac{1}{1+\eta^2-2\sqrt{1+\eta^2}\sqrt{1-\mu^2}\cos(\nu-\nu_1)+1-\mu^2}$$

This is a solution of Laplace's equation having zero normal velocity on the aerofoil and a singularity at the point $\eta = 0,\ u = 0,\ \nu = \nu_1$ which lies either at leading or at the trailing edge. The singularity is of the type $\sqrt{(\cos\alpha)/r^3}$, where r is the distance from a point on the aerofoil to the singular point and α the angle between the vector v and the radius of the circle. Thus the singular solution is,

$$\psi_2(\eta,\mu,\nu) = \int_{\pi/2}^{3\pi/2} a(\nu_1) G_{\mu_1}(\eta,\mu,\nu;0,0,\nu_1)\,d\nu_1 \ .$$

where the integration is along the leading edge only, since no singularities are admitted at the trailing edge. As in the two dimensional case the singularity in ψ_2 is of the type $\sqrt{1/r}$, where r is the distance from the leading edge. The function a (r_1) should be determined from the condition that the normal velocity at all points on the aerofoil due to the total acceleration potential $\psi_1 + \psi_2$ agree with the prescribed normal velocity. Hence the normal velocity at all points due to the acceleration potential $\psi_1 + \psi_2 - \psi^*$ should be equal to zero. This leads to an integral equation which may be solved by Fourier series expansions.

On examining this solution carefully, we find that very large frequencies of oscillation or at the starting instant $(\psi_1 + \psi_2 - \psi^*)$ is independent of frequency. Hence we conclude that the solution corresponding to the virtual inertia loads is,

$$\psi_I^* = \int_0^2 \int_0^1 \mu_1 \left(\frac{\partial^2}{\partial t^2} z(\mu_1, \nu_1) \right) G(\eta,\mu,\nu;0,\mu_1,\nu_1)\,d\nu_1 d\mu$$

Like the regular solution this is not singular at both the leading and trailing edges.

The effect of compressibility may be taken into account by means of spheroidal wave functions. Also the oscillating elliptic wing can be treated when Lame functions are used. However, these analytical

solutions are not really exact and the degree of computations is enormous when compared to numerical methods. Hence these techniques are not too useful.

Numerical techniques. - Numerical techniques may be broadly classified into two groups (a) finite element methods and (b) kernel function techniques. The doublet lattice method of Albano and Rodden [26] and potential flow methods [18] in subsonic flow and the Mach box method in supersonic flow [75, 76] are examples of the first type. The kernel function methods of Laschka [25], Cunningham [23] and Rowe [24] in subsonic flow and Müller's method [67] in supersonic flow are examples of the latter type. Two of the methods that were actually used in a slightly modified form during the course of this work are briefly described.

The doublet lattice method: This method for lifting surfaces is based on the developments of Albano and Rodden. The surfaces are divided into trapezoidal panels, the downwash being taken at the midspan of the 3/4 chord. A distribution of acceleration potential doublets whose strength is to be determined, is assumed along the quarter chord of each panel. The assumed pressure loading is then integrated along the quarter chord line. In the original method, the integrals were obtained by approximating the kernel function in each box with a parabola in the direction of the quarter chord of each panel, divided by r_1^2, where $r_1^2 = y_0^2 + z_0^2$, y_0 and z_0 being relative y and z distances of the midpoints of the quarter chords (sending points) and the three quarter chord (receiving points).

The force on the panel due to the pressure distribution is assumed to be equal to the force on the doublet line segment. The accuracy of the method was remarkable for aeroelastic purposes. However for large frequencies (reduced frequencies $k > 1$) it was found that the method was not only not accurate, but also did not converge to the results obtained by piston theory. It was found that by approximating the kernel in each box with a quartic in the spanwise direction of the quarter chord point of each panel divided by r_1^2, the results were tremendously improved for planar lifting surfaces for high frequencies.

Using the same notation as Rodden, Giesing and Kalman [77] we may rewrite equation 27b of Ref. 77 as,

$$\frac{P(\eta)}{(\bar{y}-\bar{\eta})^2} = \frac{[K_1 \exp\{-i\omega(\bar{x}-\bar{n}\tan\lambda\, s)/V\} - K_{10}]}{(\bar{y}-\bar{\eta})^2}$$

$$= A_0\bar{\eta}^2 + B_0\bar{\eta} + \frac{A_1\bar{\eta}^2 + B_1\bar{\eta} + C_1}{(\bar{y}-\bar{\eta})^2}$$

Assuming that $P(\bar{\eta})$ is evaluated at $\bar{\eta} = \pm ae, \pm be$ and 0, where e is the semi-span of each panel we have,

$$A_0 = \frac{1}{2(a^2-b^2)e^2}\left[\frac{1}{a^2}(P(ae)+P(-ae)-2P(0)) - \frac{1}{b^2}(P(be)+P(-be)-2P(0))\right]$$

$$B_0 = 2A_0\bar{y} + \frac{1}{2(a^2-b^2)e^3}\left[\frac{1}{a}(P(ae)-P(-ae)) - \frac{1}{b}(P(be)-P(-be))\right]$$

$$B_1 = -B_e \bar{y}^{-2} + \frac{a^2 b^2}{2(b^2-a^2)e} \left[\frac{1}{a^3}(P(ae)-P(-ae)) - \frac{1}{b^3}(P(be)-P(-be)) \right]$$

$$C_1 = P(0)$$

'a' and 'b' were chosen to be 1.0 and 0.5 respectively. For $A_0 = B_0 = 0$, the formulas for A_1, B_1 and C_1 reduce to those given by Albano and Rodden. The above approximation is very good for high frequencies, especially for swept wings ($\lambda s \neq 0$). At high frequencies, for swept wings, P ($\bar{\eta}$) varies rapidly for different values of $\bar{\eta}$. However extensive numerical experiments have to be carried out determine the optimum values of a, b and the receiving and sending points in various frequency domains.

In spite of the improvement in the results for moderately high frequencies, the results did not converge to the piston theory limit for certain mode shapes. For convergence the distance between the sending and receiving point on each panel must vanish as this condition is known to hold in the case of piston theory. This would require, theoritically, an infinite number of boxes in the chordwise direction. Also for a proper spanwise pressure distribution, which critically effects the aerodynamic loads a large number of spanwise boxes are required at all frequencies. This leads to an excessively large computer storage requirements and thus the method is not too attractive for high frequencies.

Laschka's kernel function method: In this method the pressure distribution is taken in the form

$$\Delta C_p(x,y) = \sum_{i=1}^{N} a_i(y) h_i(x) \frac{\ell s}{c(y)}$$

Following Laschka, the terms in the kernel function which are singular are separated from the part that is regular. The singular terms are integrated analytically while the regular terms are integrated numerically. The integral equation is reduced to a linear system and the values of the unknown coefficients $a_i(y)$ are obtained at different spanwise and chordwise stations. For the chordwise integration, the integrations points and the collocation points may be chosen independentally. For high frequencies one may choose fewer collocation points and a large number of integration points, in order to converge to piston theory. Thus the kernel function method is more efficient than the doublet lattice method.

Control surfaces may be handled by both methods, without taking into account the singularities at their leading edges. However, the computational time for high frequencies is quite high when compared to the corresponding time at low frequencies, in both methods.

APPENDIX D

PADÉ APPROXIMANTS AND INTEGRAL EQUATIONS

Padé Approximants

The [N,M] Padé approximant of a matrix function $F(z)$ is defined by

$$F(z) = P(z)R^{-1}(z)$$

where

$P(z)$ is a matrix polynomial of degree M and

$R(z)$ is a matrix polynomial of degree N

If in particular $F(z)$ is a power series defined by,

$$F(z) = \sum_{i=0}^{L} F_i z^i \quad \text{and if}$$

$$P(z) = \sum_{i=0}^{M} P_i z^i, \; R(z) = \sum_{i=0}^{M} R_i z^i, \; R_N \triangleq I \tag{D.2}$$

we have the following equations for P_i and R_i

$$\sum_{J=0}^{N-1} F_{k-j} R_j + F_{k-N} = P_k, \quad k = 0, 1, 2, 3, \ldots M$$

$$\sum_{J=0}^{N-1} F_{k-j} R_j = -F_{k-N}, \quad k = M+1, M+2, M+3, \ldots L \tag{D.3}$$

For $L \geq M + N$, equations D.3 may be solved for the matrices R_j and P_k successively.

On the other hand, if $F(z)$ is known for $z = z_k$, $k = 0,1,2,3 \ldots L$ we have

$$F(z_k)z_k^N = \sum_{i=0}^{M} P_i z_k^i - F(z_k) \sum_{i=0}^{N-1} R_i z^i, \quad k = 0,1,2,3,\ldots L \tag{D.4}$$

It is now assumed that P_0 and P_M are known apriori. (If P_M is not known, we may increase value of M by 1 and assume that $P_{M+1} = [0]$). From the L known values of z_k, we pick M-1 values, z_{k_1}, $k_1 = 1,2,3,$ ... M-1, and rewrite equations D.4 in part as

$$\sum_{i=1}^{M-1} P_i z_k^i = F(z_{k_1})z_{k_1}^N - P_0 - P_M z_{k_1}^M + F(z_{k_1}) \sum_{i=0}^{N-1} k_i z_{k_1}^i$$

$$k_1 = 1, 2, 3, \ldots M-1$$

We now have M-1 unknowns P_i and M-1 equations and hence we may solve for the unknowns P_i in terms of R_i as

$$P_i = \sum_{J=0}^{N-1} B_{ij} R_j + B_0 \tag{D.6}$$

Hence equations D.4 reduce to a system of L-M+1 equations for the N unknowns R_j, $j = 0,1,2, \ldots N-1$, which may determine by least squares provided the system of equations are solvable. On the other hand it is also possible to solve equation D.4 directly by least squares. These equations are also applicable for scalar quantities. Properties of Padé approximants are discussed further in [78].

Properties of Integral Equations Related to Padé Approximants

([79] and [80])

In this section some of the basic definitions and properties of integral equations of the form

$$\varphi(x) = f(x,s) + s \int_a^b dy\ K(x,y,s)\varphi(y) \tag{D.7}$$

where $f(x,s)$ and $K(x,y,s)$ are defined on the closed internal $[a,b]$, are discussed. We can regard,

$$K = \int_a^b dy\ K(x,y,s)(\cdot) \tag{D.8}$$

in equation D.7 as an operator acting on the function φ. In operator form the integral equation is

$$\varphi = f + sK\varphi \tag{D.9}$$

The function $K(x,y,s)$ is the kernel of the equation and in order to ensure a valid definition and a unique solution of D.7, various restrictions can be imposed on φ, f, and K. It is usual to assume φ and f are functions of bounded norm $\|\cdot\|$ in the Hilbert space L^2 of functions defined on the interval $[a,b]$; for example,

$$\|\varphi\|^2 = \int_a^b |\varphi(x)|^2 dx \ < \infty \tag{D.10}$$

A sequence of functions $\{f_n\}$ is bounded if

$$\| f_n \| \leq B < \infty \tag{D.11}$$

Bounded operators. - The operator defined by D.8 is bounded if there is a finite constant M, such that

$$\| Kh \| \leq M \| h \| \tag{D.12}$$

for all functions h of finite norm. This is a different condition from the boundedness of the function K (x,y,s) given by $|K(x,y,s)| \leq c < \infty$. The norm of a bounded operator K is the least value of M satisfying D.12. The operator is unbounded if no finite M can be found such that (D.12) holds for all h.

Kernels of finite rank. - A kernel K_n is of finite rank n if it is expressible in the form

$$K_n(x,y,s) = \sum_{i=1}^{n} \alpha_i(x)\beta_i(y) \tag{D.13}$$

where $\{\alpha_i\}$ and $\{\beta_i\}$ are linearly independent sets of functions in L^2. If the kernel K(x,y,s) is a kernel of finite rank and α_i and β_i are rational functions or polynomials of s equation (D.7) may be solved exactly. For simplicity it is assumed that f(x,s) is independent of s.

The kernel function method. - The scalar product of functions f and g in L^2 is

$$(f,g) = \int_a^b dy\ f(y)g(y) \tag{D.14}$$

Substituting (D-13) in (D.7) gives,

$$\varphi(x) = f(x) + s \sum_{j=1}^{n} (\varphi,\beta_i)\alpha_i(x) \tag{D.15}$$

The coefficients (φ,β_i) are complex numbers and any solution of (D.7) may be of the form,

$$\varphi = f(x) + \sum_{j=1}^{n} \xi_j\ \alpha_j$$

where the coefficients ξ_j and to be determined.

Substituting (D.16) in (D.15), ξ_j are determined by

$$\sum_{i=1}^{n} [\delta_{ij} - s(\alpha_i,\beta_j)]\xi_i = s(f_i,\beta_j).$$

Let $\Delta(s)$ be the determinant of the coefficients of ξ_j and the minor associated with i,j^{th} element be Δ_{ij}.

Then $$\xi_i = \Delta^{-1} \sum_{J=1}^{n} \Delta_{ij} s(f,\beta_j)$$

and

$$\varphi = f(x) + \sum_{J=1}^{n} \Delta^{-1} \sum_{i=1}^{n} \Delta_{ji} s(f,\beta_i)$$

Hence, $$\varphi = \Delta^{-1}[\Delta f(x) + \sum_{j=1}^{n} \sum_{i=1}^{n} \Delta_{ji}\ s(f(x),\beta_i(x))\alpha_j] \tag{D.16}$$

As a function of the parameter s, this a rational function, the numerator degree and the denominator degree being dependent on α_i and β_j.

Compact operators. - Let T be a linear operator that transforms any function h in L^2 into another function Th of L^2; in particular T could be of the form given by equation D.8. Every linear operator of this type is continuous in the sense that it transfors a sequence $\{h_n\}$ converging in the mean to h into a sequence $\{Th_n\}$ converging to Th.

Compactness or complete continuity of a linear operator is a stronger condition than continuity. Let $\{f_n\}$ be any bounded infinite sequence in L^2, so that $\{Tf_n\}$ is another infinite sequence in L^2. Then if for all bounded $\{f_n\}$,$\{Tf_n\}$ contains a subsequence converging to some function h as $n \to \infty$, so that

$$\| Tf_n - h \| = 0$$

then T is completely continuous. Reiz and St.-Nagy [80] give necessary and sufficient conditions for complete continuity.

Completely continuous operators can be uniformly approximated by operators with kernels of finite rank. Also, if a kernel function can be approximated with kernels of finite rank, then the operator is completely continuous. In unsteady aerodynamics the kernels are implicitly approximated by kernels of finite rank and resulting solutions are known to converge to the exact pressure distributions uniformly, for all frequencies.

Thus there exists an infinite sequence of kernels $K_1, K_2, K_3 \cdots$ of rank 1, 2, 3, ... such that

$$\| (K - K_n)h \| < \epsilon_n \| h \|$$

with $\epsilon_n \to 0$ as $n \to \infty$ for all $h \in L^2$, uniformly for all s.

Let K_n be of the form $\sum_{i=1}^{m} \alpha_i(s,x)\beta_i(s,y)$ where $\alpha_i(s,x)$ and $\beta_i(s,x)$ are rational functions or polynomials in the variables s. Hence it may be assumed that as $s \to \infty$ K_n is of $O(s^E)$ for all n. Then from equations D.16 we obtain a sequence of solutions, which are rational functions of s. The degree of the numerator would be N-E and that of the denominator N where $N \to \infty$ as $n \to \infty$.

Neumann series solutions. -

Another method of solving (D.7) is to substitute the series

$$\varphi(x) = f(x) + \sum_{n=1}^{\infty} s^n f_n(x,s) \qquad (D.17)$$

and equate the coefficients of s on each side. This gives

$$f_{n+1}(x,s) = \int_a^b dy\ K(x,y,s) fn(y,s)$$

$$n = 1,2,3, \ldots$$

The series (D.17) is known as a series and may be written in operator notation as,

$$\varphi(x) = f(x) + Kf(x) + K^2 f(x) \ldots$$

When K is uniformly bounded in the norm, then the series converges in the norm if,

$$|s| \leq \|K\|^{-1}$$

When s does not satisfy this condition Chisholm [79] has shown that Padé approximants of the series may be formed which will give approximations to the solution for all s.

From Chisholm's theorem it follows that: If the kernel function $K(x, y, s)$ of the integral equation D.7 can be approximated by a sequence of kernels of finite rank, then there exists a sequence of solutions which are rational functions in the 's' domain, the degree of the numerator being $N + J$ and the degree of the denominator being N, which converges uniformly to the exact solution as $N \to \infty$, where J depends on the limiting behavior of $K(x,y,s)$ and $f(x,s)$ as $s \to \infty$.

Thus if the behavior of the pressure distributions in unsteady aerodynamics are known for high frequencies and in steady flow and if it is possible to show that the associated kernel functions are completely continuous for all s, then it is possible, in principle, to construct Padé approximants for the aerodynamic loads from the numerically obtained solutions.

6. REFERENCES

1. Bisplinghoff, R. L., et al., "Aeroelasticity," 1st ed., Addison-Wesley Publish Company, Inc., 1955.

2. Bisplinghoff, R. L. and Ashley, H., "Principles of Aeroelasticity," John Wiley and Sons, Inc., 1962.

3. Fung, Y. C., "An Introduction to the Theory of Aeroelasticity," Dover Publications, 1969.

4. Leipholz, H., "Stability Theory," Academic Press, 1970.

5. Przemieniecki, J. S., "Theory of Matrix Structural Analysis," McGraw-Hill Book Company, 1968.

6. Flannelly, W. G., et al., "Research on Structural Dynamic Listing by Impedance Methods," USAAMRDL-TR-72-63, Nov., 1972.

7. Garrick, I. E., "On Some Fourier Transforms in the Theory of Non-Stationary Flows," Proc. Fifth Int. Cong. Appl. Mech. (Cambridge, Mass., 1938). AIAA Selected Reprint Series on "Aerodynamic Flutter," Vol. V, March, 1969, pp 32-35.

8. Theodorsen, Theodore, "General Theory of Aerodynamic Instability and the Mechanism of Flutter," NACA Rept. 496, 1935.

9. Sears, W. R., "Some Aspects of Non-Stationary Airfoil Theory and Its Practical Application," Jour. Aero Sci., Vol. 8, No. 3, Jan. 1941, pp 104-108.

10. Jones, R. T., "The Unsteady Lift of a Wing of Finite Aspect Ratio," NACA Rept. 681, 1940.

11. Jones, W. P., "Aerodynamic Forces on Wings in Non-Uniform Motion," R. & M. No. 2117, British A.R.C., Aug. 1945.

12. Lomax, H., et al., "Two-and Three-Dimensional Unsteady Lift Problems in High Speed Flight," NACA Rept. 1077, 1952.

13. Mazelsky, B. and Drischler, J. A., "Numerical Determination of Indicial Lift and Moment Functions for a Two-Dimensional Sinking and Pitching Airfoil at Mach Numbers 0.5 and 0.6," NACA TN 2739, 1952.

14. Drischler, J. A., "Calculation and Compilation of the Unsteady Lift Functions for a Rigid Wing Subjected to Sinusoidal Gusts and to Sinusoidal Sinking Oscillations," NACA TN 3748, Oct. 1956.

15. Miles, J. W., "Transient Loading of Wide Delta Airfoils at Supersonic Speeds," Jour. Aero. Sci., Vol. 18, No. 8, Aug. 1951, pp 543-554.

16. Miles, J. W., "Transient Loading of Supersonic Rectangular Airfoils," Jour. Aero. Sci., Vol. 17, No. 10, Oct. 1950, pp 647-652.

17. Djojodihardjo, R. H. and Widnall, S. E., "A Numerical Method for the Calculation of Nonlinear Unsteady Lifting Potential Flow Problems," AIAA Journal, Vol. 7, No. 10, Oct. 1969, pp 2001-2009.

18. Hess, J. L., "Calculation of Potential Flow About Arbitrary Three-Dimensional Lifting Bodies," Douglas Aircraft Company Rept. No. MDC J5679-01, Oct. 1972.

19. Ashley, H., et al., "New Direction in Lifting Surface Theory," AIAA Journal, Vol. 3, No. 1, Jan. 1965, pp 3-16.

20. Landahl, M. T. and Stark, V. J. E., "Numerical Lifting Surface Theory-Problems and Progress," AIAA Journal, Vol. 6, No. 11, Nov. 1968, pp 2049 - 2058.

21. Woodcock, D. L., "A Comparison of Methods used in Lifting Surface Theory," AGARD Rept. No. 583.

22. Ashley, H., "Some considerations relative to the predictions of unsteady airloads on lifting configurations," Journal of Aircraft, Vol. 8, No. 10, Oct. 1971, pp 747-756.

23. Cunningham, A. M., Jr., "Unsteady Subsonic Collocation Method for Wings with and without Control Surfaces," Jour. of Aircraft, Vol. 9, No. 6, June 1972, pp 413-419.

24. Rowe, W. S., "Collocation Method for Calculating the Aerodynamic Pressure Distributions on Lifting Surfaces Oscillating in Subsonic Compressible Flow," AIAA Symposium on Structural Dynamics and Aeroelasticity, Boston, Mass., Aug. 30-Sept. 1, 1965, pp 31-45.

25. Laschka, B., "Zur Theorie der Harmonisch Schwingenden tragenden Fläche bei Unterschallströmung," Zeitschrift für Flugwissenschaften II, July 1963, pp 265-291.

26. Albano, E. and Rodden, W. P., "A Doublet-Lattice Method for Calculating Lift Distributions on Oscillating Surfaces in Subsonic Flows," AIAA Journal, Vol. 7, No. 2, Feb. 1969, pp 279-285.

27. Gwin, L. B. and McIntosh, S. C. Jr., "Large Scale Flutter Optimization of Lifting Surfaces," AFFDL-TR-73-91, January 1974.

28. Theodorsen, T. and Garrick, I.E., "Non-Stationary flow about a wing-aileron-tab combination including aerodynamic balance," Rept. No. 736, NACA, 1942.

29. Jones, W. P., "Aerodynamic Forces on an Oscillating Aerofoil-Aileron-Tab Combination" R.& M.1948, British A.R.C., Sept. 1941.

30. Buchek, P. M., et al., "Modern Control Techniques in Active Flutter Suppression Using a Control Moment Gyro," (Stanford University; NASA Grant NGL-05-020-498.) NASA CR-138494, 1973.

31. Cooley, J. W. and Tukey, J. W., "An Algorithm for the Machine Computation of Complex Fourier series," Digital Signal Processing, Edited by Rabiner, L. R. and Rader, C. M., IEEE Press, New York 1972, pp 223-227.

32. Golub, G. H. and Pereyra, V., "The Differentation of Pseudo-Inverses and Nonlinear least squares problems whose variables separate," SIAM J. Numer. Anal., Vol. 10, No. 2, April 1973.

33. Baker, G. A.,Jr., "The Padé Approximant Method and Some Related Generalizations," The Padé Approximant in Theoritical Physics,

Edited by Baker, G. A., Jr. and Gammel, J. V., 1st Ed., Academic Press, New York, 1970.

34. Jones, W. P., "Summary of Formulae and Notations Used in Two Dimensional Derivative Theory," British A.R.C., R.&M. No. 1958, April 1942.

35. Luke, Y. L., "Approximate Inversion of a class of Laplace Transforms Applicable to Supersonic Flow Problems," Quart. J. of Mech. and Appl. Math., Vol. 17, 1964, pp 97-103.

36. Kemp, N. H., "On the Lift and Circulation of Airfoils in Some Unsteady-Flow Problems," Journ. Aero. Sci., Vol. 19, No. 10, Oct. 1952, pp 713-714.

37. Horlock, J. H., "Fluctuating Lift Forces on Aerofoils Moving Through Transverse and Chordwise Gusts," ASME Jour. Basic. Engg., Dec. 1968, pp 494-500.

38. Hewson-Browne, R. C., "The Oscillations of a Thick Aerofoil in an Incompressible Flow," Quarterly J. of Mechanics and Applied Mathematics, 16, 1963, pp 79-92.

39. Wood, L. C., "The Lift and Moment Acting on a Thick Aerofoil in Unsteady Motion," Phil. Trans. A., Vol. 267, 1954, pp 131.

40. Chen, C. F. and Wirtz, R. A., "Second order theory for flow past oscillating airfoils," AIAA J., Vol. 6 , No. 8 , 1968, pp 1556-1562/

41. Dat, R. and Meurzec, J. L., "Exploitation par lissage mathematique des mesures d'admittance d'um systéme linéare," Extráct de la Recherche Aérospatiale, No. 1972-4, 1972, pp 209-215.

42. Miles, J. W., "Quasi-Stationary Thin Airfoil Theory," Jour. of Aero. Sci., Vol. 16, 1949, pp 440.

43. Smilg, B., "The Instability of Pitching Oscillations of an Airfoil in Subsonic Incompressible Potential Flow," Jour. Aero. Sci., Vol. 16, 1949, pp 691-696.

44. Garrick, I. E. and Rubi··ow, S. I., "Flutter and Oscillating Air-Force Calculations for an Airfoil in Two Dimensional Supersonic Flow," NACA Rept. No. 846, 1946.

45. Hassig, H. J., "Aerodynamic Flutter Coefficients for an Airfoil with Leading- and Trailing-Edge flaps in Two-Dimensional Supersonic Flow," Journ. Aero. Sci., Vol. 21, No. 2, Feb. 1954, pp 131-132.

46. Landahl, M. T., "Unsteady Transonic Flow," Pergamon Press, N.Y., 1961.

47. Kuo, Y. H., "On the stability of two-dimensional smooth transonic flows," Jour. Aero. Sci., vol. 18, 1951.

48. Pearcey, H. H., "The Aerodynamic Design of Section Shapes for Swept Wings," Advances in Aeronautical Sciences, Vol. 3, London 1962.

49. Nieuwland, G. Y. and Spee, B. M., "Transonic Airfoils: Recent Developments in Theory, Experiment, and Design," Annual Review of Fluid Mechanics, Vol. 5, 1973, pp 119-150.

50. Jones, W. P., "Calculation of Additional Mass and Inertia Coefficients for Rectangular Plates in Still Air," R.& M. No. 1947, British A.R.C., Nov. 1941.

51. Bryson, A. E.,Jr., "Stability Derivatives for a slender missile with application to a Wing-Body Vertical Tail Configurations," Journal of the Aeronautical Sciences, Vol. 20, No. 3, pp 297-308, May 1953.

52. Bryson, A. E.,Jr., "Comment on the stability derivatives of a wing-body-vertical tail cross section," Journal of the Aeronautical Sciences, Reader's Forum, Vol. 21, No. 1, pp 59, January 1954.

53. Bryson, A. E.,Jr., "Evaluation of the Inertia Coefficients of the Cross Section of a Slender Body," Readers Forum, Journal of Aeronautical Sciences, Vol. 21, No. 6, pp 424-427, June 1954.

54. Van Spiegel, E., "Boundary value problems in lifting surface theory," Technical Rept. W1, National Luchtvaartlaboratorium, Amsterdam, March 1958.

55. Benthem, J. P. and Wouters, J. G., "The calculation of aerodynamic forces on the circular wing in unsteady incompressible flow," Nationaal Lucht-En Ruimtevaartlaboratorium,NLR-TN-W25, 1963.

56. Summa, M. J., "Potential Flow About Three Dimensional Streamlined Lifting Configurations, with Applications to Wings and Rotors," AIAA, 13th Aerospace Sciences Meeting, Pasadena, Calif., Jan., 1975.

57. Wolvovich, W. A., "The determination of state space representations of linear multivariable systems," Automatica, Vol. 9, No. 1, 1973.

58. Silverman, L., "Realizations of linear dynamical systems," IEEE Transactions on Automatic Control, Vol. AC-16, No. 6, 1971.

59. Gopinath, B., "On the control of linear multiple input-output systems," The Bell System Technical Journal, Vol. 50, No. 3, March 1971, pp 1063-1081.

60. Lyons, M. G., et al., "Control Law Synthesis and Sensor Design for Active Flutter Suppression," AIAA paper No. 73-832, 1973.

61. Hall, W. E., Jr. and Bryson, A. E.,Jr., "Synthesis of Hover Autopolits for Rotary-Wing VTOL Aircraft," (Stanford University; NASA Grant NAS2-5143.) NASA CR-132053, 1973.

62. Segenriech, S., "Weight Optimization under Flutter Constraint," Doctoral Dissertation, Dept. of Aeronautics and Astronautics, Stanford University, Jan. 1975.

63. Drischler, J., "An Integral Equation Relating the General Time-Dependent Lift and Downwash Distributions on Finite Wings in Subsonic Flow," NASA, TN D-1521, 1963.

64. Watkins, C. E., et al., "On the Kernel function of the Integral Equations relating the Lift and Downwash distribution of Oscillating Finite Wings in Subsonic Flow," NACA TN 3131, January 1954.

65. Landahl, M. T., "Kernel Function for Nonplanar Oscillating Surfaces in Subsonic Flow," AIAA Journal, Vol. 5, No. 5, May 1967, pp 1045-1046.

66. Mangler, K. W.,"Improper Integrals in Theoretical Aerodynamics," RAE Report Aero 2424, ARC 14394, June, 1951.

67. Milne, R. D., "Asymptotic Solution of Linear Stationary Integro-differential Equations," British ARC, R.& M. Rept. No. 3548, July 1966.

68. Runyan, H. L. and Watkins, C. E., "A systematic Kernel function procedure for determining aerodynamic forces on oscillating or steady finite wings at subsonic speeds," NASA Tech. Rept. No. R-48, pp 8.

69. Müller, A., "Berechrung Der Druckverteilung an Schwingenden Tragflügeln in überschallströmung mittels eines kollokations-verfahrens für die Küssnersche Integralgleichung," Doktor-Ingenieurs Dissertation, Der Technischen Universität München, July, 1973.

70. Fettis, H. E., "An approximate method for the calculation of non-stationary airforces at subsonic speeds," WADC Technical Rept. No. 52-56, Wright Air Development Center, 1952.

71. Osborne, C., "Unsteady Thin-Airfoil Theory for Subsonic Flow," AIAA Journal, Vol. 11, No. 2, Feb. 1973, pp 205-209.

72. Kemp, N. H., "Lift and Moment for Arbitrary Power-Law Upwash in Oscillating Subsonic Unsteady Thin-Airfoil Theory," AIAA Journal, Vol. 12, No. 3, March 1974, pp 413-415.

73. Hsu, P. T., "Some Recent Developments in the Flutter Analysis of Low-Aspect-Ratio Wings," Proceedings of the National Specialists Meeting on Dynamics and Aeroelasticity at Fort Worth, Texas, Nov. 6-7, 1958, pp 7-26.

74. Miles, J. W., "On Solving Subsonic Unsteady Flow Lifting Surface Problems by Separating Variables," Jour. Aero. Sci., Vol. 21, No. 6, June,1954, pp 427-428.

75. Zartarian, G. and Hsu, P. T., "Theoretical Studies on the Prediction of Unsteady Supersonic Airloads on Elastic Wings," WADC Technical Report 56-97, Dec. 1955.

76. Moore, M. and Andrew, L., "Unsteady Aerodynamics for Advanced Configuration, Part IV, Application of the Supersonic Mach Box Method to Intersecting Planar Surfaces," FDL-TDR-64-152, May 1965.

77. Rodden, W. P., Giesing, J. P. and Kalman, T. P., "New Development and Applications of the Subsonic Doublet-Lattice Method for Nonplanar Configurations," Symposium in Unsteady Aerodynamics for Aeroelastic Analysis of Interfering Surface, AGARD Conference Proceedings No. 80-71, Part II, 1971.

78. Baker, G. A.,Jr., "Essentials of Padé Approximants," Academic Press, New York, 1974.

79. Chisholm, J. S. R., "Padé Approximants and Linear Integral Equations," The Padé Approximant in Theoritical Physics, Edited by Baker, G. A. Jr. and Gammel, J. V., 1st Ed., Academic Press, New York, 1970.

80. Riesz, F. and B. St.-Nagy, "Functional Analysis," Ungar Publishing Co., New York, 1955.

TABLE 1

Coefficients of Rational Function Approximations to Non-dimensional Aerodynamic Load Coefficients for a Two-dimensional Airfoil, M = 0.3

$$q_{ij} = \frac{a_0 s^5 + a_1 s^4 + a_2 s^3 + a_3 s^2 + a_4 s + a_5}{b_1 s^4 + b_2 s^3 + b_3 s^2 + b_4 s + b_5}$$

	n =	0	1	2	3	4	5
q_{11}*	a_n	-13.3333	-8.2878	-1.0658	0.0		
	b_n		1.0	1.8934	0.1652		
q_{12}	a_n	0.0	5.1195	0.4359	0.002294		
	b_n		1.0	0.06875	0.0003483		
q_{13}	a_n	-0.8333	-0.2602	-0.4845	-0.007393		
	b_n		1.0	0.1315	0.001843		
q_{21}	a_n	0.0	-3.2091	-0.2865	0.0		
	b_n		1.0	1.3876	0.08859		
q_{22}	a_n	-4.4444	-2.7331	5.9498	1.6230	0.06558	0.0003981
	b_n		1.0	3.2552	0.5873	0.02078	0.0001209
q_{23}	a_n	0.6944	0.1763	-0.05832	-0.001091		
	b_n		1.000	0.1243	0.001694		
q_{31}	a_n	-0.8333	-0.2893	-0.03348	0.0		
	b_n		1.0	5.0413	0.4632		
q_{32}	a_n	0.6944	0.1816	0.05998	0.001501		
	b_n		1.0	0.8534	0.02033		
q_{33}	a_n	-0.2778	-0.1496	-0.05678	-0.001284		
	b_n		1.0	0.4687	0.01039		

* 1 refers to plunging, 2 to pitching about midchord, and 3 to the flap mode.

TABLE 2.

Coefficients of Rational Function Approximations to Non-dimensional Aerodynamic Load Coefficients for a Two-dimensional Airfoil, M = 0.4

$$q_{ij} = \frac{a_0 s^5 + a_1 s^4 + a_2 s^3 + a_3 s^2 + a_4 s + a_5}{b_1 s^4 + b_2 s^3 + b_3 s^2 + b_4 s + b_5}$$

	n=	0	1	2	3	4	5
q_{11}	a_n	-10.0	-4.2809	-0.5572	0.0		
	b_n		1.0	0.9880	0.08310		
q_{12}	a_n	0.0	5.1427	0.4830	0.003379		
	b_n		1.0	0.07400	0.0004929		
q_{13}	a_n	-0.6250	-2.5884	-0.4890	-0.007481		
	b_n		1.0	0.1286	0.001792		
q_{21}	a_n	0.0	-2.4349	-0.2007	0.0		
	b_n		1.0	1.0187	0.05968		
q_{22}	a_n	-3.3333	2.2341	0.2630	0.002297		
	b_n		1.0	0.08196	0.0006703		
q_{23}	a_n	+0.5208	0.2902	-0.06122	-0.001284		
	b_n		1.0	0.1325	0.001916		
q_{31}	a_n	-0.6250	-0.2129	-0.02345	0.0		
	b_n		1.0	3.6174	0.3122		
q_{32}	a_n	0.5208	0.1361	0.03746	0.0008860		
	b_n		1.0	0.5157	0.01153		
q_{33}	a_n	-0.2083	-0.1392	-0.03399	-0.0006823		
	b_n		1.0	0.2700	0.005306		

TABLE 3.

Coefficients of Rational Function Approximations to Non-dimensional Aerodynamic Load Coefficients for a Two-dimensional Airfoil, M = 0.5

$$q_{ij} = \frac{a_0 s^5 + a_1 s^4 + a_2 s^3 + a_3 s^2 + a_4 s + a_5}{b_1 s^4 + b_2 s^3 + b_3 s^2 + b_4 s + b_5}$$

	n=	0	1	2	3	4	5
q_{11}	a_n	-8.0	1.9012	-0.2370	0.0		
	b_n		1.0	0.4188	0.03350		
q_{12}	a_n	0.0	5.1602	0.5418	0.004743		
	b_n		1.0	0.07965	0.0006537		
q_{13}	a_n	-0.5	-2.5522	-0.5019	-0.007814		
	b_n		1.0	0.1264	0.001769		
q_{21}	a_n	0.0	-1.8000	-0.1324	0.0		
	b_n		1.0	0.7177	0.03728		
q_{22}	a_n	-2.6667	2.0138	0.3523	0.004771		
	b_n		1.0	0.1075	0.001315		
q_{23}	a_n	0.4167	0.4154	-0.06066	-0.001380		
	b_n		1.0	0.1324	0.001945		
q_{31}	a_n	-0.5	-0.1565	-0.01673	0.0		
	b_n		1.0	2.5786	0.2109		
q_{32}	a_n	0.4167	0.1098	0.02341	0.0005031		
	b_n		1.0	0.3072	0.006189		
q_{33}	a_n	-0.1667	-0.1373	-0.02097	-0.0003418		
	b_n		1.0	0.1576	0.002512		

TABLE 4.

Coefficients of Rational Function Approximations to Non-dimensional Aerodynamic Load Coefficients for a Two-dimensional Airfoil, M = 0.6

$$q_{ij} = \frac{a_0 s^5 + a_1 s^4 + a_2 s^3 + a_3 s^2 + a_4 s + a_5}{b_1 s^4 + b_2 s^3 + b_3 s^2 + b_4 s + b_5}$$

	n=	0	1	2	3	4	5
q_{11}	a_n	-6.6667	-0.3912	-0.03194	0.0		
	b_n		1.0	0.06952	0.004192		
q_{12}	a_n	0.0	5.1775	0.6040	0.006246		
	b_n		1.0	0.08373	0.0007953		
q_{13}	a_n	-0.4167	-2.4886	-0.5178	-0.008246		
	b_n		1.0	0.1230	0.001724		
q_{21}	a_n	0.0	-1.4269	-0.09561	0.0		
	b_n		1.0	0.5401	0.02494		
q_{22}	a_n	-2.2222	1.7875	0.4201	0.006742		
	b_n		1.0	0.1225	0.001717		
q_{23}	a_n	0.3472	0.5631	-0.05650	-0.001371		
	b_n		1.0	0.1242	0.001786		
q_{31}	a_n	-0.4167	-0.1191	-0.01195	0.0		
	b_n		1.0	1.8696	0.1397		
q_{32}	a_n	0.3472	0.09421	0.01391	0.0002472		
	b_n		1.0	0.1700	0.002809		
q_{33}	a_n	-0.1389	-0.1416	-0.01319	-0.0001351		
	b_n		1.0	0.09149	0.0009170		

TABLE 5.

Coefficients of Rational Function Approximations to Non-dimensional Aerodynamic Load Coefficients for a Two-dimensional Airfoil, M = 0.7

$$q_{ij} = \frac{a_0 s^5 + a_1 s^4 + a_2 s^3 + a_3 s^2 + a_4 s + a_5}{b_1 s^4 + b_2 s^3 + b_3 s^2 + b_4 s + b_5}$$

	n=	0	1	2	3	4	5
q_{11}	a_n	-5.7143	-6.2792	-1.8266	-0.1182	-0.001456	0.0
	b_n		1.0	1.4214	0.2952	0.01515	0.0001671
q_{12}	a_n	0.0	5.1783	0.6671	0.007819		
	b_n		1.0	0.08515	0.0008887		
q_{13}	a_n	-0.3571	-2.3670	-0.5349	-0.008739		
	b_n		1.0	0.1174	0.001631		
q_{21}	a_n	0.0	-1.1951	-0.07606	0.0		
	b_n		1.0	0.4297	0.01780		
q_{22}	a_n	-1.9048	1.5229	0.4675	0.008228		
	b_n		1.0	0.1271	0.001870		
q_{23}	a_n	0.2976	0.7544	-0.04855	-0.001240		
	b_n		1.0	0.1077	0.001442		
q_{31}	a_n	-0.3571	-0.09268	-0.008365	0.0		
	b_n		1.0	1.3504	0.08779		
q_{32}	a_n	0.2976	0.08782	0.007694	0.00008373		
	b_n		1.0	0.08386	0.0008493		
q_{33}	a_n	-0.1190	-0.2074	-0.08238			
	b_n		1.0	0.4992			

TABLE 6.

Coefficients of Rational Function Approximations to Non-dimensional Aerodynamic Load Coefficients for a Two-dimensional Airfoil, M = 1.5

$$q_{ij} = \frac{a_0 s^5 + a_1 s^4 + a_2 s^3 + a_3 s^2 + a_4 s + a_5}{b_1 s^4 + b_2 s^3 + b_3 s^2 + b_4 s + b_5}$$

	n=	0	1	2	3	4	5
q_{11}	a_n	-2.6667	-2.3055	1.2222	0.0		
	b_n		1.0	0.9173	0.3416		
q_{12}	a_n	0.0	2.8534	2.5706	1.2507		
	b_n		1.0	0.9981	0.3496		
q_{13}	a_n	-0.1667	-1.1533	-2.8005	-2.2150		
	b_n		1.0	3.0072	2.4765		
q_{21}	a_n	0.0	-0.2075	-0.00003146	0.0		
	b_n		1.0	0.5392	0.2188		
q_{22}	a_n	-0.8889	-0.8296	-0.06073	0.0		
	b_n		1.0	0.7373	0.2545		
q_{23}	a_n	0.1389	0.8734	1.9139	1.4918		
	b_n		1.0	2.7295	2.2238		
q_{31}	a_n	-0.1667	-0.06846	-0.03584	0.0		
	b_n		1.0	0.5401	0.1603		
q_{32}	a_n	0.1389	0.2915	0.1301	0.04485		
	b_n		1.0	0.7090	0.2006		
q_{33}	a_n	-0.05556	-0.2632	-0.4221	-0.1319		
	b_n		1.0	1.8483	0.5898		

TABLE 7.

Coefficients of Rational Function Approximations to Non-dimensional Aerodynamic Load Coefficients for a Two-dimensional Airfoil, M = 1.75

$$q_{ij} = \frac{a_0 s^5 + a_1 s^4 + a_2 s^3 + a_3 s^2 + a_4 s + a_5}{b_1 s^4 + b_2 s^3 + b_3 s^2 + b_4 s + b_5}$$

	n=	0	1	2	3	4	5
q_{11}	a_n	-2.2857	-2.1596	-1.1955	0.0		
	b_n		1.0	0.9832	0.4292		
q_{12}	a_n	0.0	2.3790	2.4545	1.2164		
	b_n		1.0	1.0930	0.4367		
q_{13}	a_n	-0.1429	-1.0139	-2.3900	-1.1392		
	b_n		1.0	3.2217	1.6360		
q_{21}	a_n	0.0	-0.1240	-0.00002064	0.0		
	b_n		1.0	0.5477	0.2773		
q_{22}	a_n	-0.7619	-0.6749	-0.1472	0.0		
	b_n		1.0	0.7679	0.3077		
q_{23}	a_n	0.1190	0.7020	1.2492	0.08993		
	b_n		1.0	2.3673	1.7221		
q_{31}	a_n	-0.1429	-0.07017	-0.03661	0.0		
	b_n		1.0	0.5891	0.2103		
q_{32}	a_n	0.1190	0.2495	0.1332	0.04389		
	b_n		1.0	0.7794	0.2521		
q_{33}	a_n	-0.04762	-0.2382	-0.3647	-0.1020		
	b_n		1.0	1.9944	0.5862		

TABLE 8.

Coefficients of Rational Function Approximations to Non-dimensional Aerodynamic Load Coefficients for a Two-dimensional Airfoil, M = 2.0

$$q_{ij} = \frac{a_0 s^5 + a_1 s^4 + a_2 s^3 + a_3 s^2 + a_4 s + a_5}{b_1 s^4 + b_2 s^3 + b_3 s^2 + b_4 s + b_5}$$

	n=	0	1	2	3	4	5
q_{11}	a_n	-2.0000	-2.0140	-1.1581	0.0		
	b_n		1.0	1.0390	0.5015		
q_{12}	a_n	0.0	2.0567	2.2596	1.1321		
	b_n		1.0	1.1418	0.4902		
q_{13}	a_n	-0.1250	-0.8956	-1.9206	0.1262		
	b_n		1.0	3.2902	0.2186		
q_{21}	a_n	0.0	-0.08493	-0.00001539	0.0		
	b_n		1.0	0.5760	0.3329		
q_{22}	a_n	-0.6667	-0.5933	-0.1827	0.0		
	b_n		1.0	0.8010	0.3560		
q_{23}	a_n	0.1042	0.6357	1.09470	0.003237		
	b_n		1.0	2.5267	0.007476		
q_{31}	a_n	-0.1250	-0.07283	-0.04096	0.0		
	b_n		1.0	0.6773	0.2838		
q_{32}	a_n	0.1042	0.2272	0.1361	0.04675		
	b_n		1.0	0.8710	0.3239		
q_{33}	a_n	-0.04167	-0.2024	-0.2618	-0.005740		
	b_n		1.0	1.8052	0.03977		

TABLE 9.

Rational Function Approximations of Generalized Aerodynamic Loads in Plunging (1), Pitching (2), Chordwise Bending $(x/r)^2$, (3) and, Spanwise Bending $(y/r)^2$ (4) for a Circular Wing in Incompressible Flow

$$q_{ij} = a_0 s^2 + a_1 s + a_2 + \frac{a_3 s}{s + \beta}$$

i	j	a_0	a_1	a_2	a_3	β
1	1	1.6316	1.7000	0.0	0.01853	0.2049
1	2	0.1617	2.4548	1.7902	0.002942	0.05175
2	1	0.03449	-0.8871	0.0	-0.009152	0.2009
2	2	0.1429	0.5283	-0.9326	0.001345	0.04781
1	3	0.5277	0.5820	1.8658	-0.003505	0.05232
1	4	0.3230	0.4199	0.0	0.005303	0.2340
2	3	-0.09445	0.5675	0.8778	0.001710	0.05202
2	4	0.009023	-0.01816	0.0	-0.002205	0.2071

TABLE 10.

Indicial Lift in Plunging for Circular and Elliptic Wings

$$K(t) = 2\pi(a \quad \delta(\tau) + a_2 H(\tau) - a_3 e^{-\beta \tau})$$

wing and method	a_1	a_2	a_3	β
Circular wing AR = $4/\pi$ using least squares for Padé approximants.	0.25945	0.28495	0.01440	0.20488
Elliptic wings: from exact asymptotes AR = 3.0	0.4545	0.5174	0.06290	0.1769
AR = 4.0	0.4707	0.5976	0.1269	0.2408
5.0	0.4797	0.6538	0.1741	0.2484
6.0	0.4849	0.6933	0.2085	0.2415
Using least squares for Padé approximants AR = 6.0	0.29298	0.6937	0.2012	0.2878
R.T.Jones AR = 3.0	0.4545	0.6	0.1698	0.54
AR = 6.0	0.4849	0.74	0.26519	0.381

TABLE 11.

Indicial Lift in Plunging

$$K(t) = 2\pi(a_1 \delta(\tau) + a_2 H(\tau) - a_3 e^{-\beta_1 \tau} + a_4 e^{-\beta_2 \tau})$$

	a_1	a_2	a_3	a_4	β_1	β_2
Rectangular Wings AR = 6.0, M = 0.0	0.3291	0.6354	0.2084	0.0001132	0.2840	0.001185
", M=0,(W.P.Jones)	0.448	0.685	0.2375	0.0	0.28	0.0
AR = 4.0, M = 0.	0.3341	0.5731	0.1069	0.0	0.2254	0.0
", M=0,(W.P.Jones)	0.430	0.596	0.166	0.0	0.3	0.0
AR = 6, M = 0.3	0.0	0.6802	0.1564	1.5982	0.1782	4.4301
" M = 0.5	0.0	0.7279	0.1754	0.7208	0.1697	2.2567
" M = 0.7	0.0	0.8246	0.2221	0.3070	0.1568	1.5834
Taper Wing, AR = 5.84, M = 0.	0.2721	0.6777	0.1962	0.0	0.2975	0.0
Swept Wing AR = 6 $\Lambda = 45^\circ$, M = 0.7	0.0	0.6031	0.2471	0.5540	0.2167	1.1159

TABLE 12.

Other Indicial Functions in Incompressible Flow

$$K(t) = 2\pi(a \quad \delta(\tau) + a_2 H(\tau) - a_3 e^{-\beta_1 \tau})$$

wing	a_1	a_2	a_3	β_1
circular wing: moment in plunging	-0.005490	0.1484	0.007249	0.2009 0.2009
Lift due to spanwise bending $z = y/r)^2$	0.05141	0.07044	0.003606	0.2340
pitching moment due to spanwise bending z) $(y/r)^2$	-0.001436	0.03059	0.001694	0.2071
rectangular wing: AR = 6, rolling moment due to impulsive rolling	0.1076	0.1391	0.01881	0.4270
swept wing, $\Lambda = 45^\circ$ AR = 6, no taper, rolling moment due to impulsive rolling	0.09421	0.1226	0.02138	0.4587

TABLE 13.

Indicial Functions for Generalized Forces for Impulsive Plunging (1) and Pitching (2) Displacements M = 0.7, AR = 6, Rectangular Planform, ref. length = semi-span

$$q_{ij} = a_1\delta(\tau) + a_2 H(\tau) + a_3 e^{-\beta_1 \tau} + a_4 e^{-\beta_2 \tau}$$

q_{ij}	a_1	a_2	a_3	a_4	β_1	β_2
q_{11}	-5.7143	0.0	-1.3131	18.3261	0.9409	9.5001
q_{12}	0.0	5.18084	-0.4940	0.0	0.5889	0.0
q_{21}	0.0	0.0	-0.04953	-1.4965	0.7069	3.7799
q_{22}	-0.05291	0.4660	-0.0007264	-0.2231	0.1312	1.3761

TABLE 14.

Coefficients of Polynomial Approximations to Mode Shapes in an Axis System Along the Free Stream (x) and Normal to it (y). (Origin at 40% Root Chord from the Leading Edge)

$$\frac{Z_R}{b} = \sum_{i=1}^{5} \sum_{j=1}^{5} A(i,j)\, x^{i-1}\, y^{j-1}$$

MODE	i	A(i,1)	A(i,2)	A(i,3)	A(i,4)	A(i,5)
1	1	-0.0008822	0.001222	0.001382	-0.0001261	0.000004556
	2	0.001281	0.003943	-0.0003256	0.000009111	0.0
	3	0.002561	-0.0002730	0.0	0.0	0.0
	4	-0.0007351	-0.000009111	0.0	0.0	0.0
	5	-0.000004556	0.0	0.0	0.0	0.0
2	1	-0.02338	0.03938	0.07274	-0.004923	0.00001540
	2	0.03795	-0.006656	-0.004997	0.00003079	0.0
	3	-0.07940	0.004774	0.0	0.0	0.0
	4	0.004848	-0.00003079	0.0	0.0	0.0
	5	-0.00001540	0.0	0.0		0.0

TABLE 15.

Quasi-steady Generalized Loads $q_{ij} = q_{ij}^{0} + ik\, q_{ij}^{1}$ by the Doublet Lattice Method

		NCB = 6, NSB = 5		NCB = 9, NSB = 5		NCB = 6, NSB = 10	
i	j	$q_{ij}^{0} \cdot 10^{+3}$	$q_{ij}^{1} \cdot 10^{3}$	$q_{ij}^{0} \cdot 10^{3}$	$q_{ij}^{1} \cdot 10^{3}$	$q_{ij}^{0} \cdot 10^{3}$	$q_{ij}^{1} \cdot 10^{3}$
1	1	-1.6338	-5.1787	-1.6338	-5.1832	-1.5354	-4.9210
1	2	28.275	9.2391	28.281	9.3084	26.554	10.904
1	3	-39.325	-5.1146	-39.793	-0.6528	-38.198	-3.8863
2	1	-5.5670	-7.1503	-5.5598	-6.9906	-5.3875	-6.9194
2	2	87.560	-141.37	87.354	-144.15	84.447	-132.15
2	3	-17.030	132.09	-20.116	138.13	-13.897	122.83
3	1	-0.5205	-3.1743	-0.5293	-3.2774	-0.4902	-3.1385
3	2	10.042	32.424	10.231	33.852	9.5354	33.163
3	3	-52.841	-72.116	-50.432	-77.856	-49.975	-70.520

TABLE 16.

Generalized Piston Theory Loads Using Lattice Integration Scheme at M = 0.6

i	j	$10^3 \cdot Mq_{ij}$			
		EXACT.	NCB=6, NSB=5	NCB=9, NSB=5	NCB=6, NSB=10
1	1	-9.49315	-9.3466	-9.3543	-9.4463
1	2	3.6133	6.9296	5.8367	7.0302
1	3	-10.6014	-12.739	-12.058	-12.745
2	1	3.61336	-0.38735	0.95867	-0.3167
2	2	-75.0865	-71.194	-73.223	-71.362
2	3	35.3091	35.517	36.032	35.519
3	1	-10.6014	-8.1457	-8.9968	-8.1479
3	2	35.3091	29.901	32.298	29.881
3	3	-79.4860	-70.789	-75.619	-70.790

TABLE 17.

Rational Function Approximations to Generalized Loads on a Swept Wing, AR = 4.1 ,
With a Control Surface in First Bending (1) First Torsion (2),
and Control Surface Modes (3)

$$q_{ij} = a_0 s + a_1 + \frac{a_2 s}{s + \beta}$$

i	j	a_0	a_1	a_2	β_1
1	1	-0.01575	-0.001535	0.007290	0.6736
1	2	0.01172	0.02655	-0.00000194	0.002384
1	3	-0.02124	-0.03820	0.001446	0.08299
2	1	-0.0005278	-0.005388	-	-
2	2	-0.1189	0.08445	-0.0001357	0.01203
2	3	0.05920	-0.01390	0.005107	0.08026
3	1	-0.01358	-0.0004902	0.01738	1.6643
3	2	0.04980	0.009535	-0.002858	0.1718
3	3	-0.1180	-0.04998	0.03816	0.8039

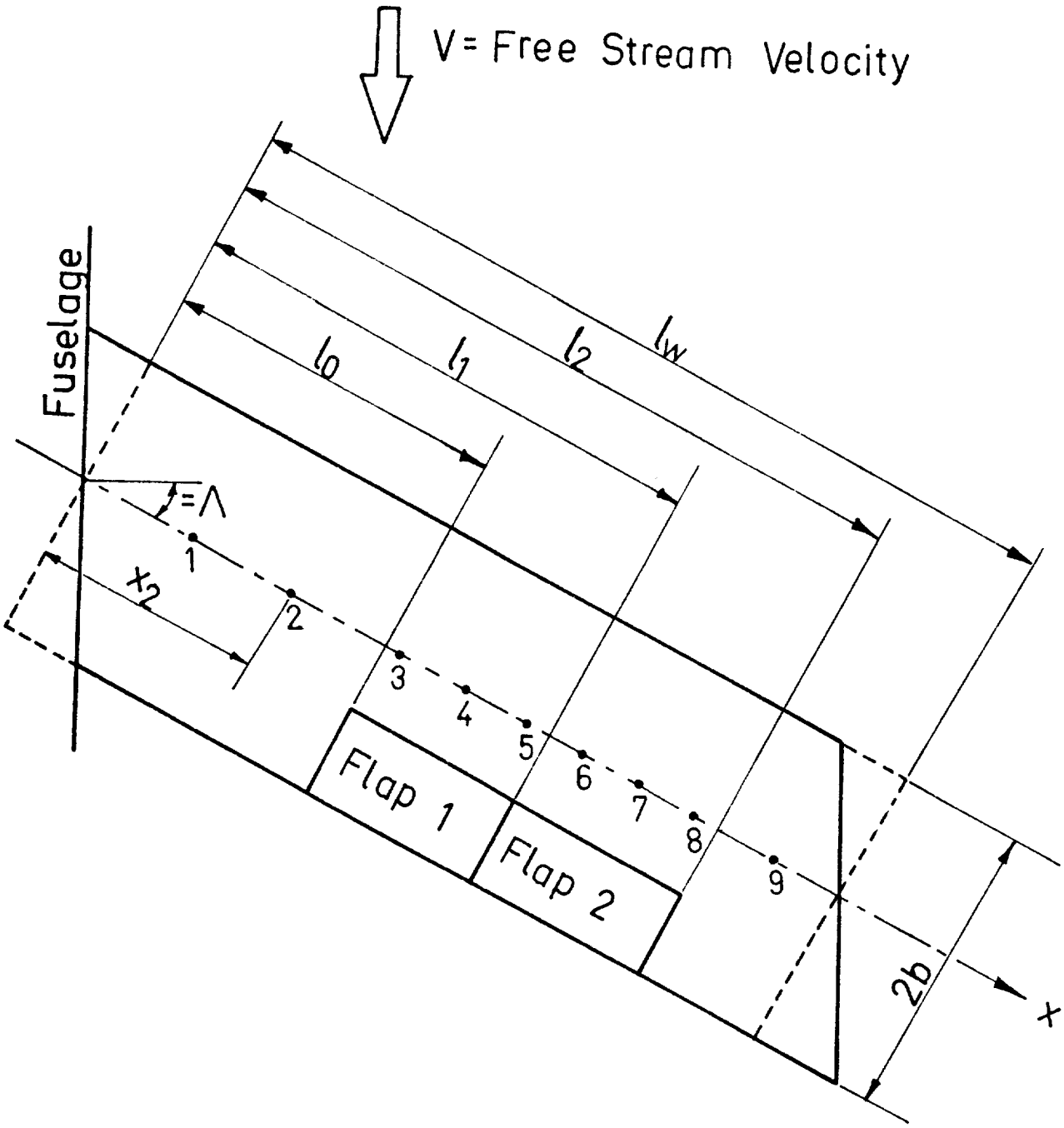

Fig. 1. Swept wing with two flaps and nine node points.

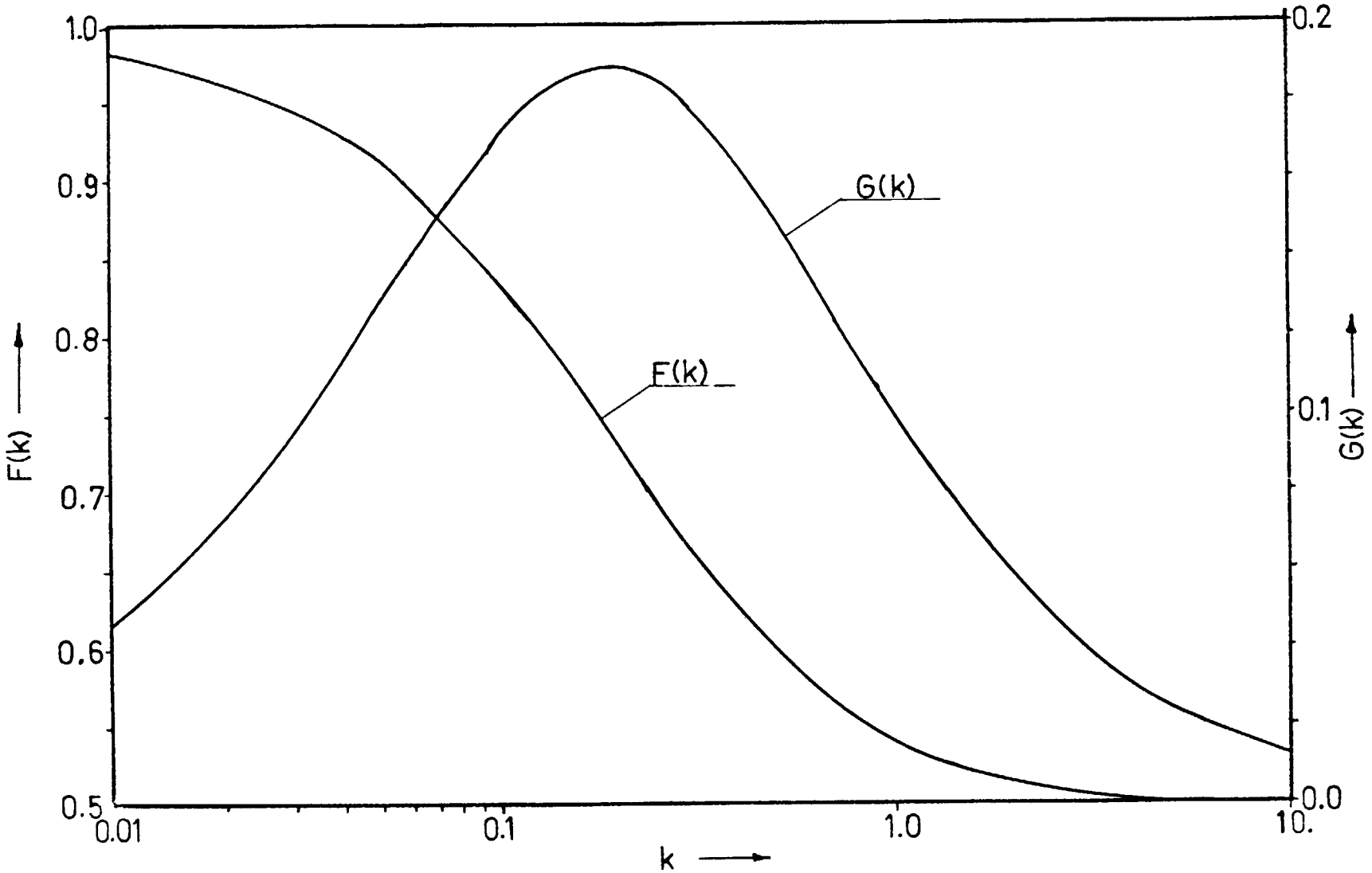

Fig. 2. Theodorsen's function $C(k) = F(k) - iG(k)$.

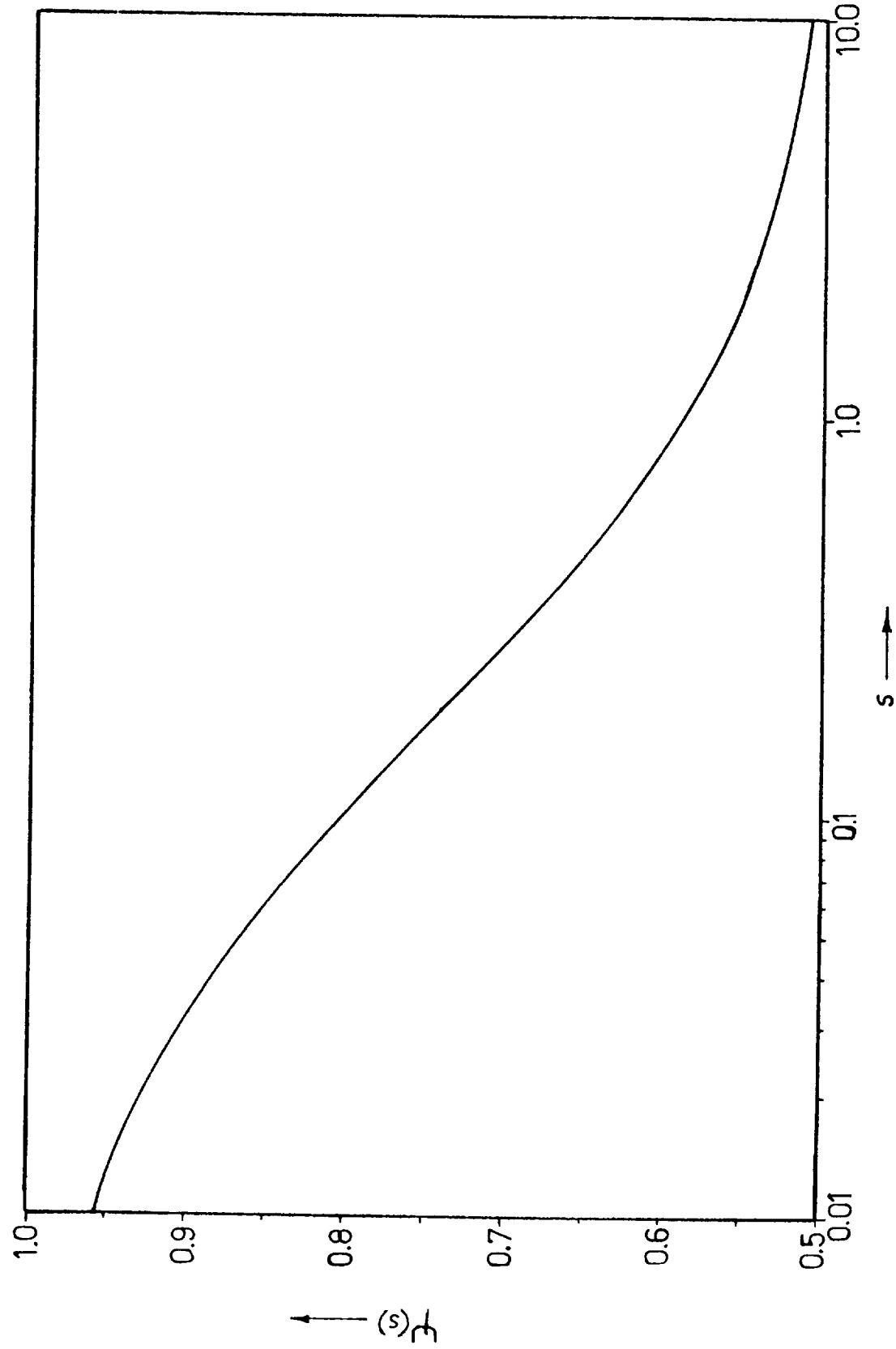

Fig. 3. $\psi(s)$ for real values of s.

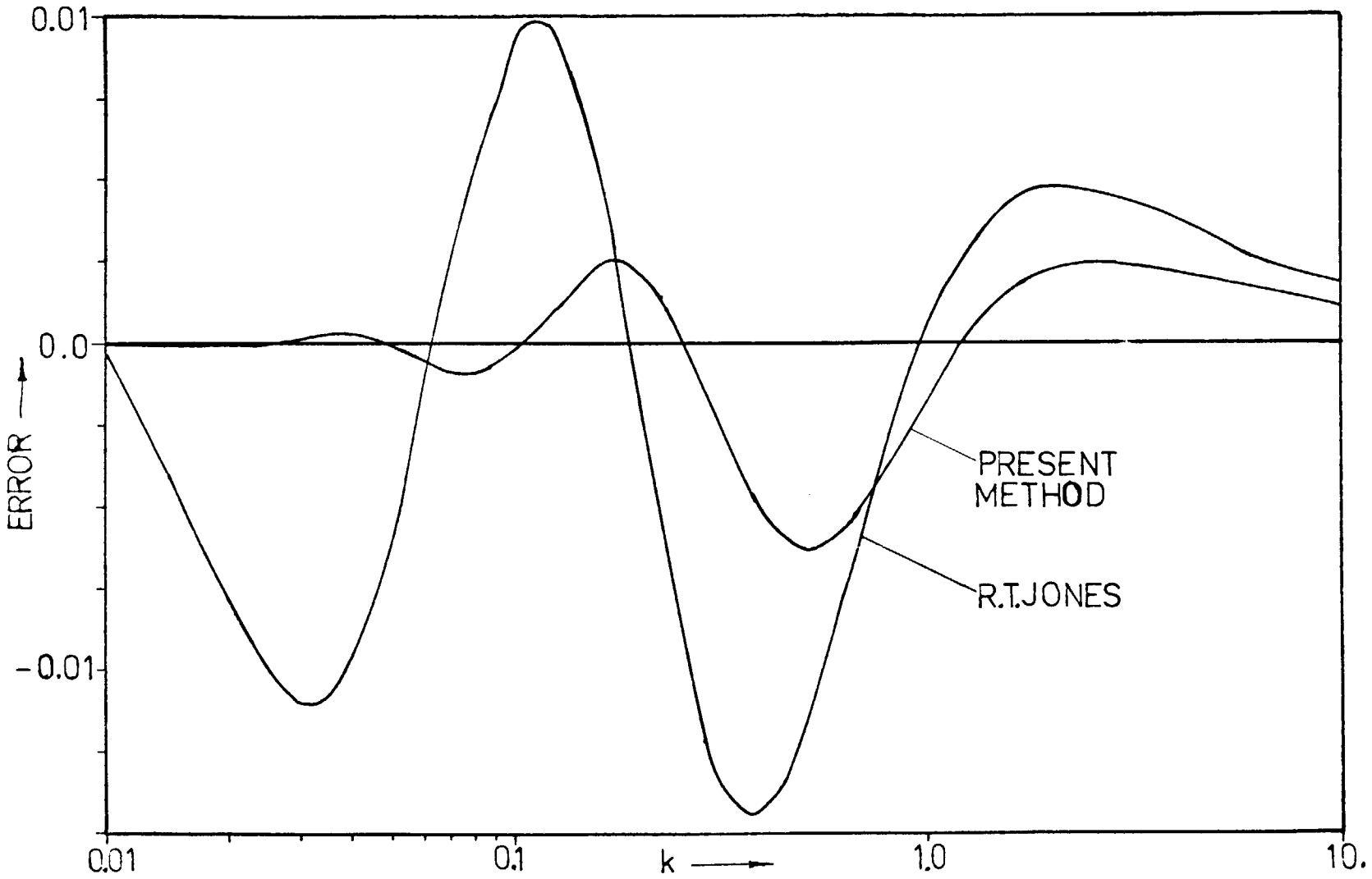

Fig. 4. Error in F(k) (True - Approximate).

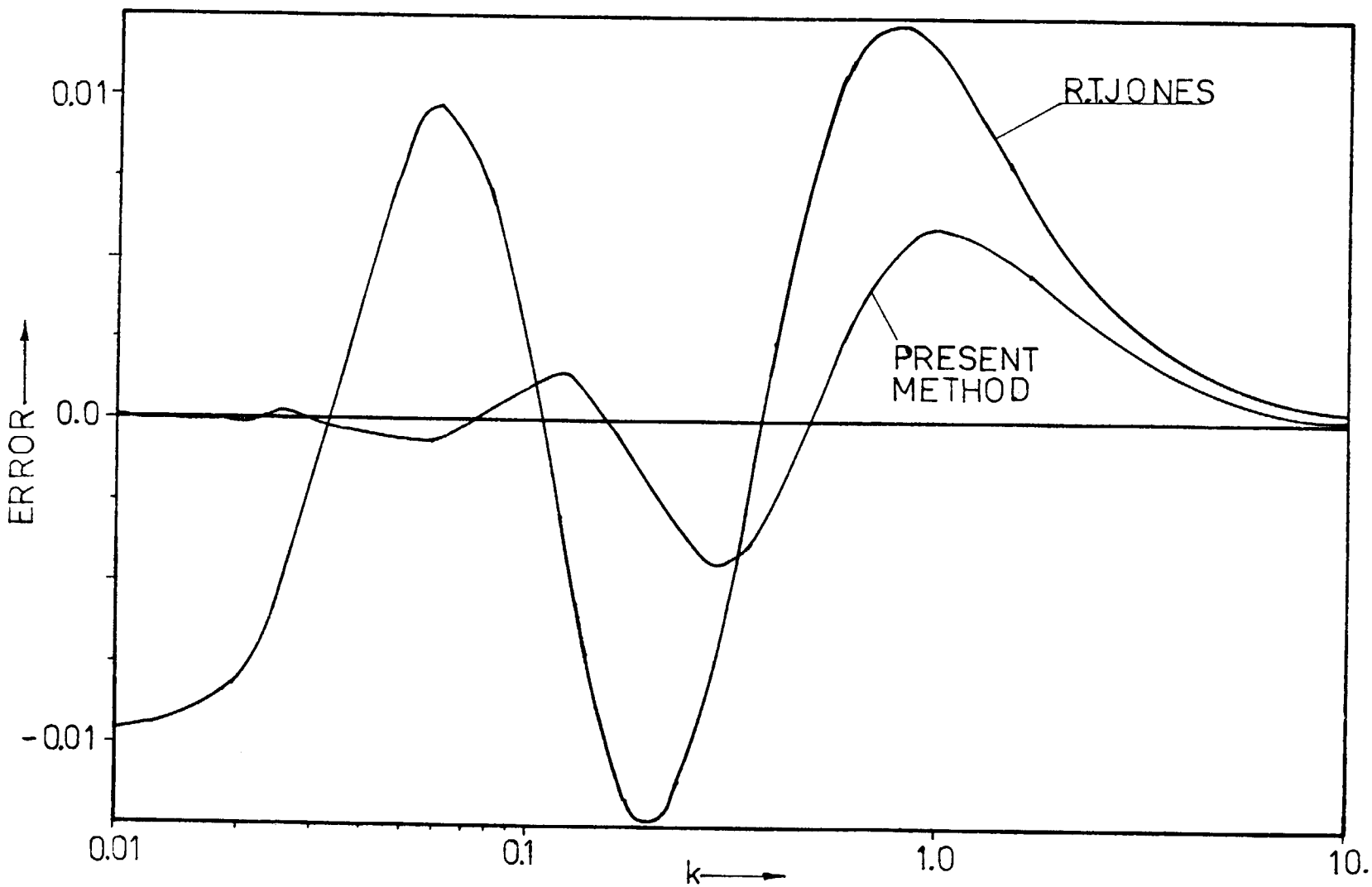

Fig. 5. Error in G(k) (True - Approximate).

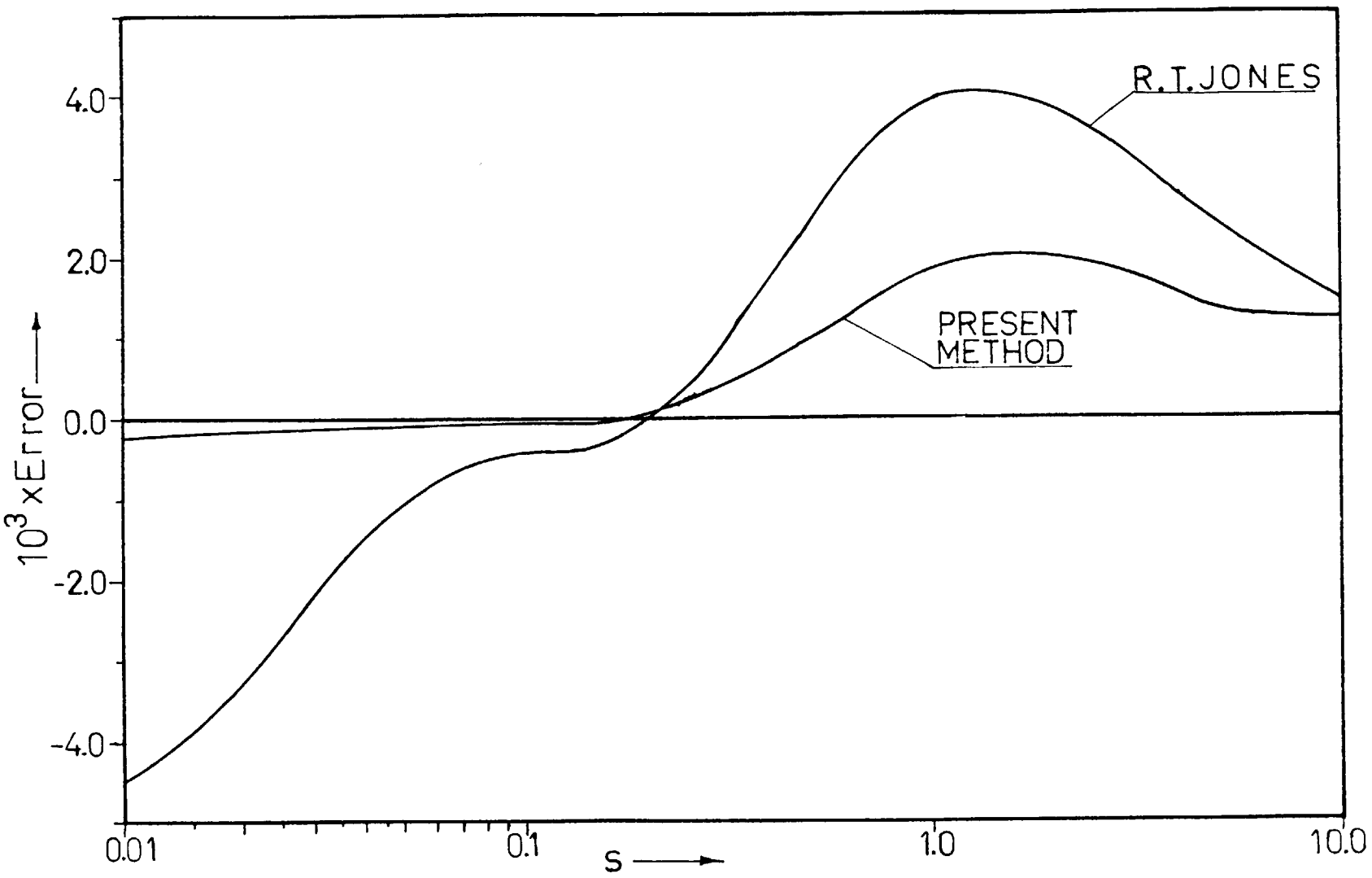

Fig. 6. Error in $\psi(s)$.

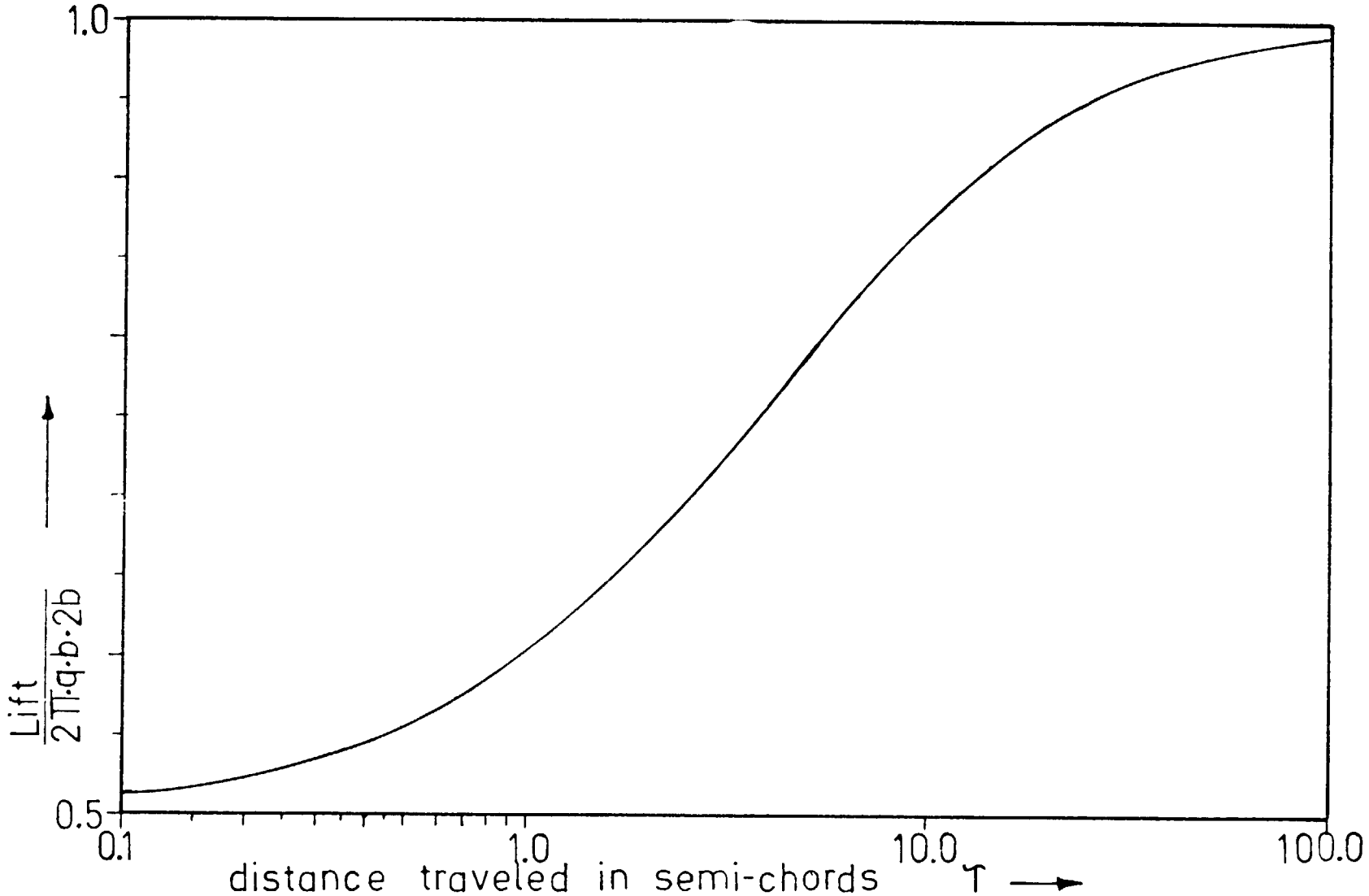

Fig. 7. Wagner's function K(t) (obtained approximately by Küssner).

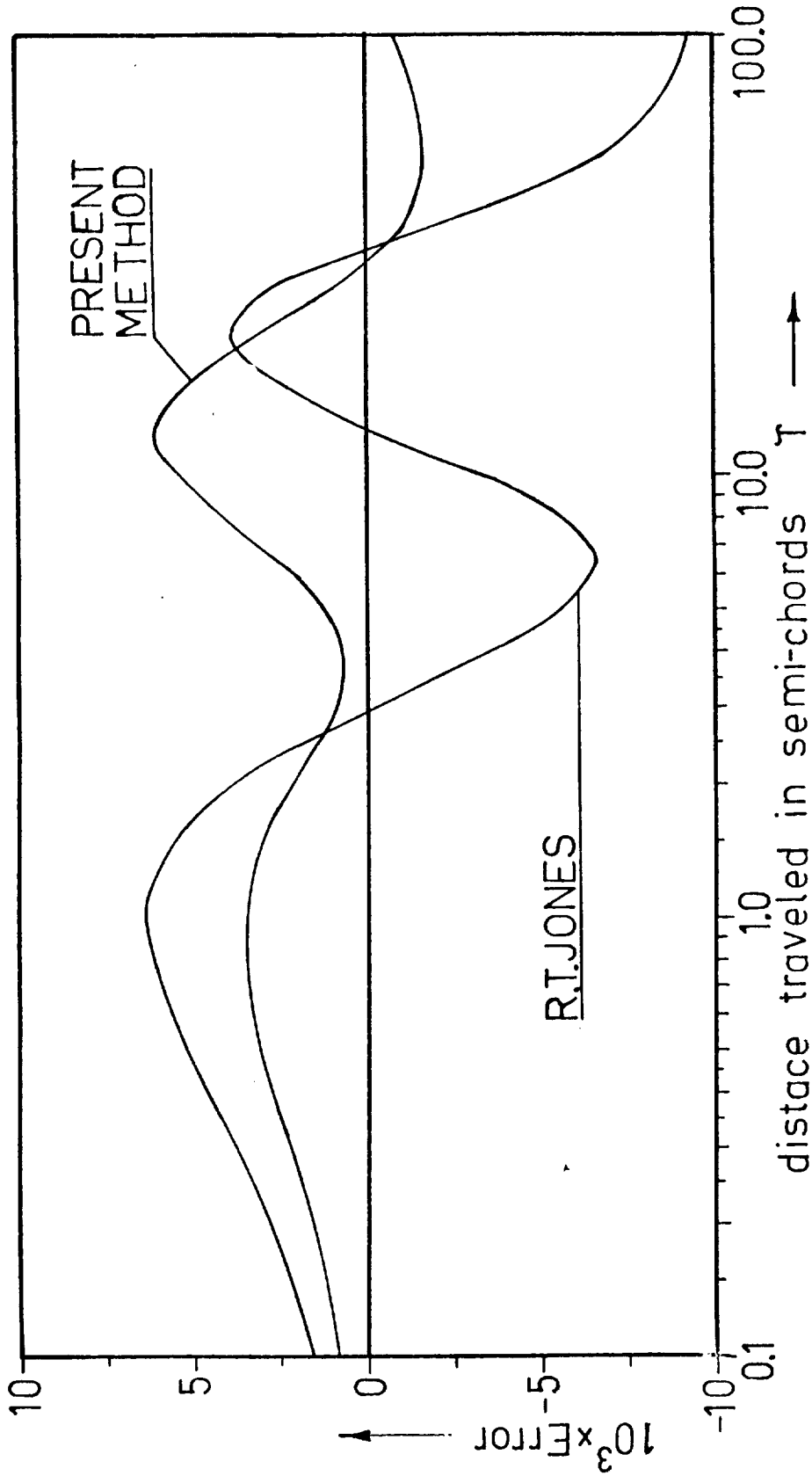

Fig. 8. Error in K(t).

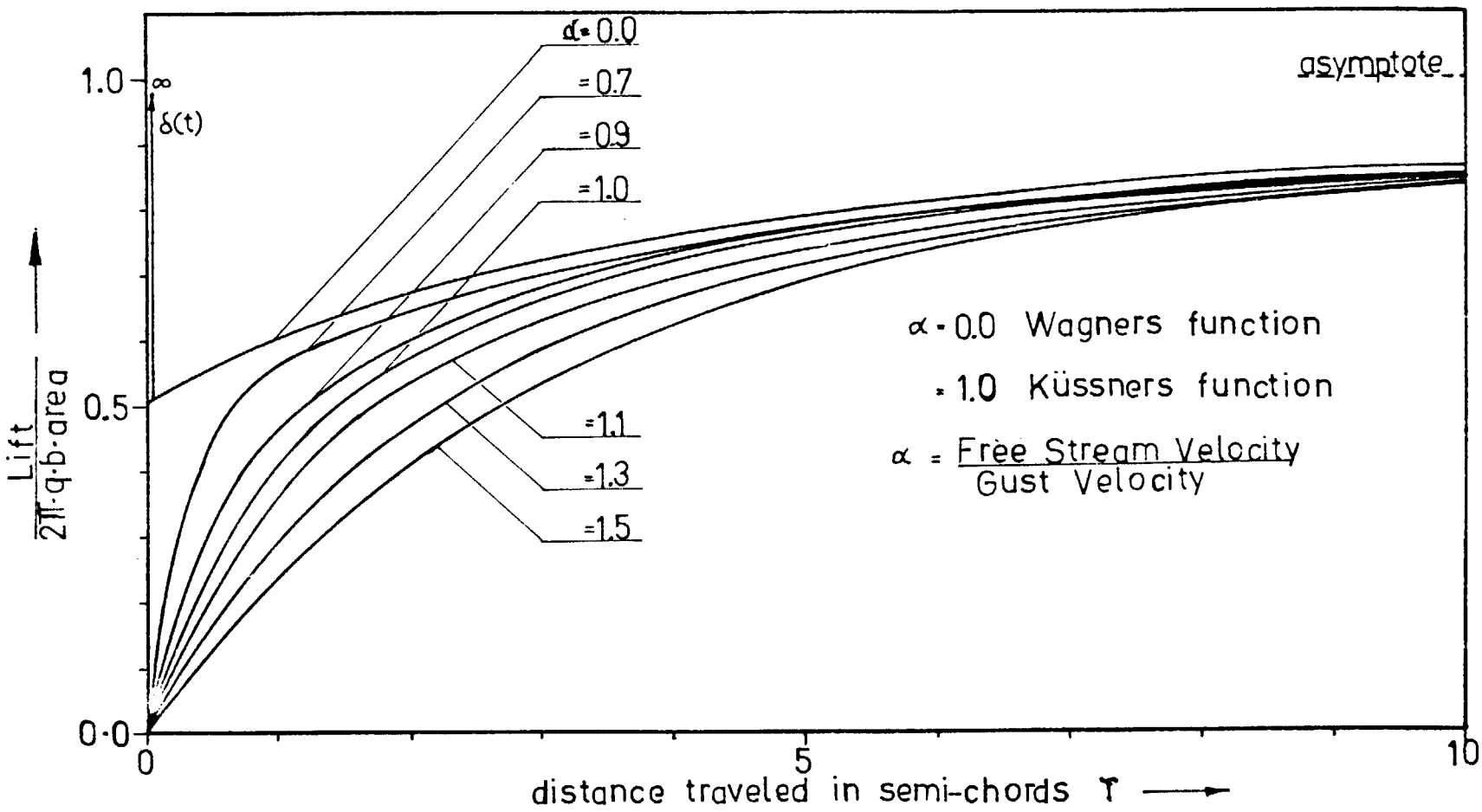

Fig. 9. Indicial response for moving transverse gusts.

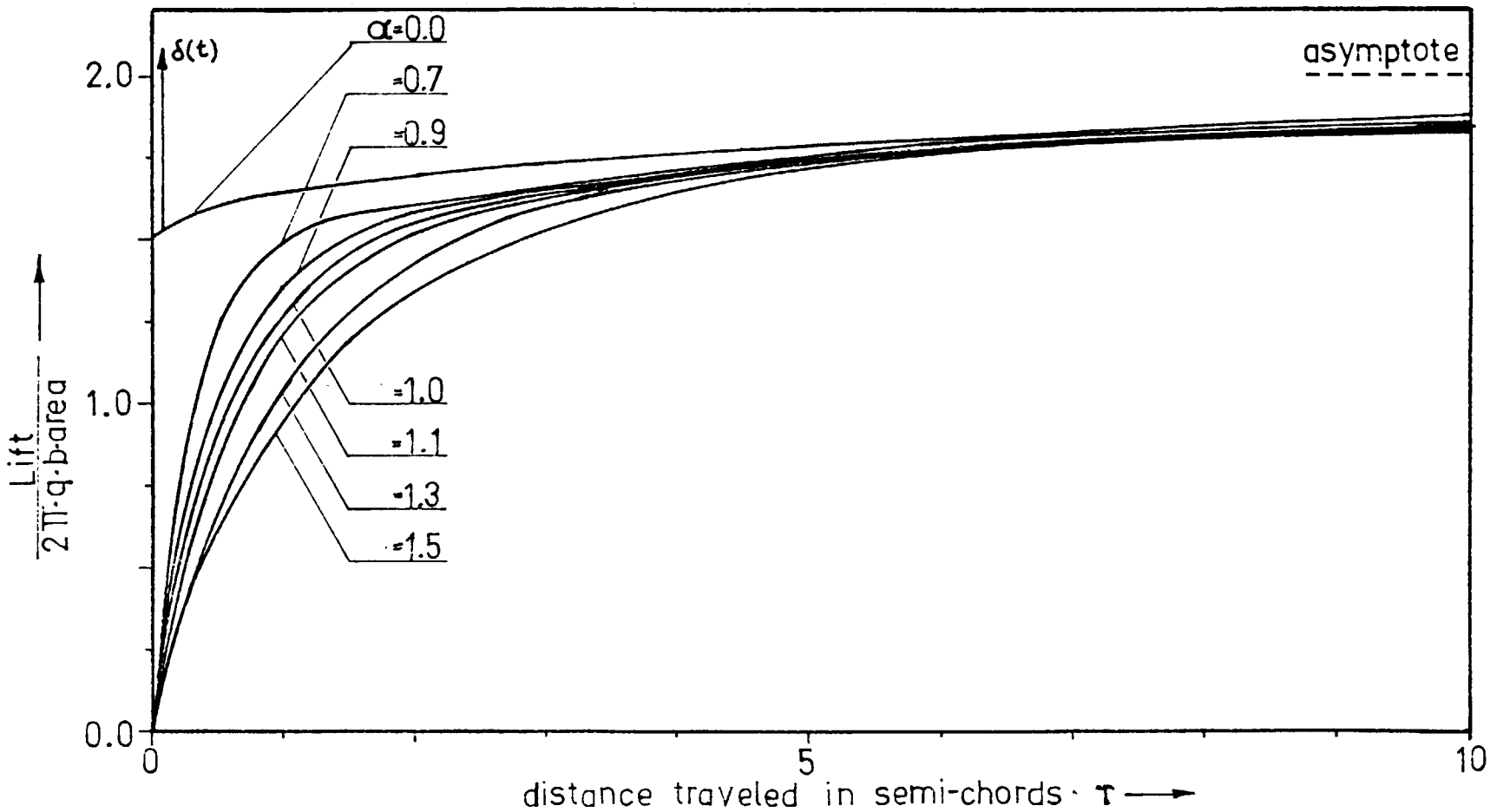

Fig. 10. Indicial response for moving chordwise gusts.

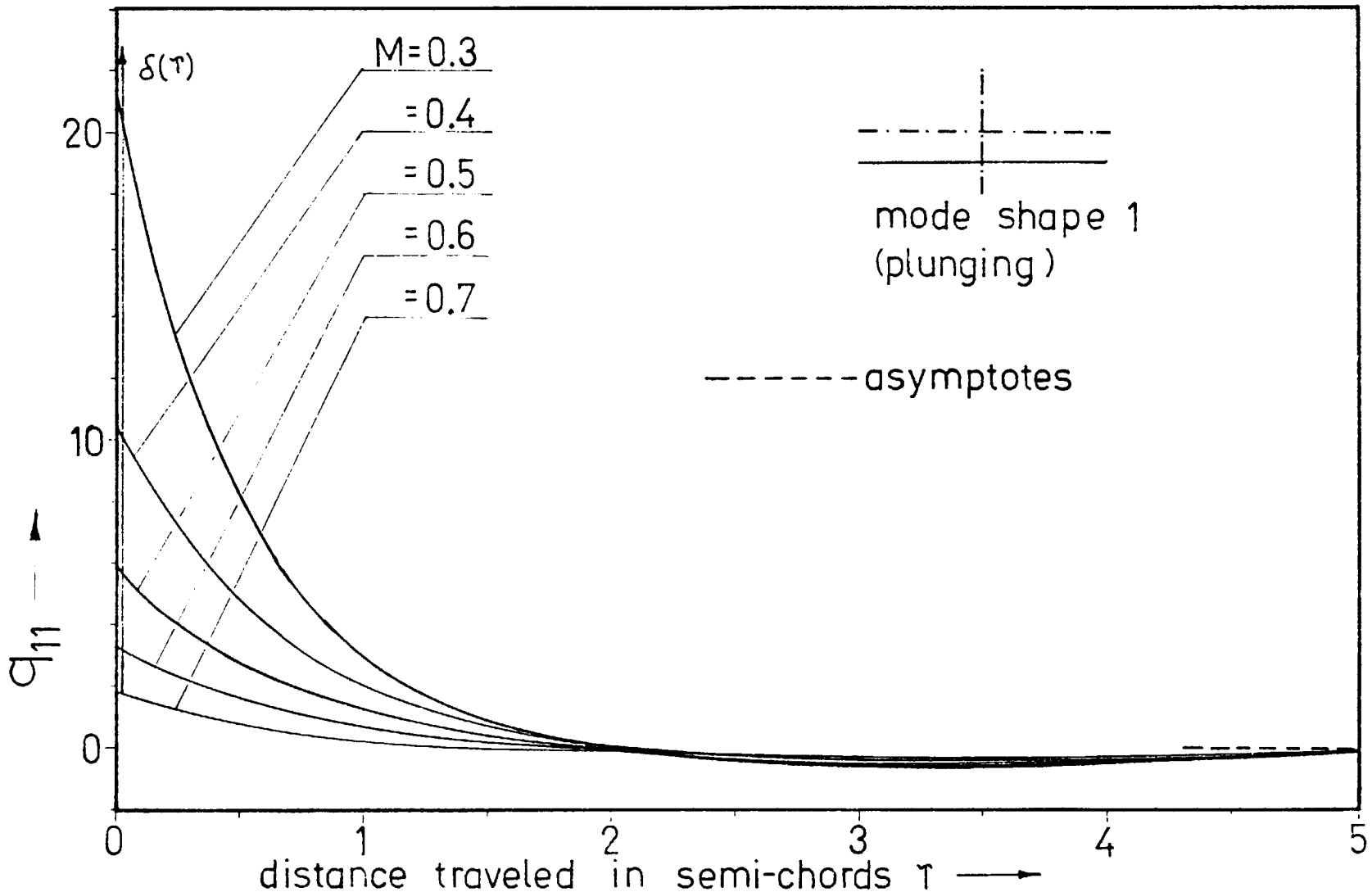

Fig. 11. Indicial lift for an impulsive plunging displacement, AR = ∞

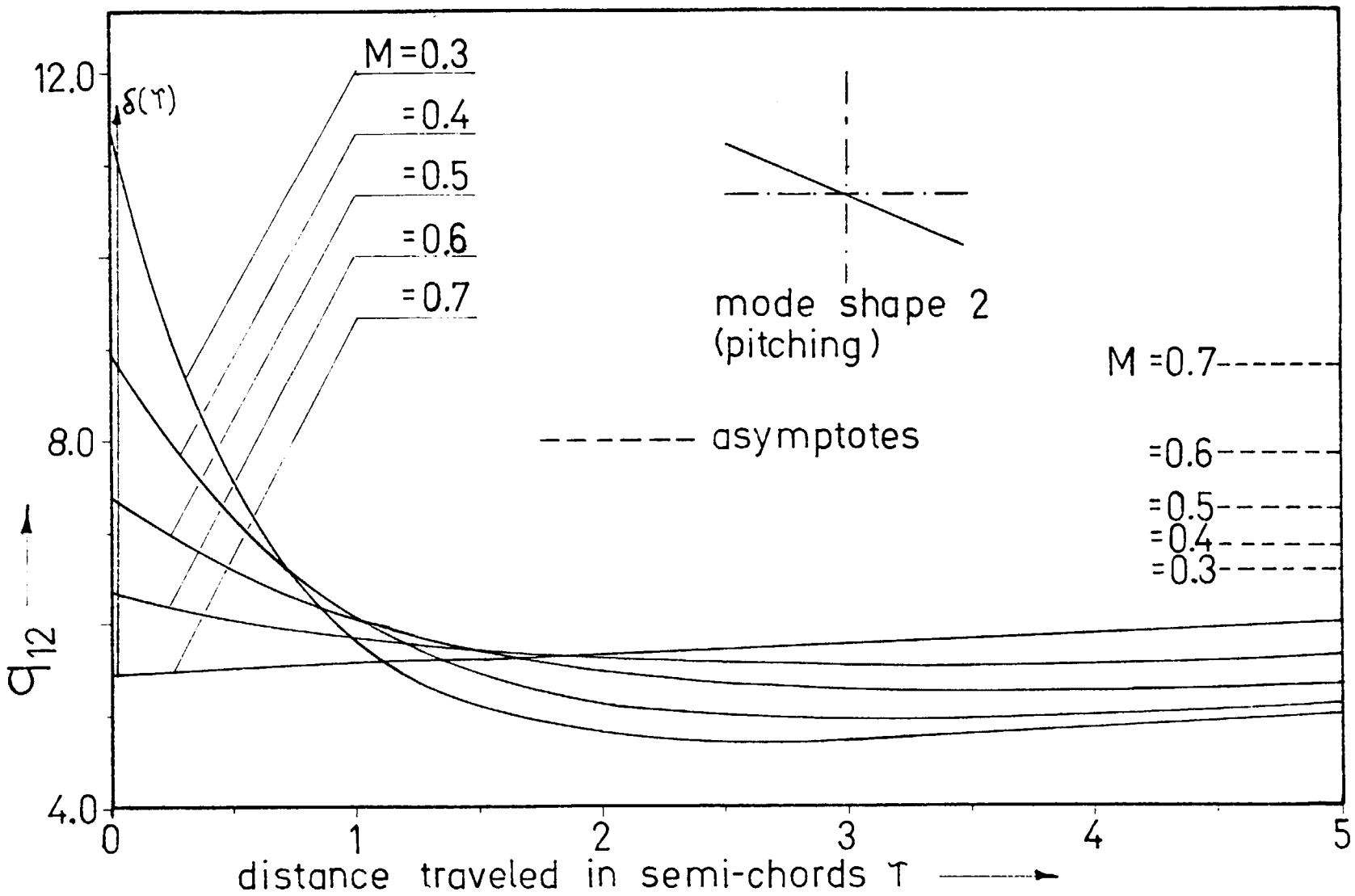

Fig. 12. Indicial lift for an impulsive pitching displacement.

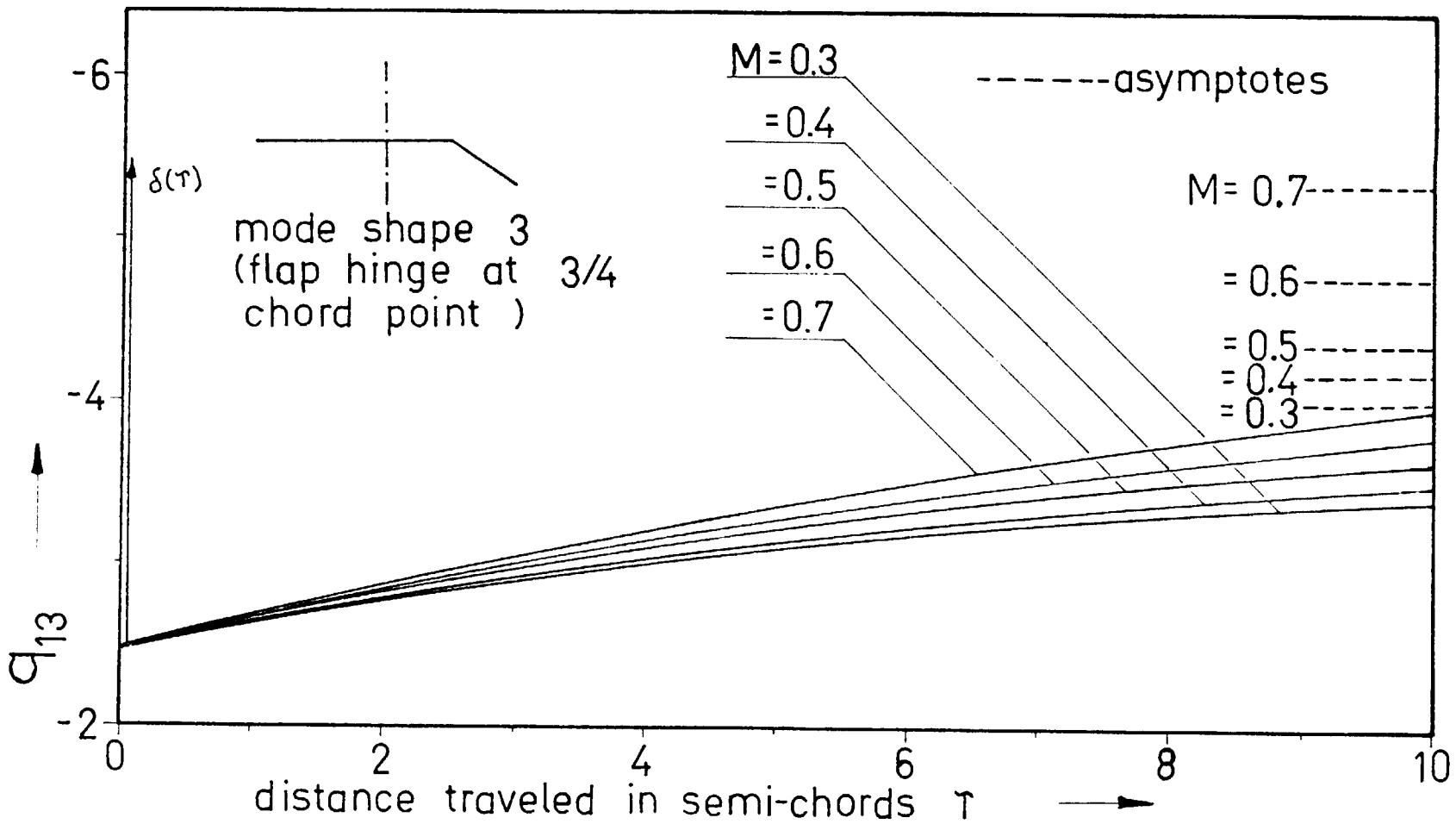

Fig. 13. Indicial lift due to impulsive flap rotation.

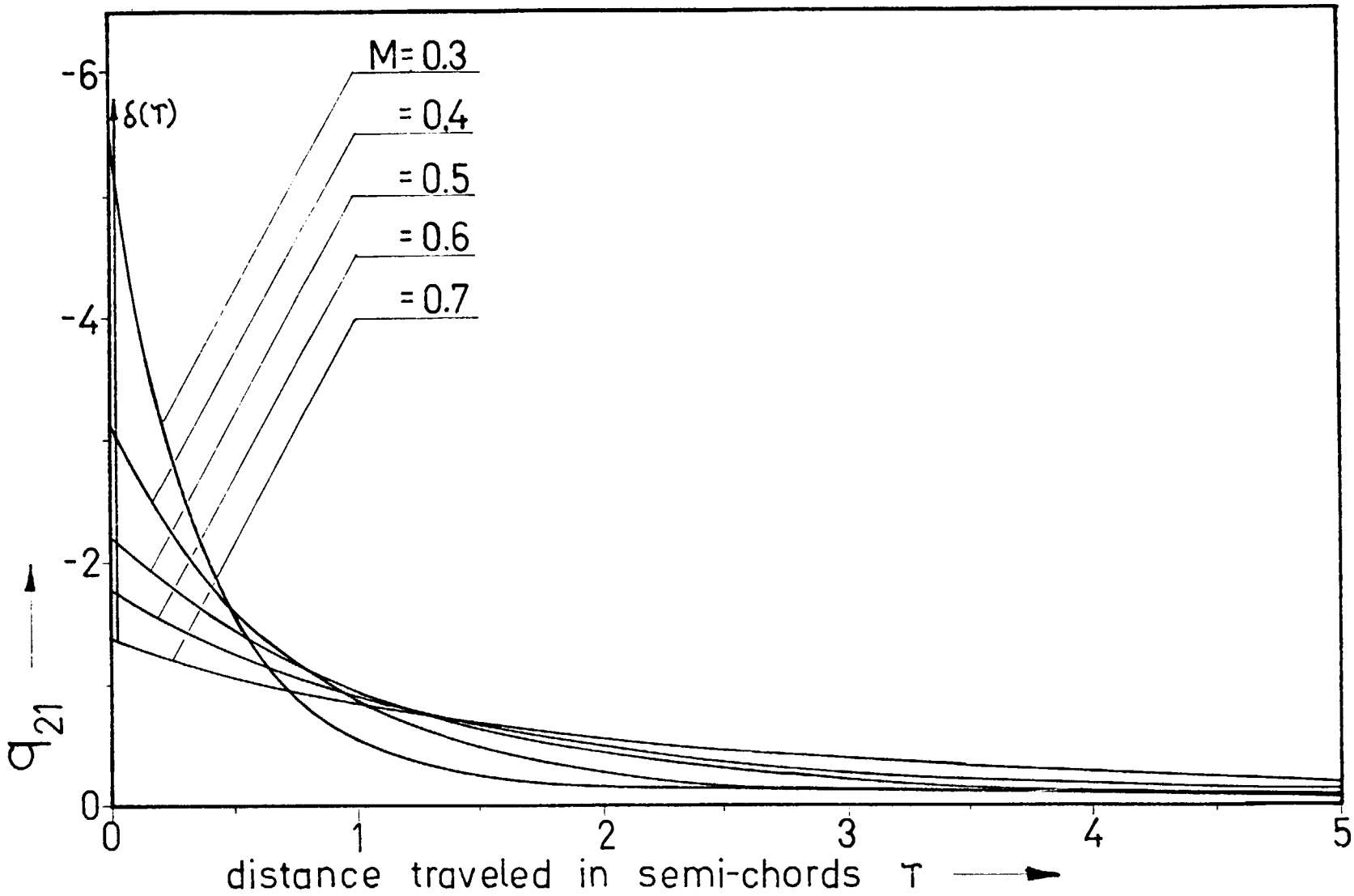

Fig. 14. Indicial moment in plunging.

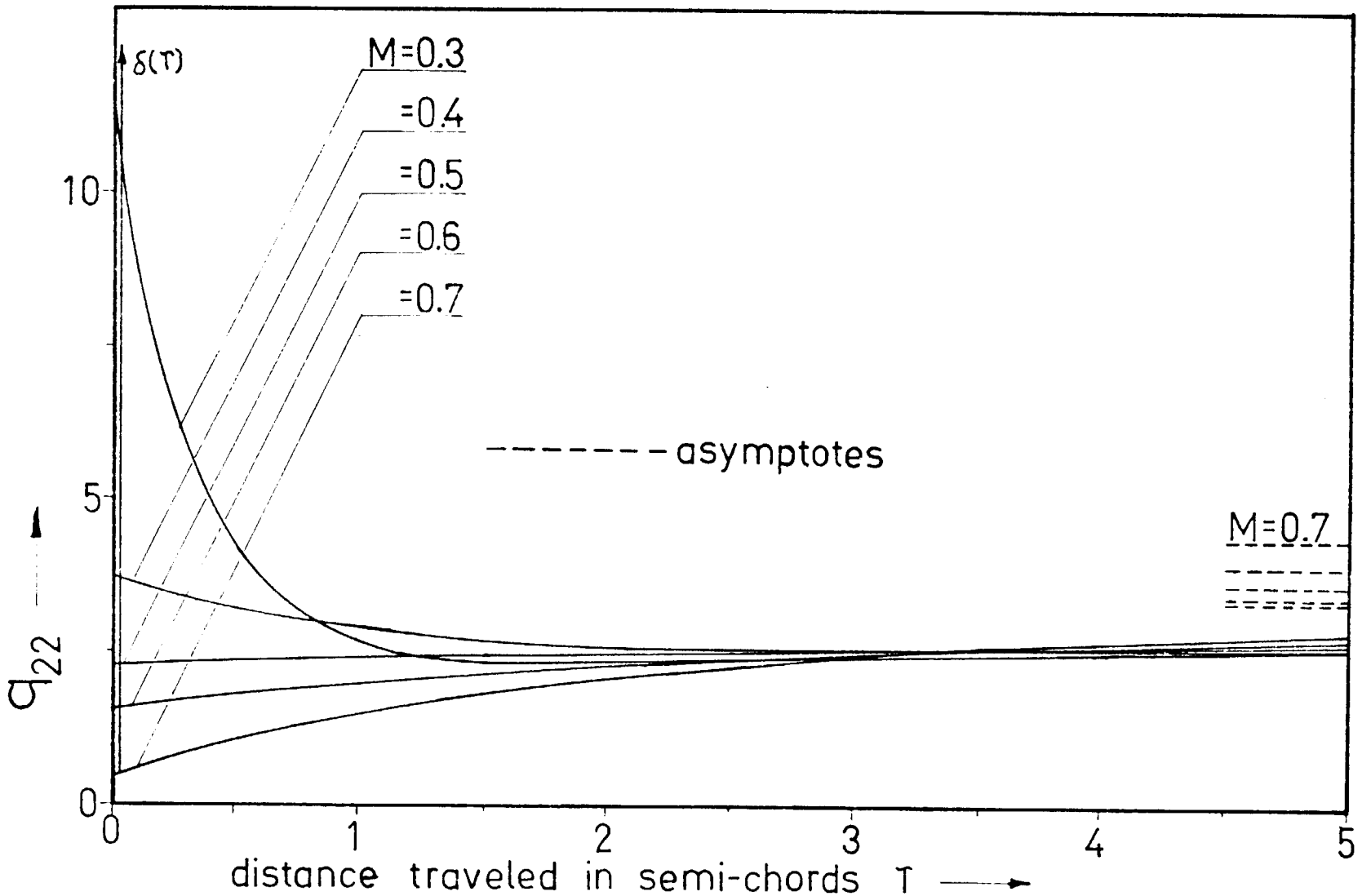

Fig. 15. Indicial moment in pitching.

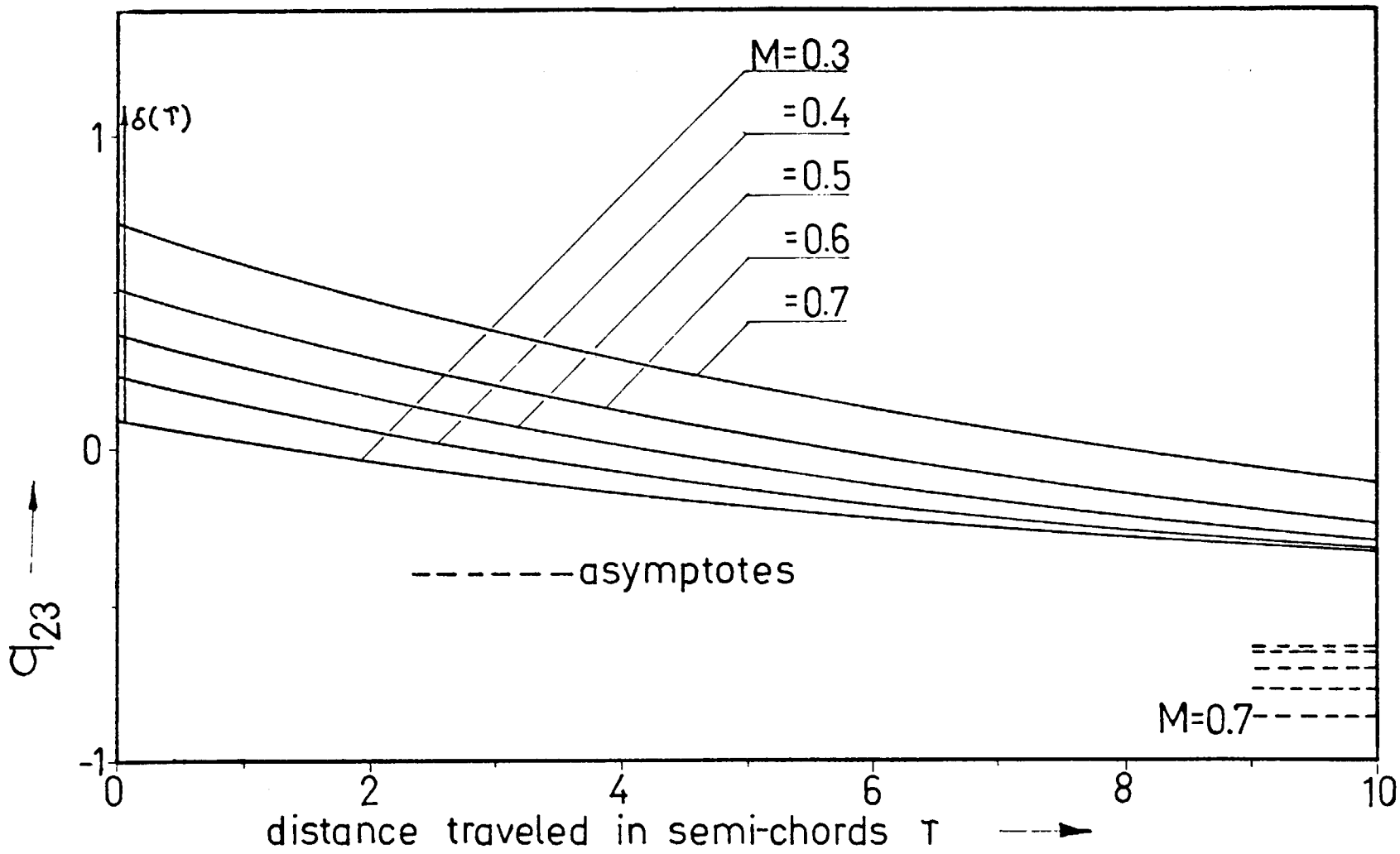

Fig. 16. Indicial moment due to flap mode.

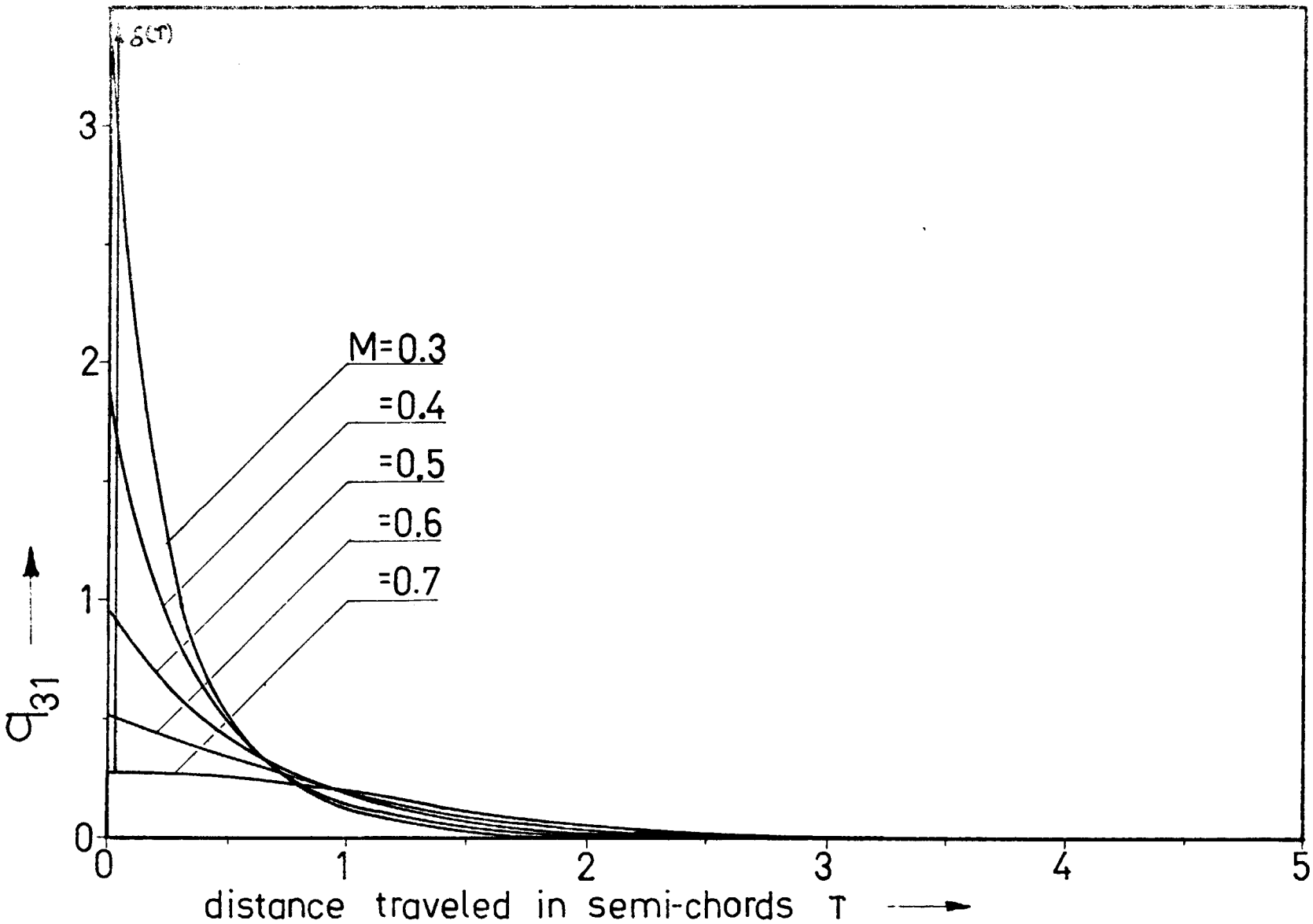

Fig. 17. Indicial partial moment in plunging.

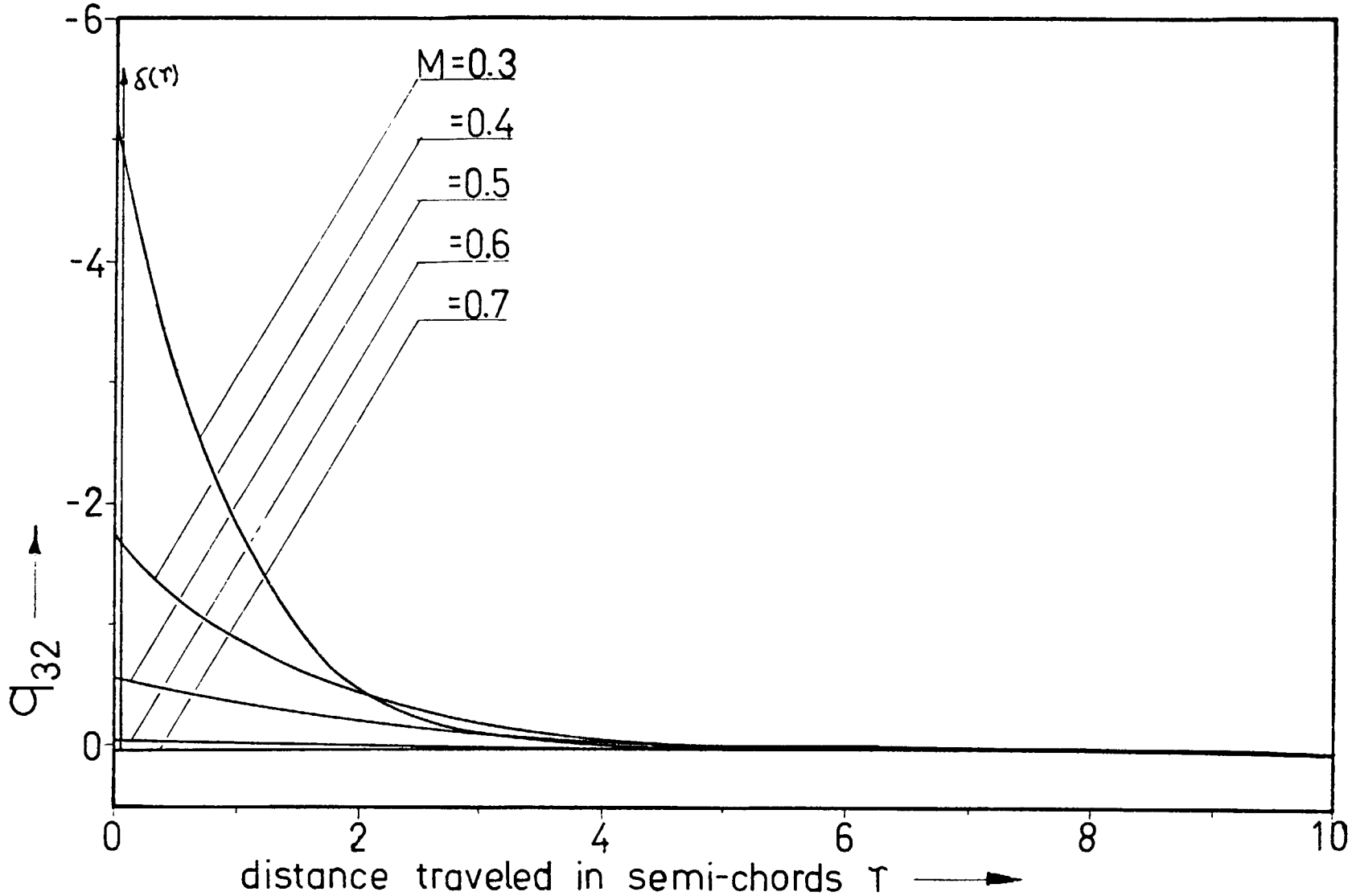

Fig. 18. Indicial partial moment in pitching.

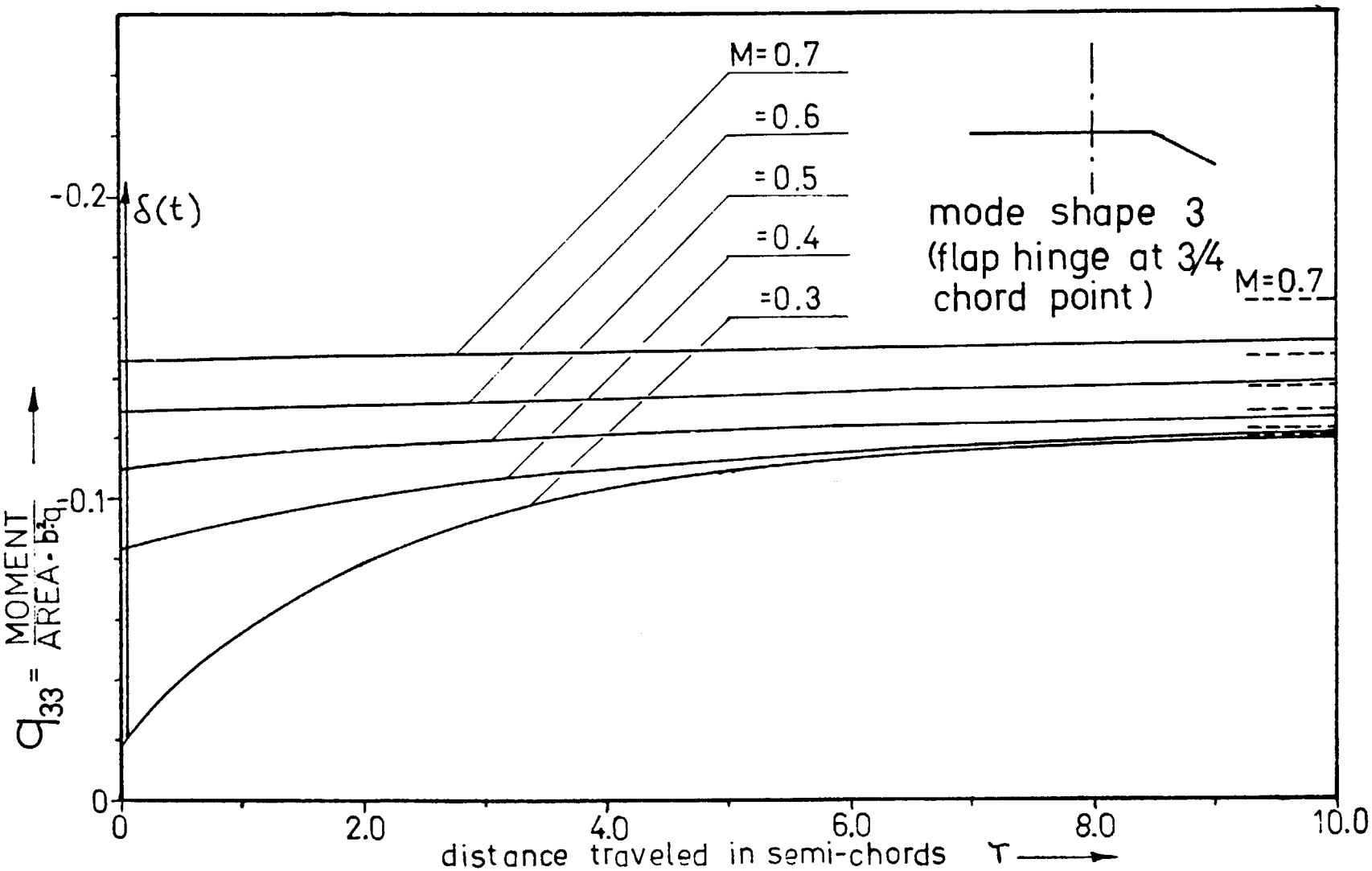

Fig. 19. Indicial partial moment due to flap mode.

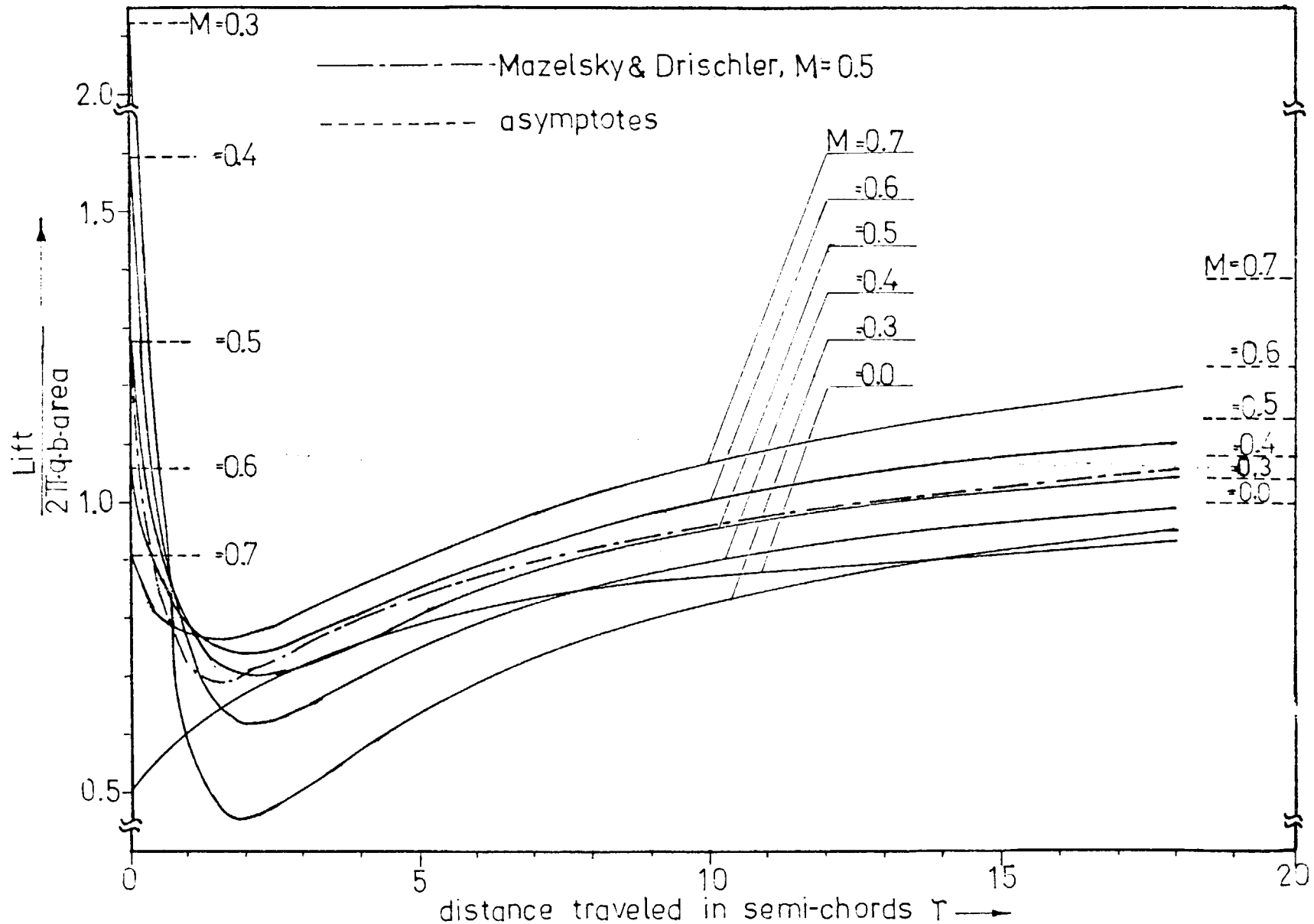

Fig. 20. Influence of compressibility on Wagner's function.

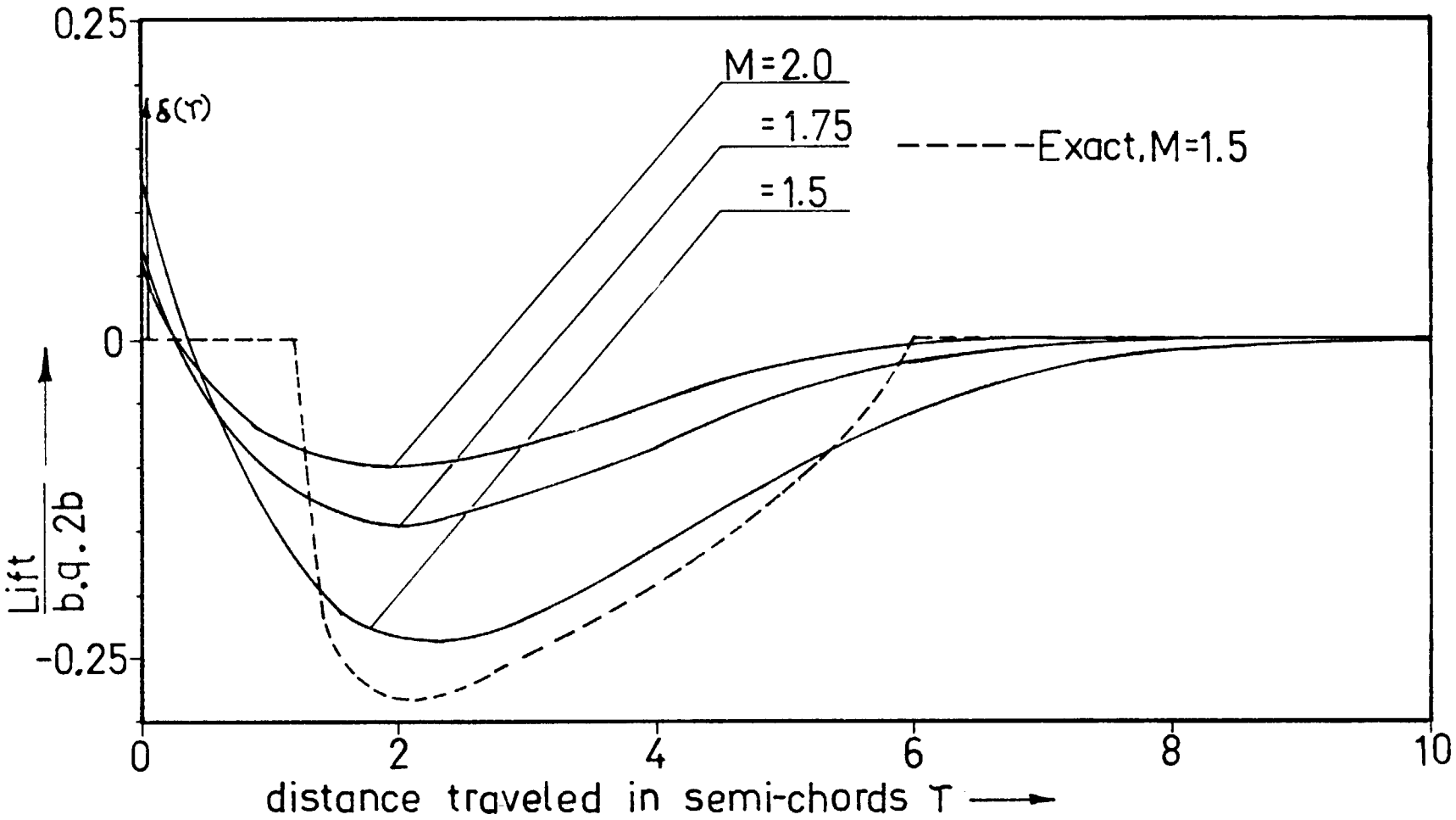

Fig. 21. Indicial lift due on impulsive plunging displacement, M > 0.

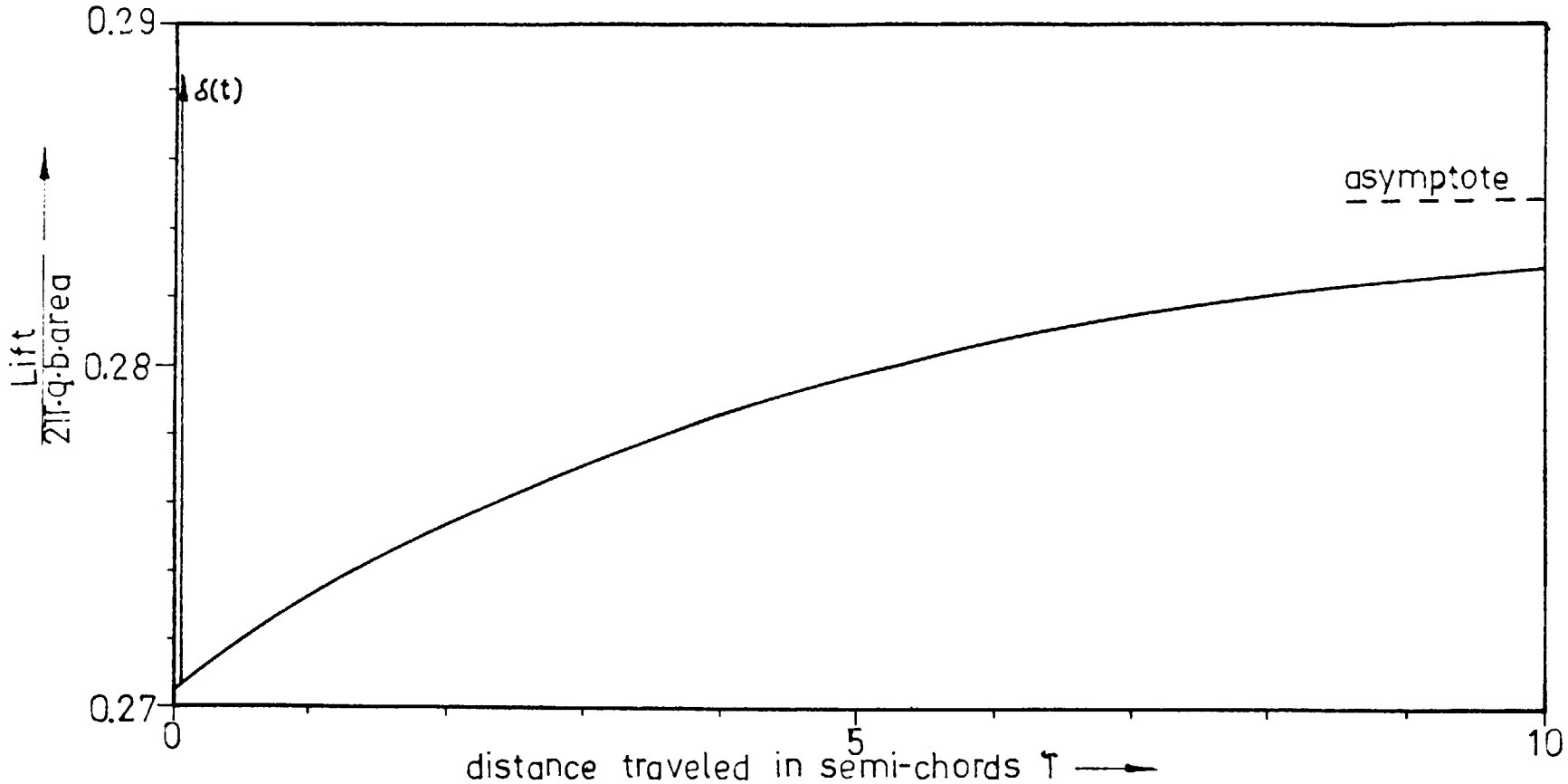

Fig. 22. Indicial lift due to impulsive plunging, circular planform, M = 0.

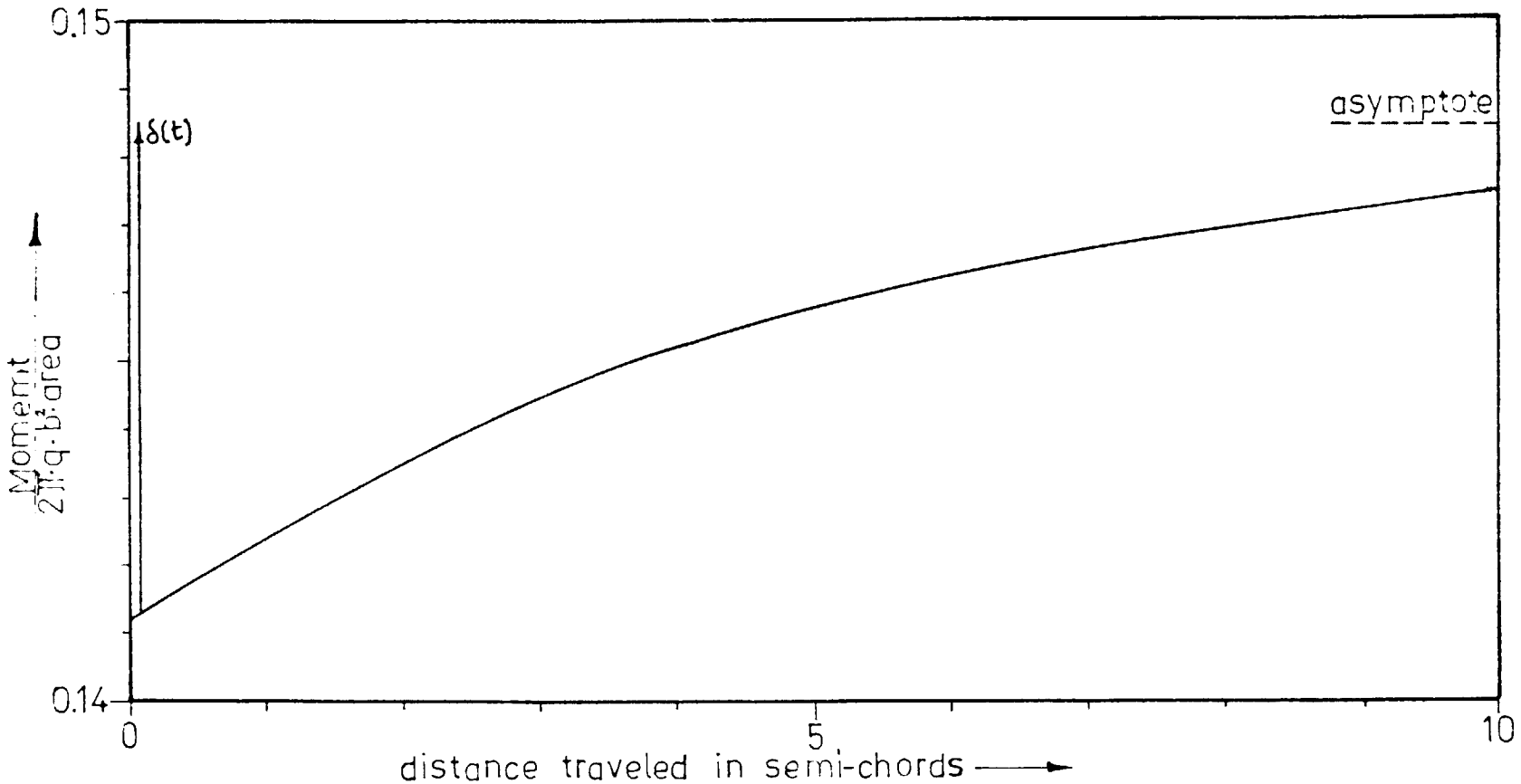

Fig. 23. Indicial moment due to the impulsive plunging, circular planform, M = 0.

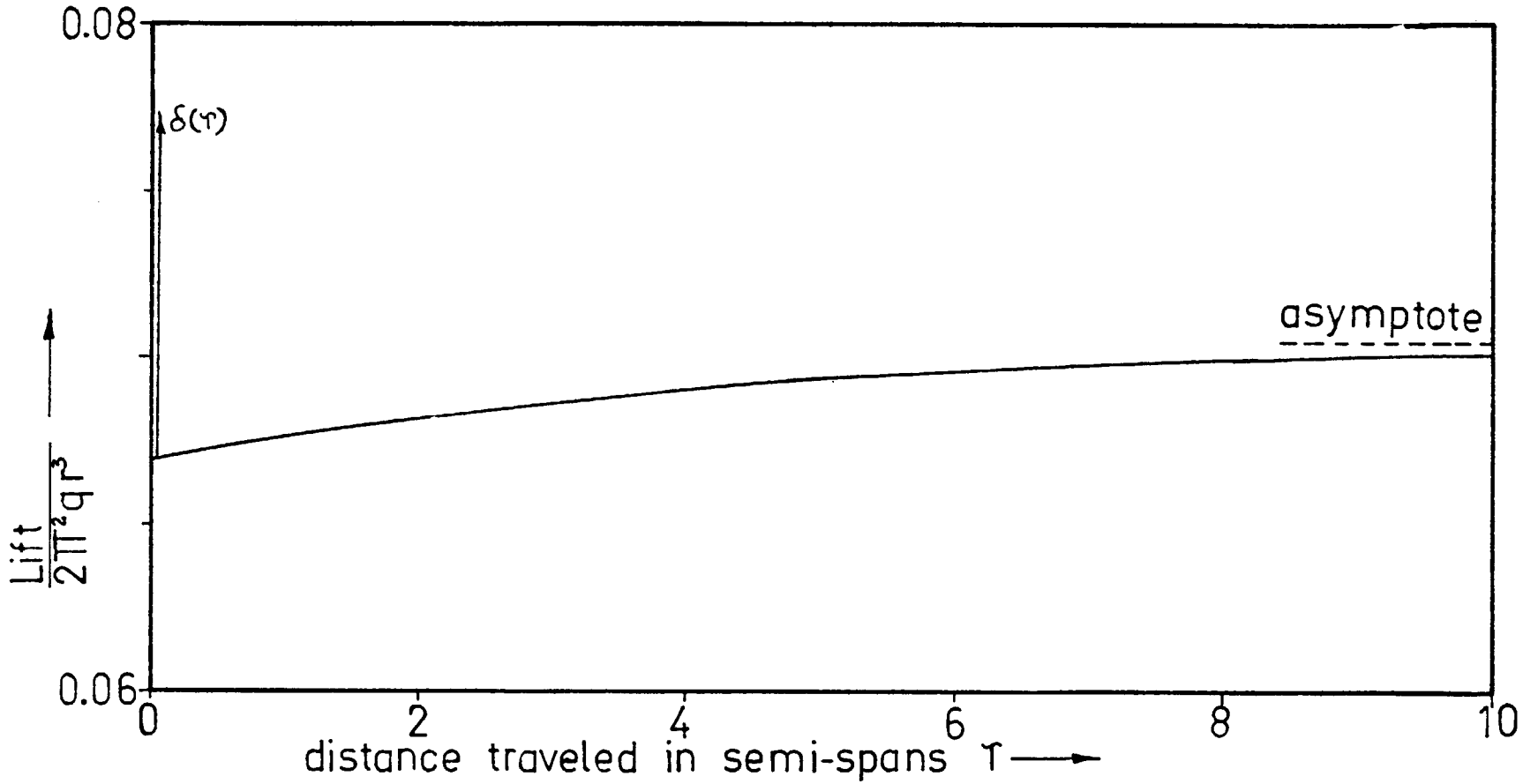

Fig. 24. Indicial lift due to an impulsive parabolic spanwise bending mode, circular planform, M = 0.

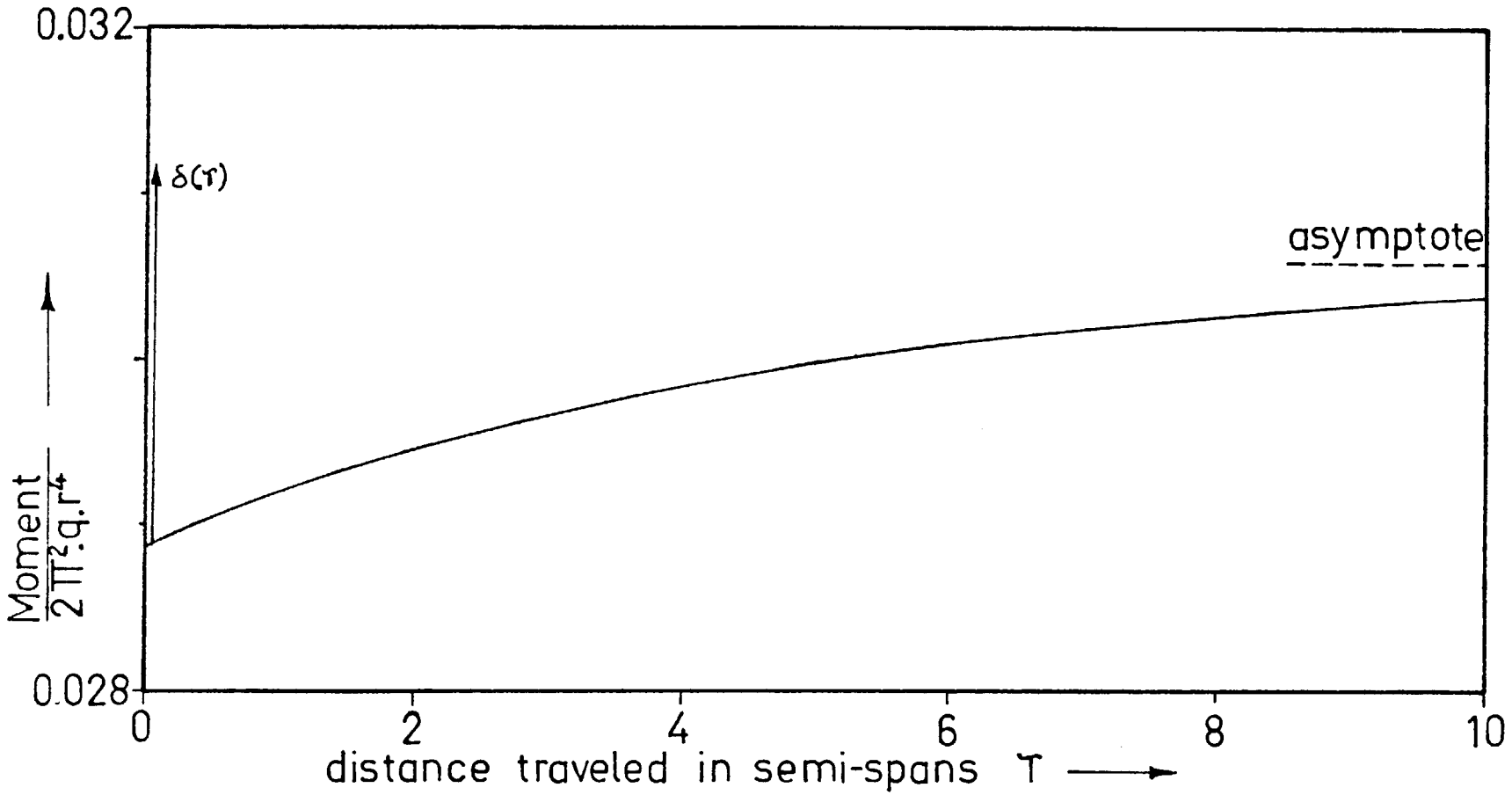

Fig. 25. Indicial moment due to an impulsive parabolic spanwise bending mode, circular planform, M = 0.

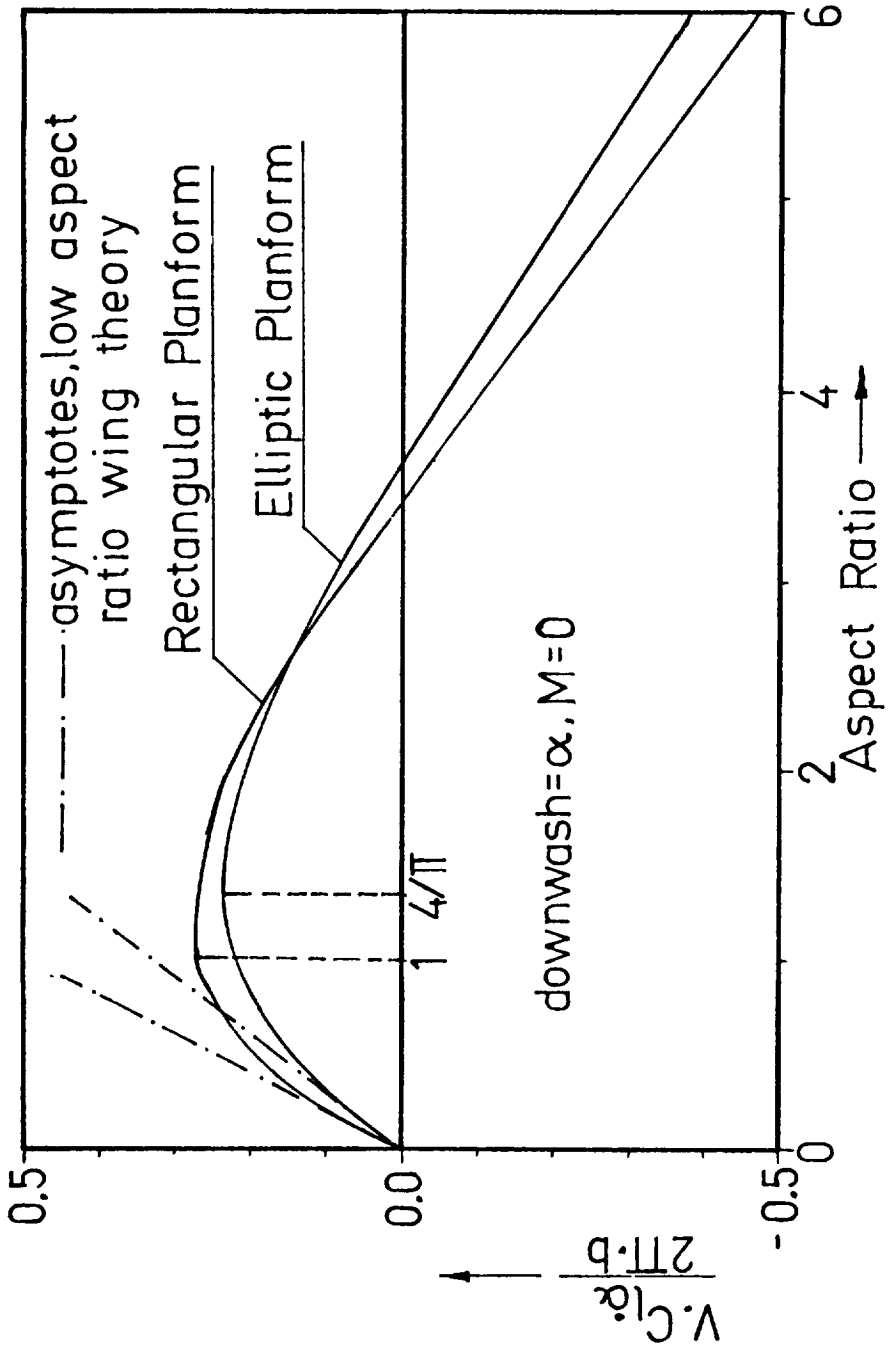

Fig. 26. Variation of $C_{l_{\dot{\alpha}}}$ with aspect ratio for rectangular and elliptic wings.

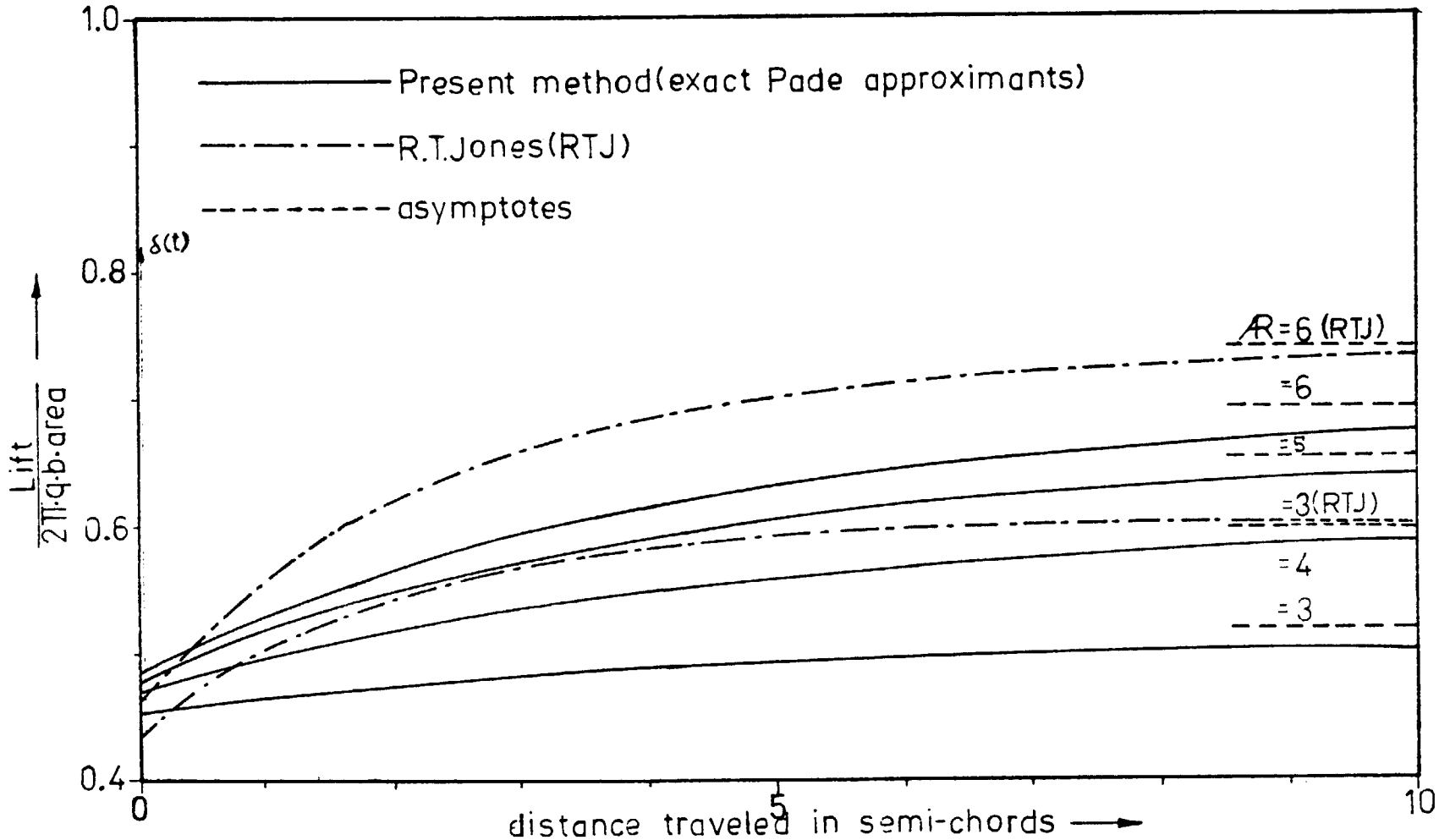

Fig. 27. Indicial lift due to impulsive plunging obtained from exact Padé approximants, elliptic planform, M = 0.

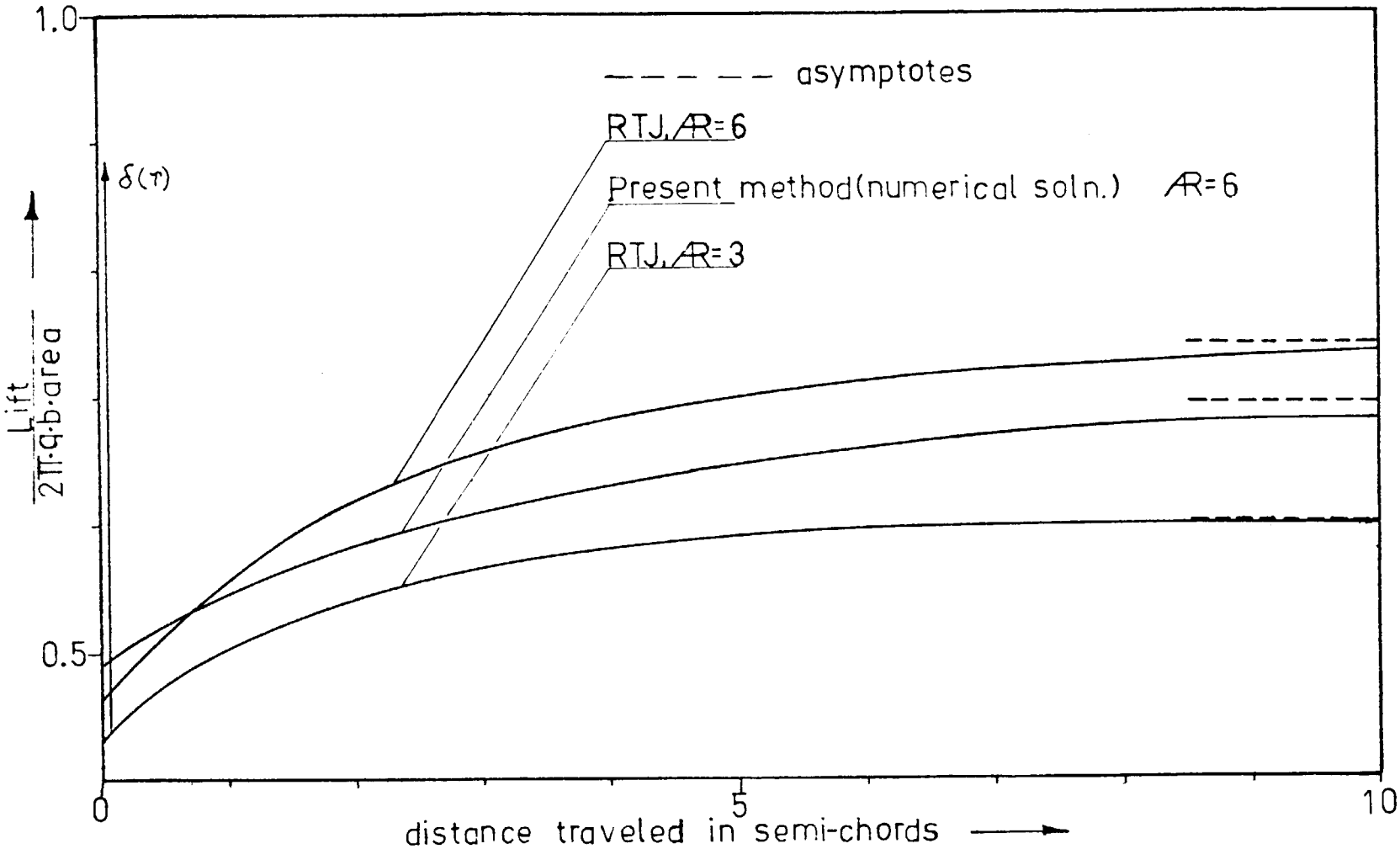

Fig. 28. Indicial lift due to impulsive plunging obtained numerically, elliptic planform, M = 0.

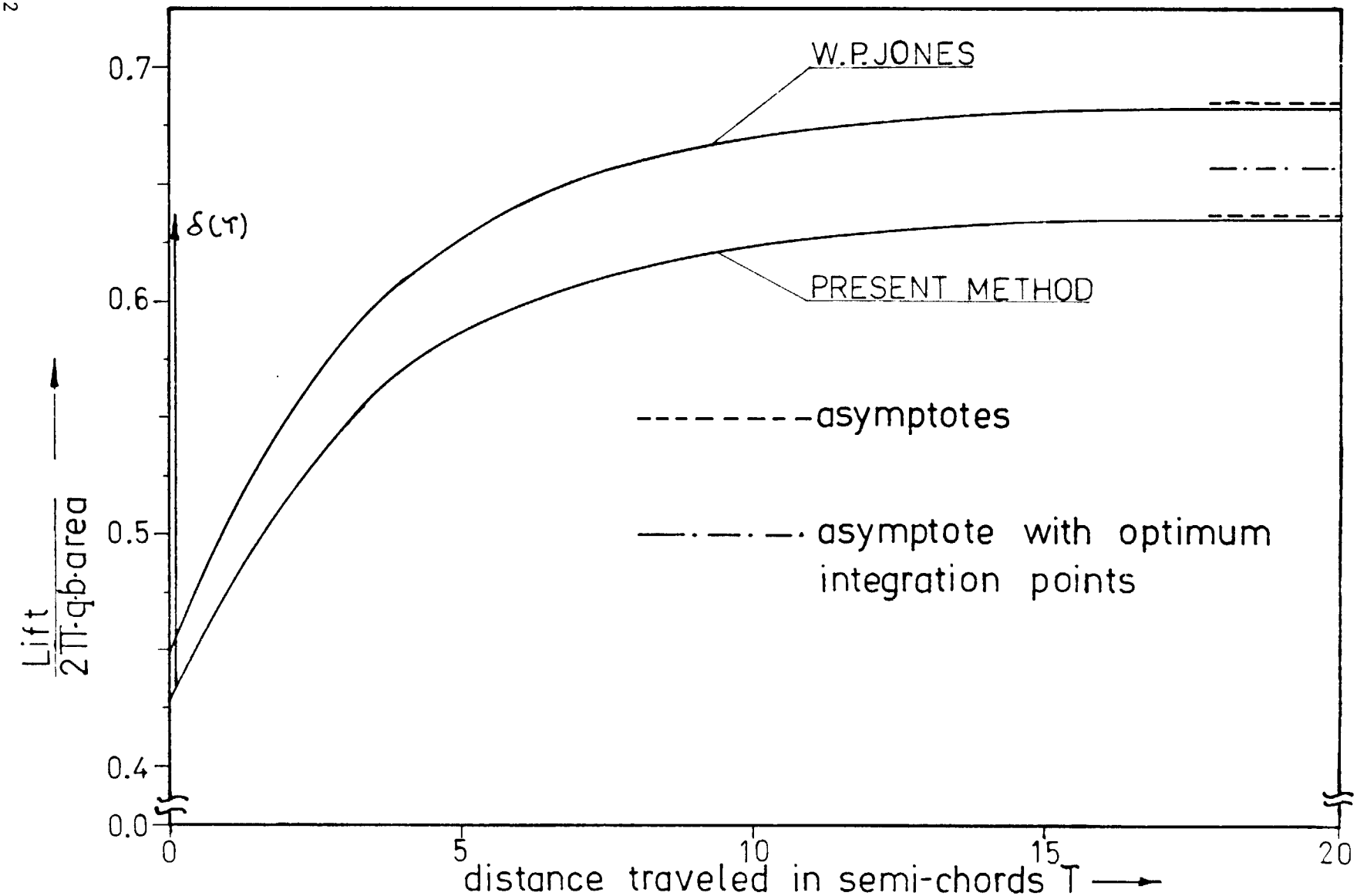

Fig. 29. Indicial lift due to impulsive plunging, rectangular planform, AR = 6.0.

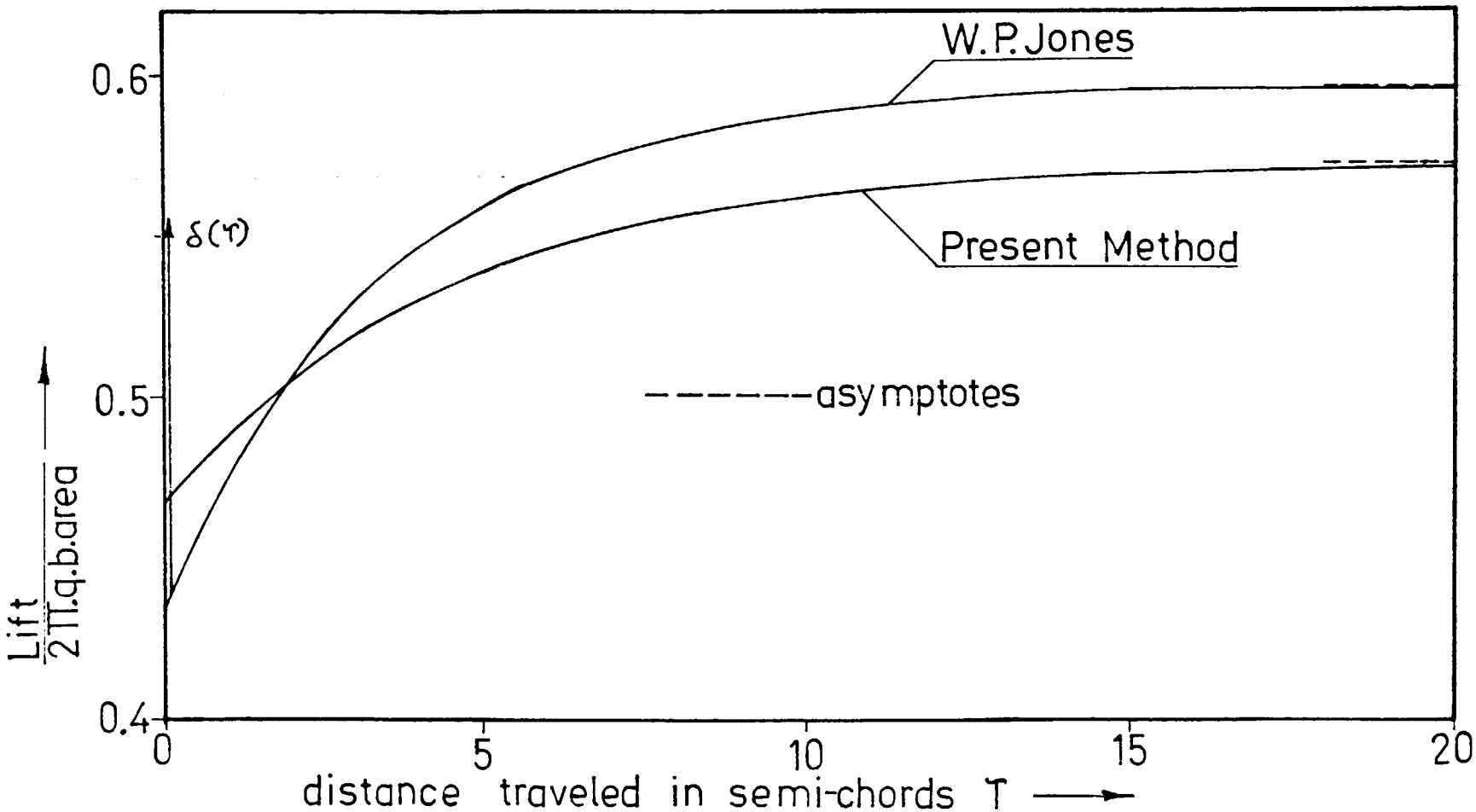

Fig. 30. Indicial lift due to impulsive plunging, rectangular planform, AR = 4.0.

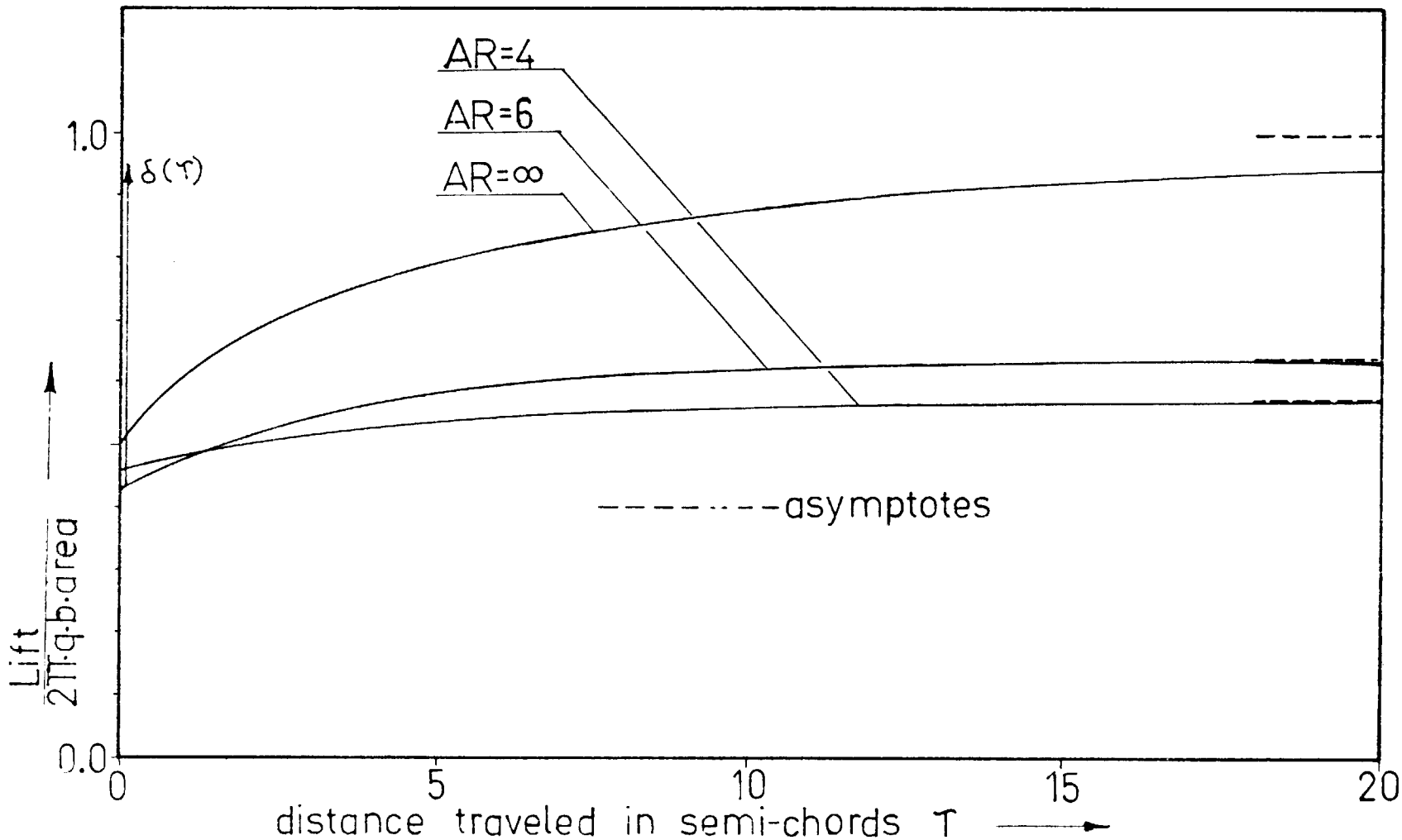

Fig. 51. Influence of AR on the indicial lift in plunging, rectangular planform, M = 0.

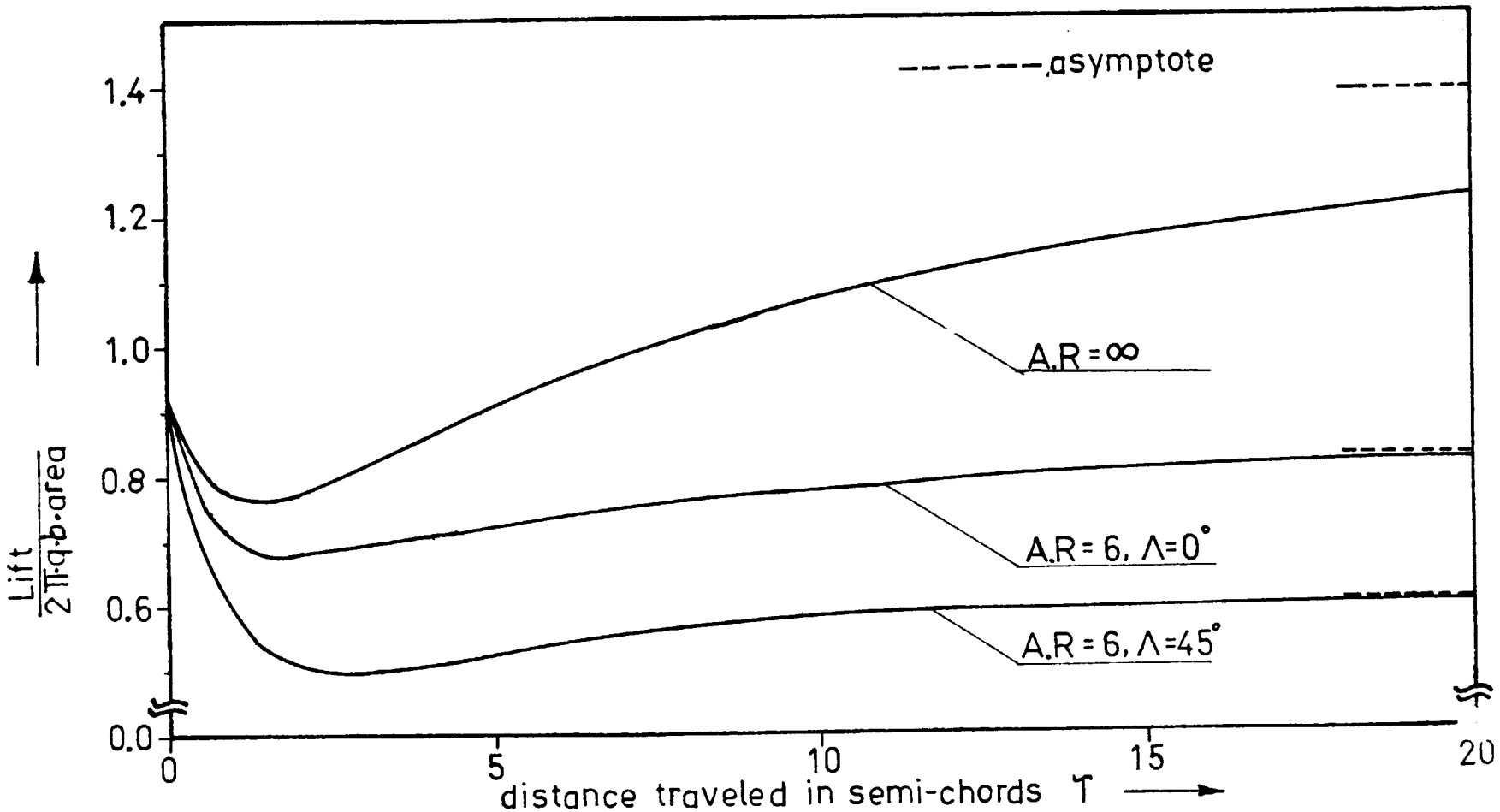

Fig. 32. Influence of finite aspect ratio and sweep on the indicial function for impulsive plunging at M = 0.7.

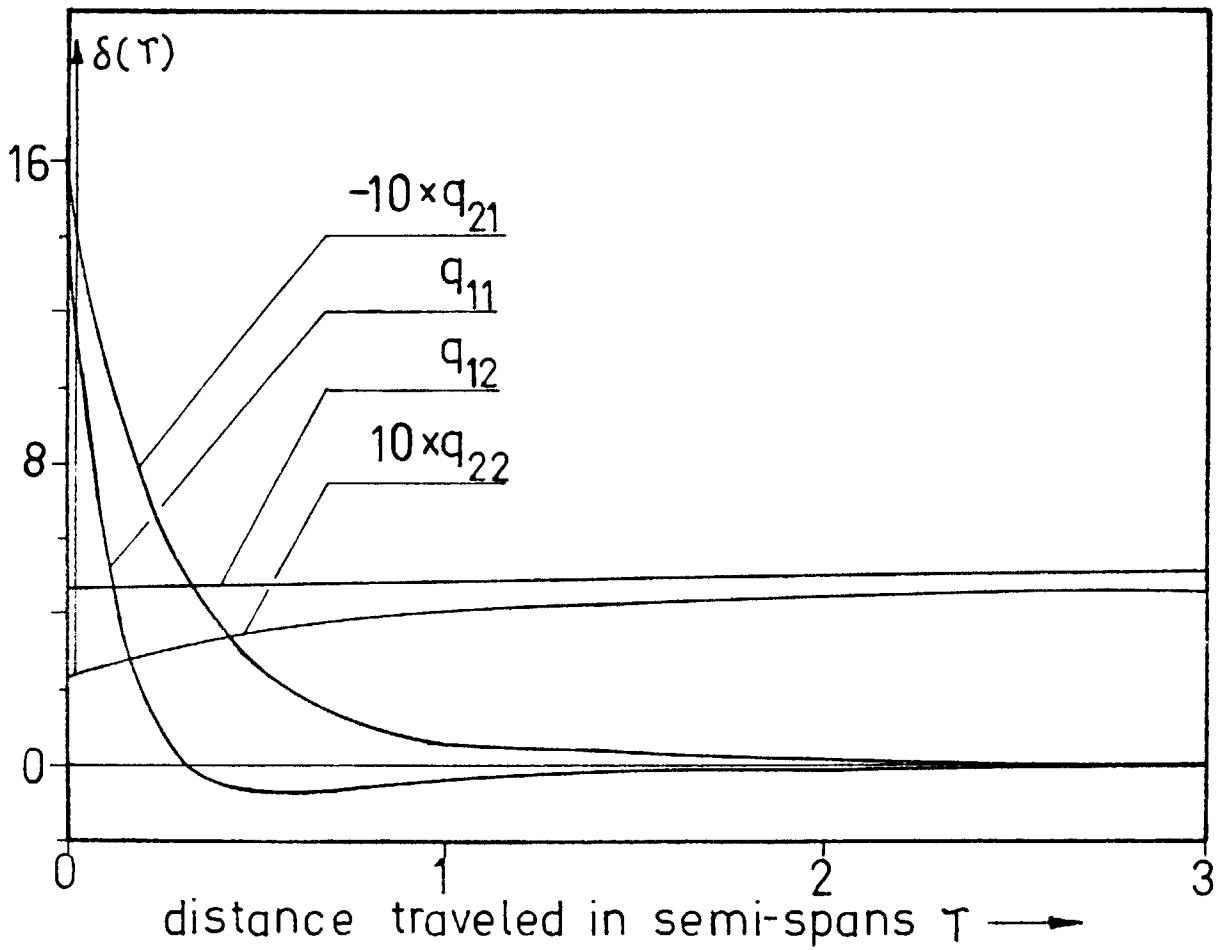

Fig. 33. Indicial generalized forces in plunging (1) and pitching (2) displacements rectangular wing AR = 6.0, M = 0.7.

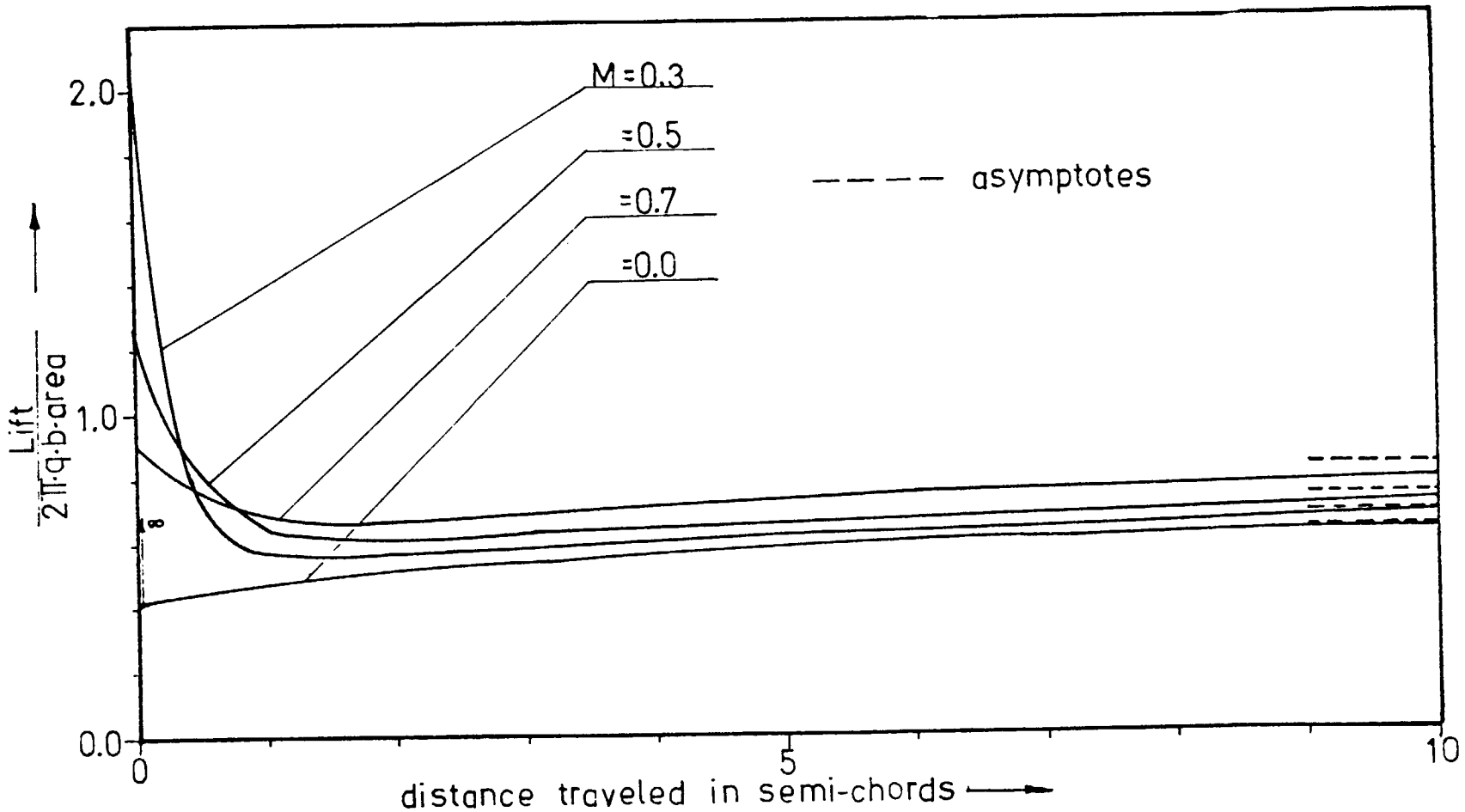

Fig. 34. Influence of compressibility on the indicial function for impulsive plunging, rectangular planform, AR = 6.0.

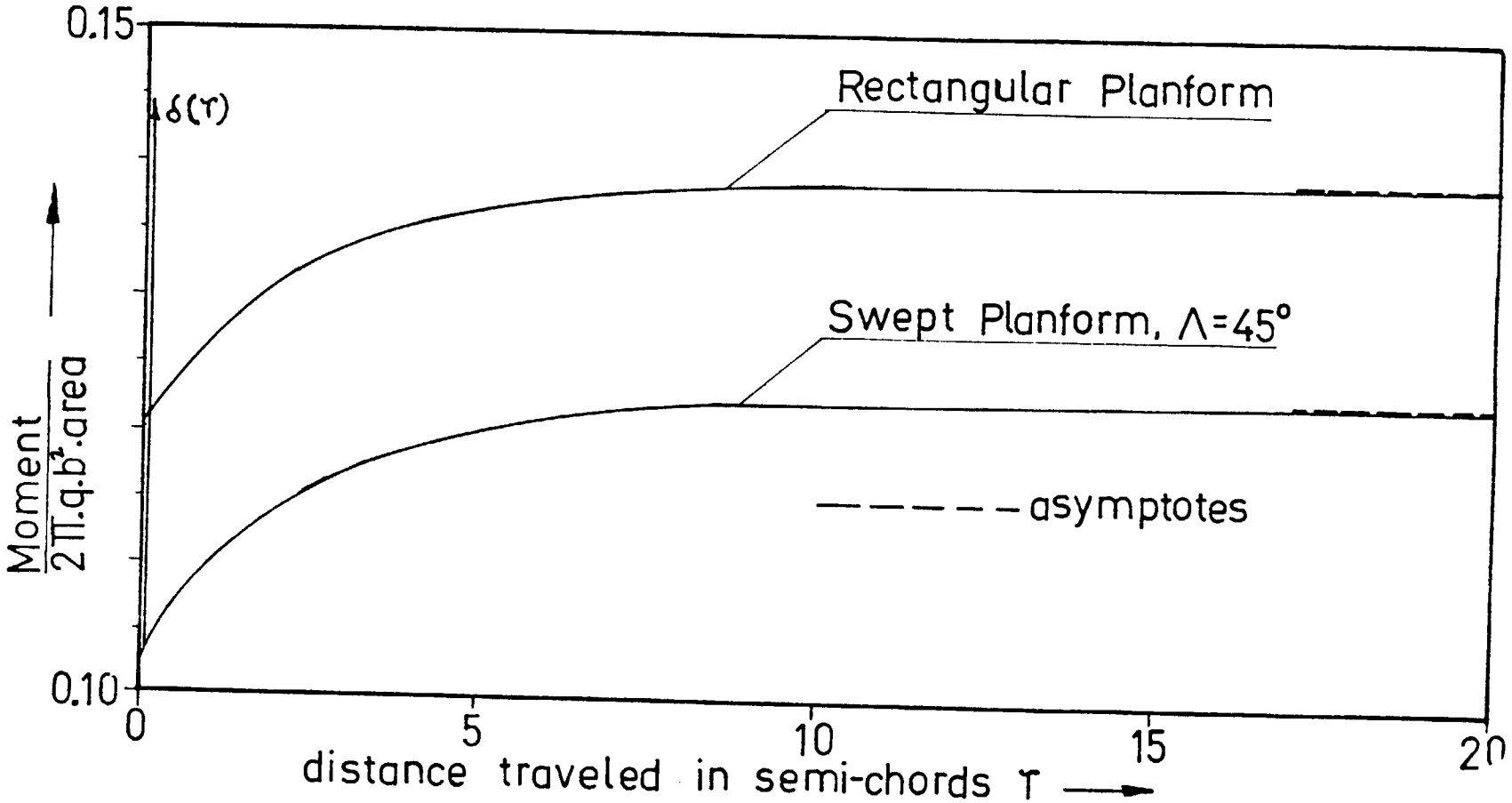

Fig. 35. Rolling moment on an impulsively rolling wing, AR = 6.0, M = 0.0.

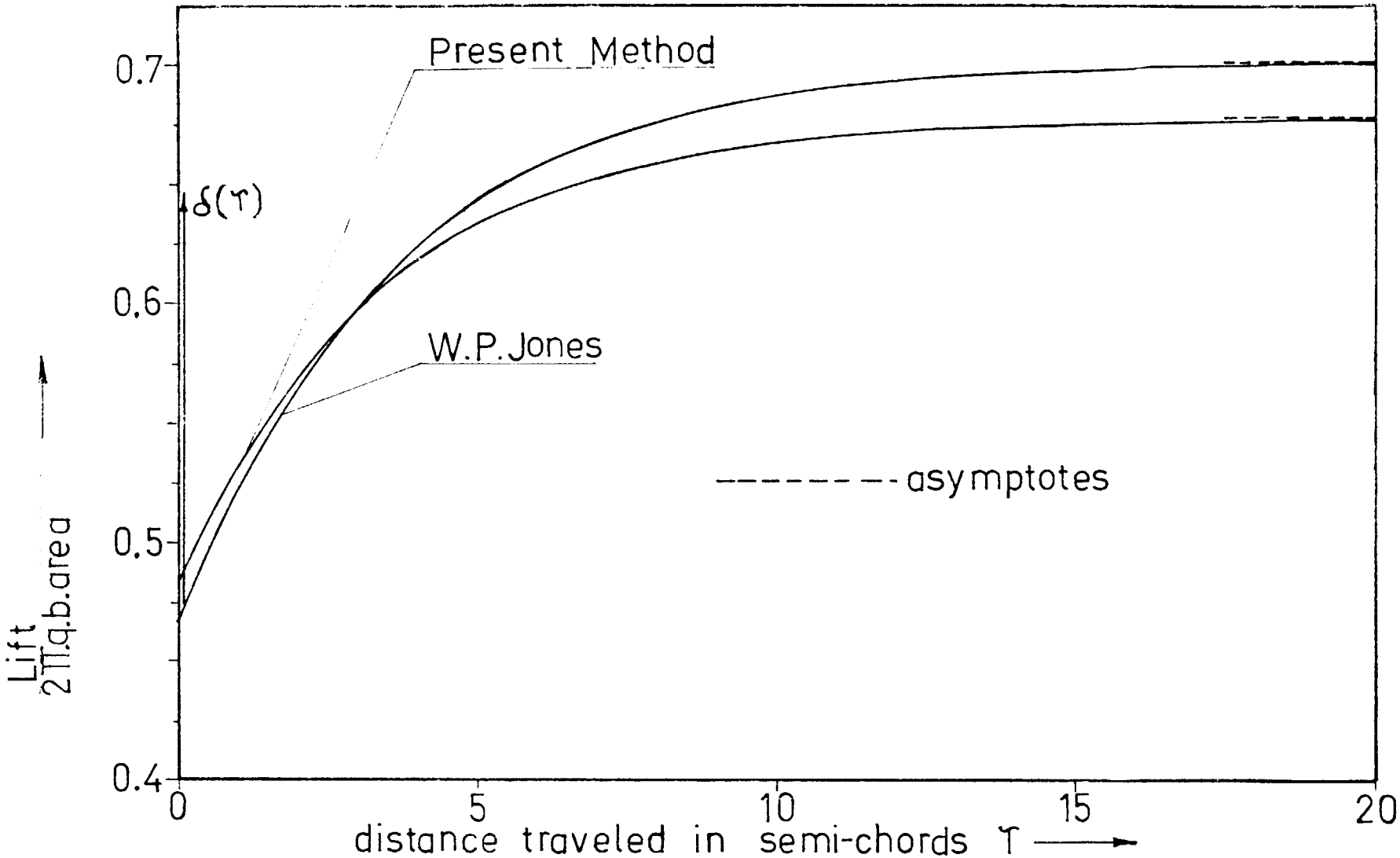

Fig. 36. Indicial lift for impulsive plunging, tapered planform, AR = 5.84, M = 0.0, TR = 0.524.

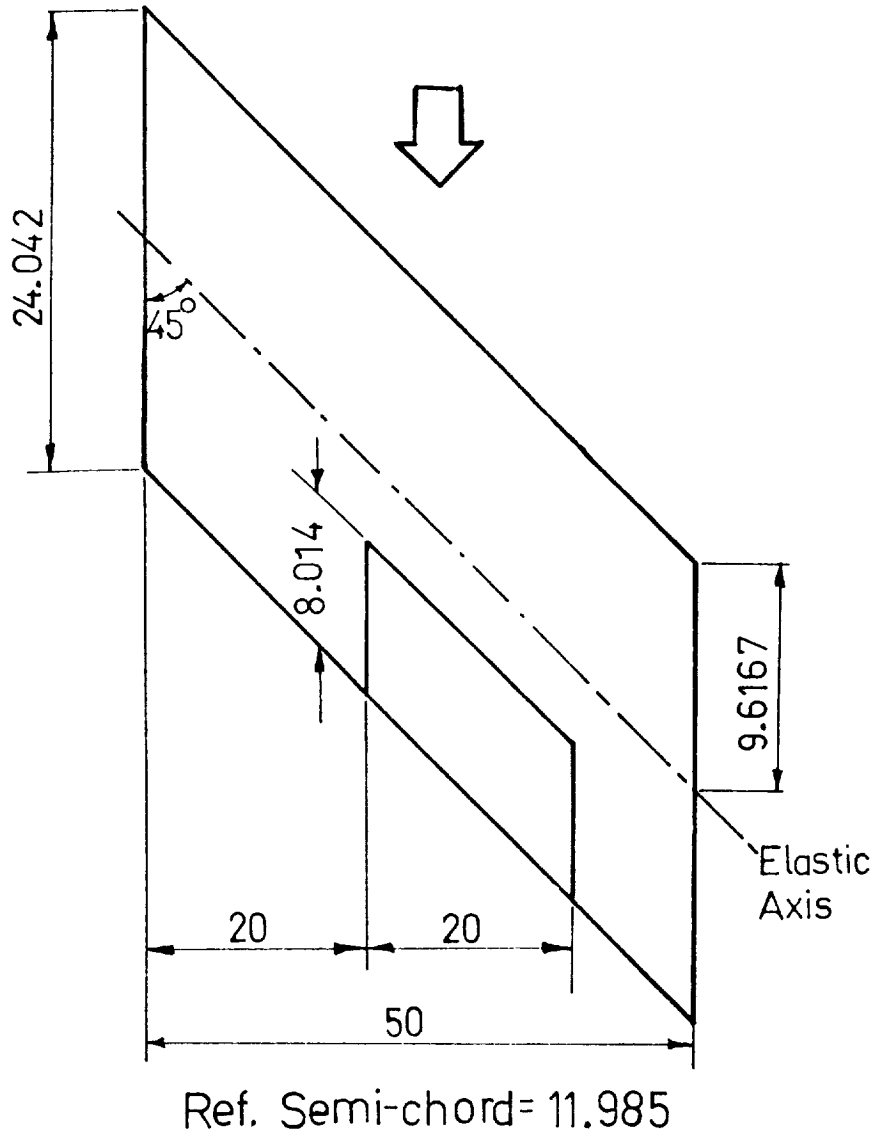

Fig. 37. Swept wing, AR = 4.16, $\Lambda = 45^{\circ}$, M = 0.6 .

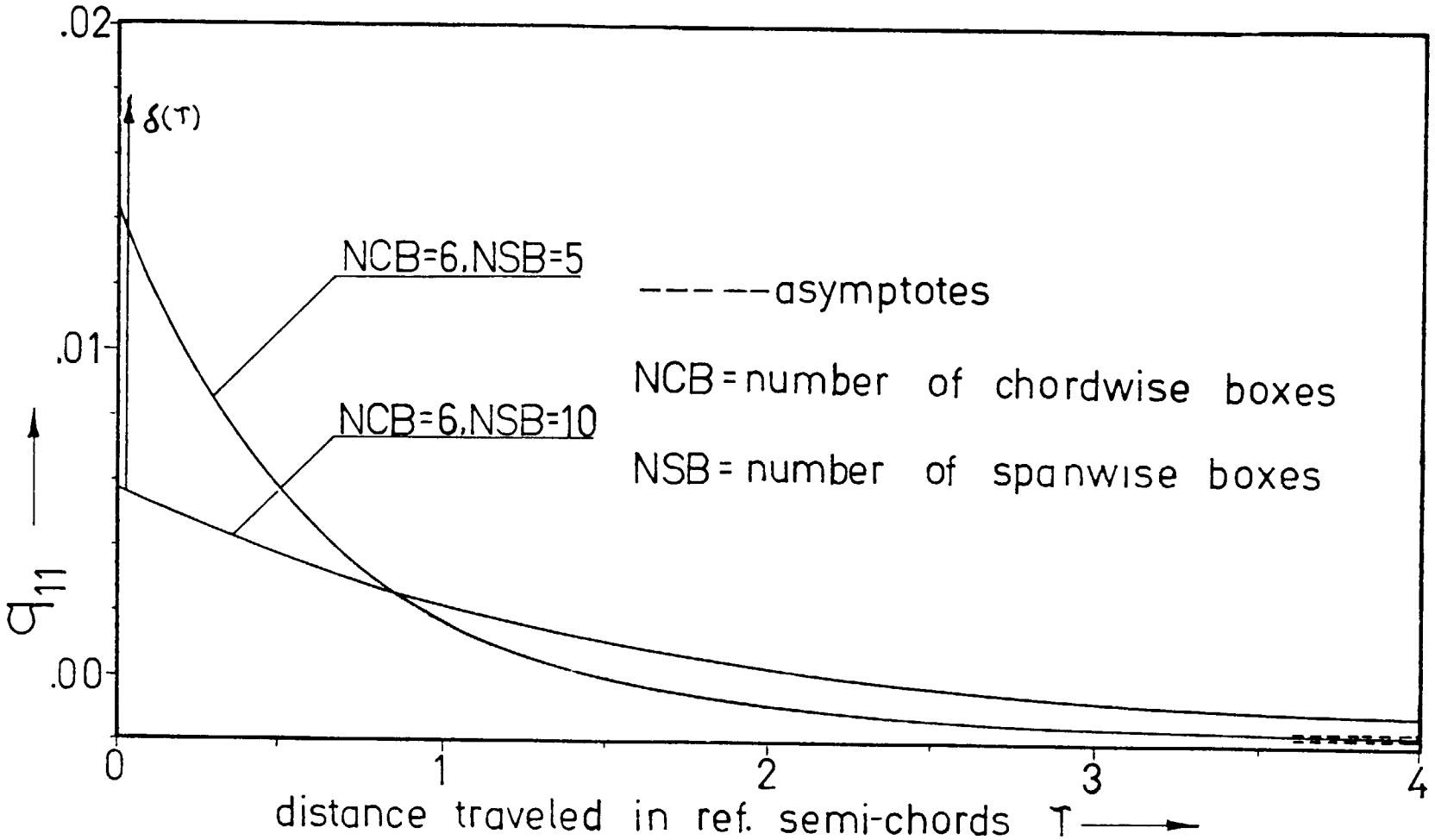

Fig. 38. Indicial function for q_{11}, due to impulsive displacement in the first bending mode, swept wing, AR = 4.16, $\Lambda = 45^{\circ}$, M = 0.6.

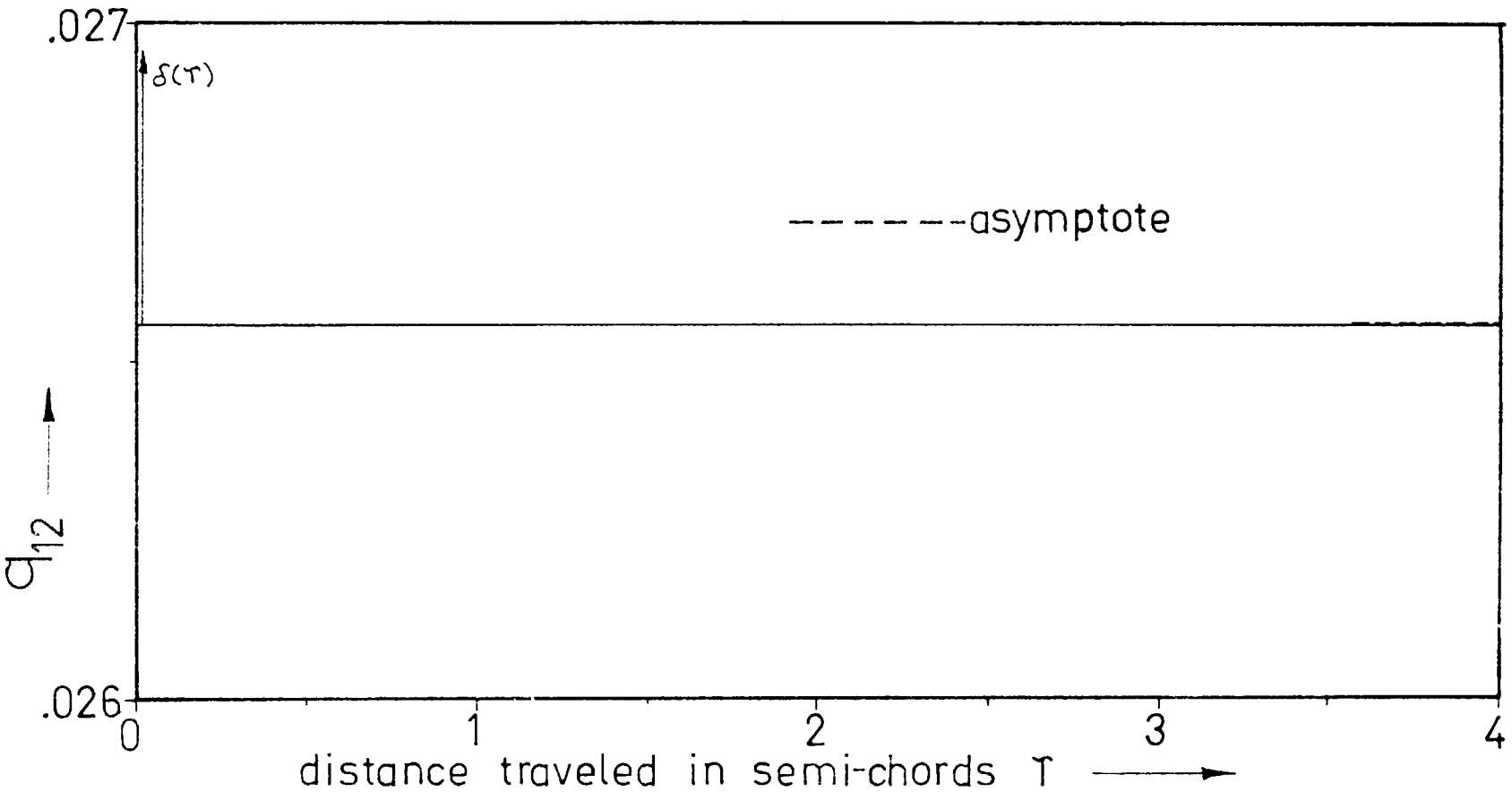

Fig. 39. Indicial function for q_{12} due to impulsive displacement in the first torsion mode, swept wing, AR = 4.16, $\Lambda = 45^{\circ}$, M = 0.6.

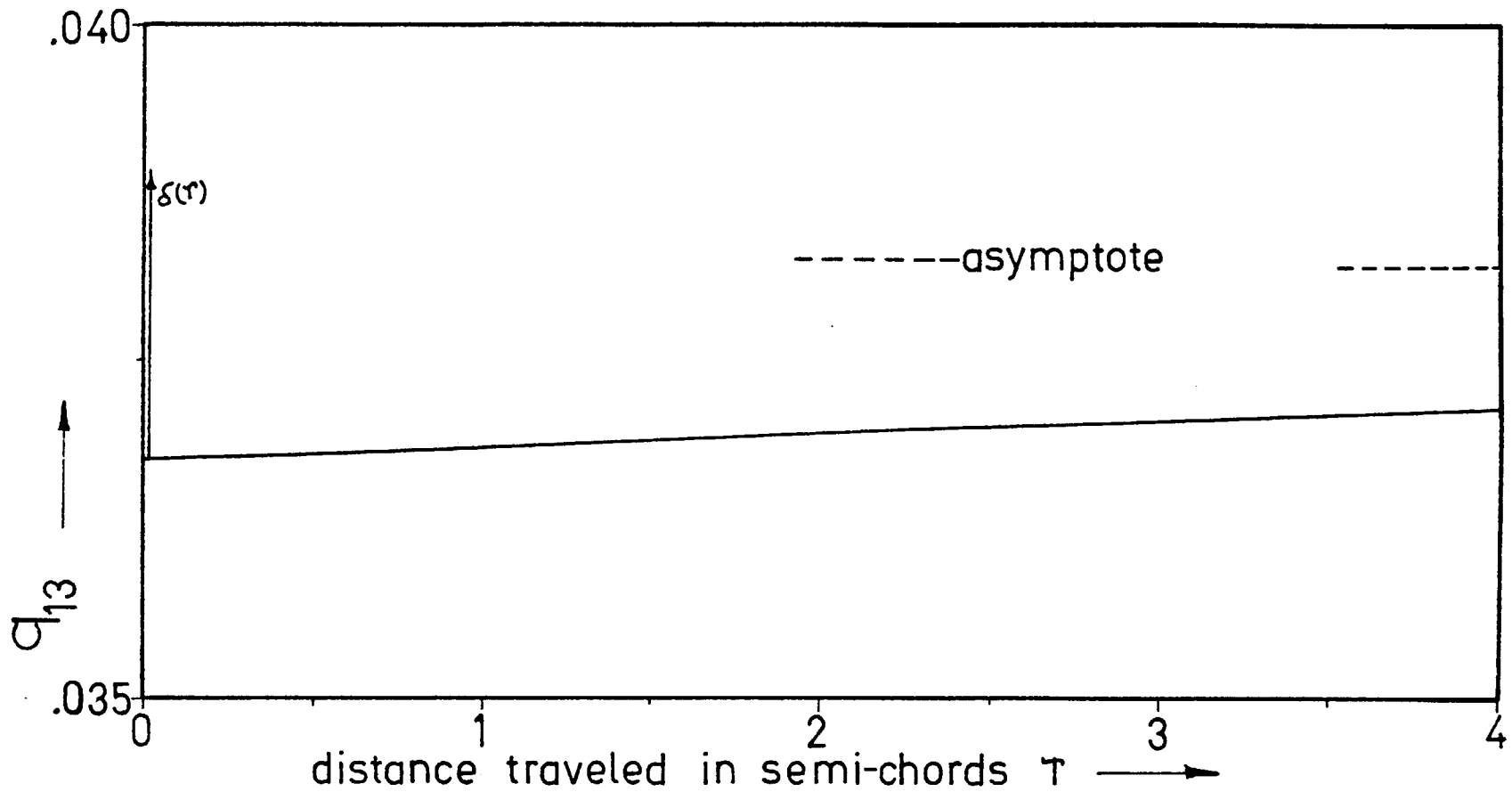

Fig. 40. Indicial function for q_{13}, due to impulsive flap rotation.

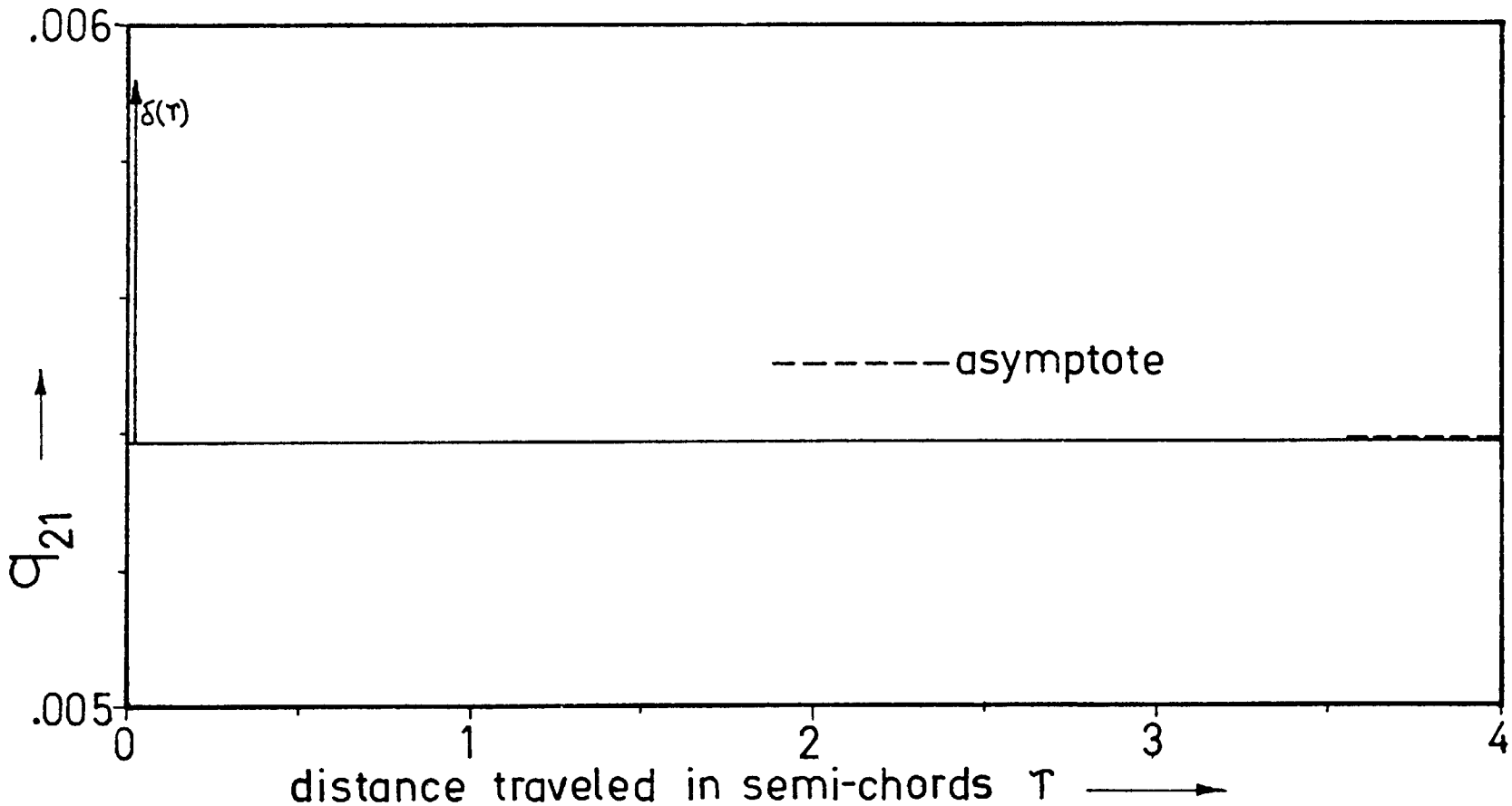

Fig. 41. Indicial function for q_{21}.

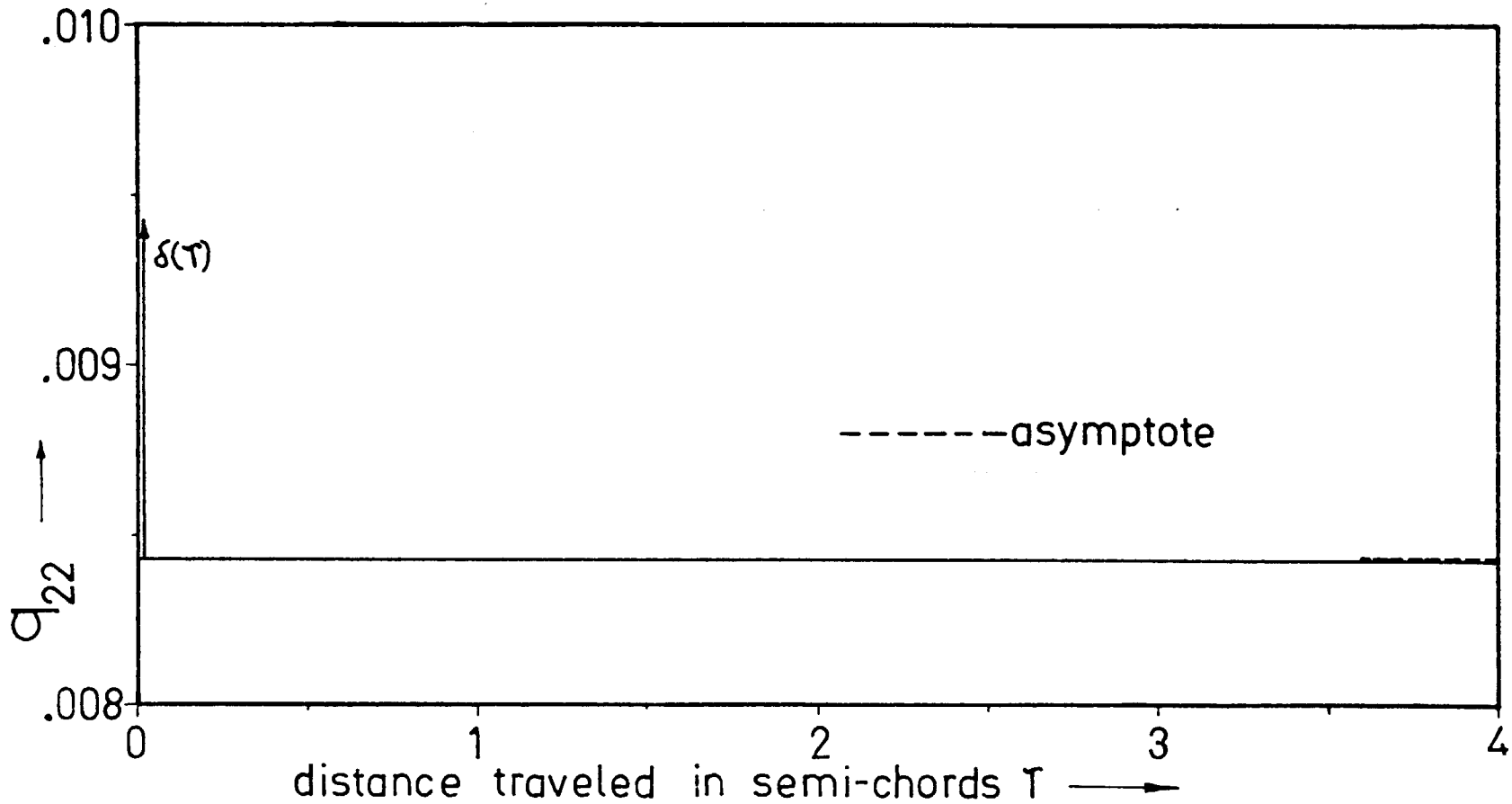

Fig. 42. Indicial function for q_{22}.

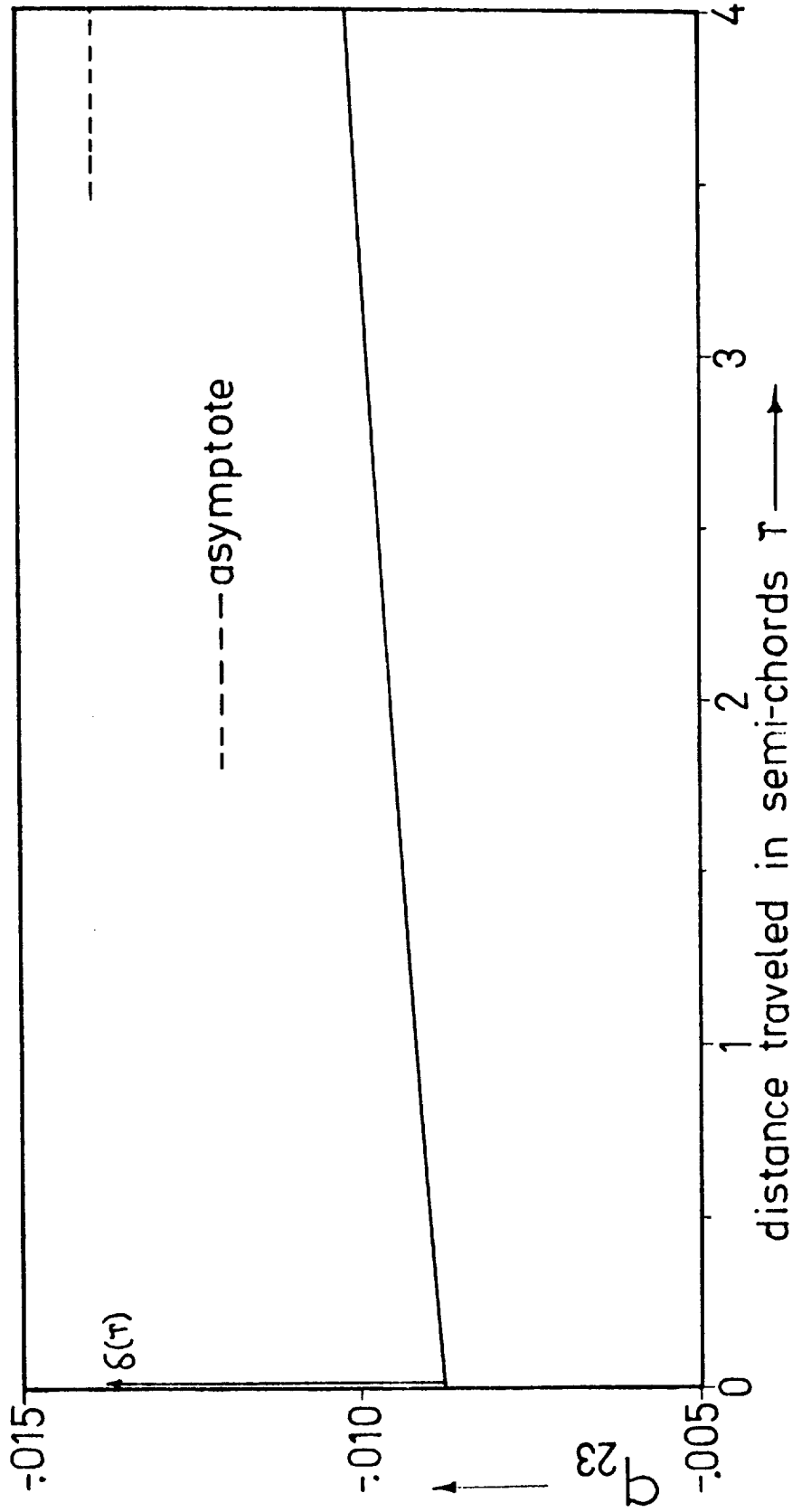

Fig. 43. Indicial function for q_{23}.

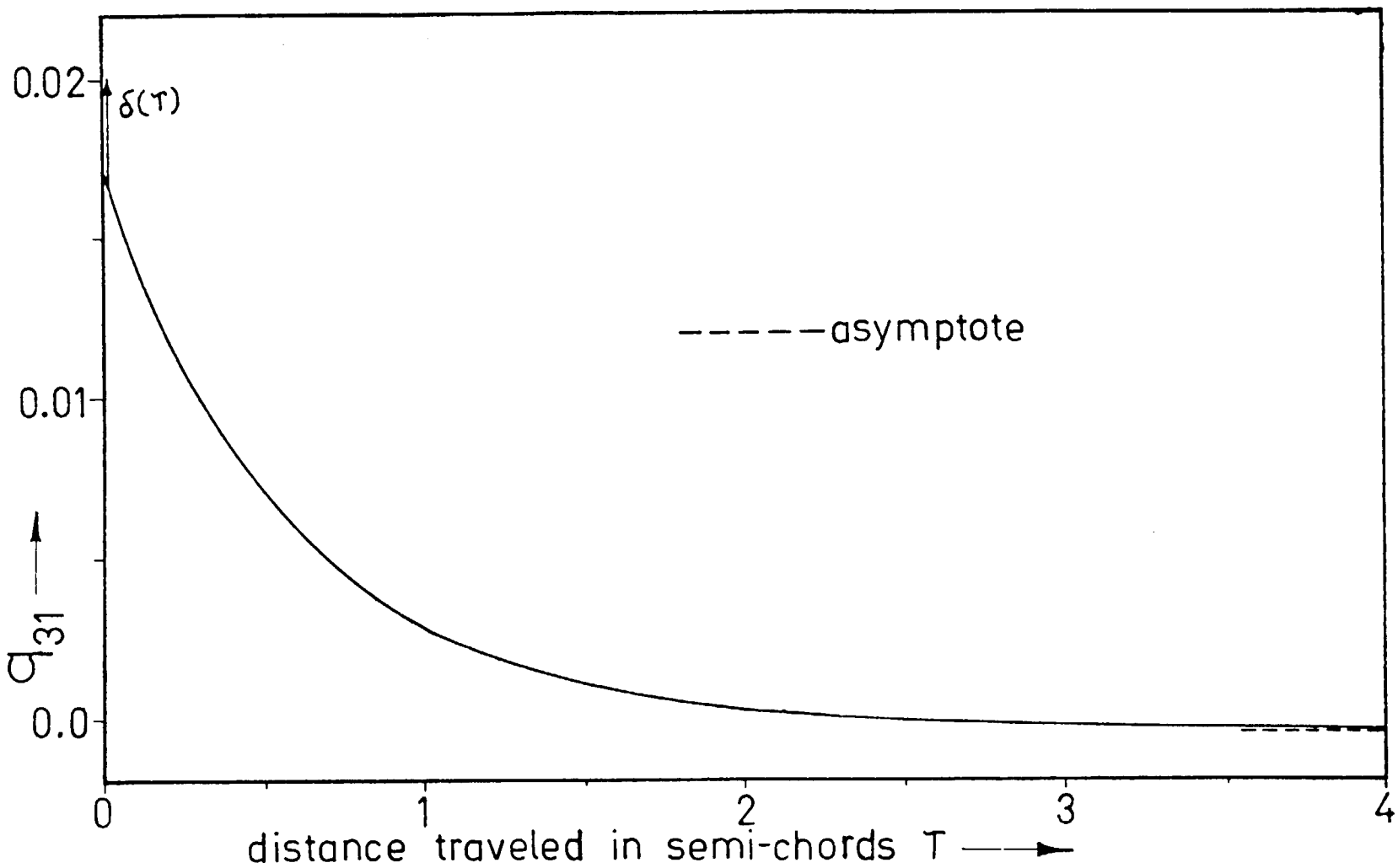

Fig. 44. Indicial function for q_{31} .

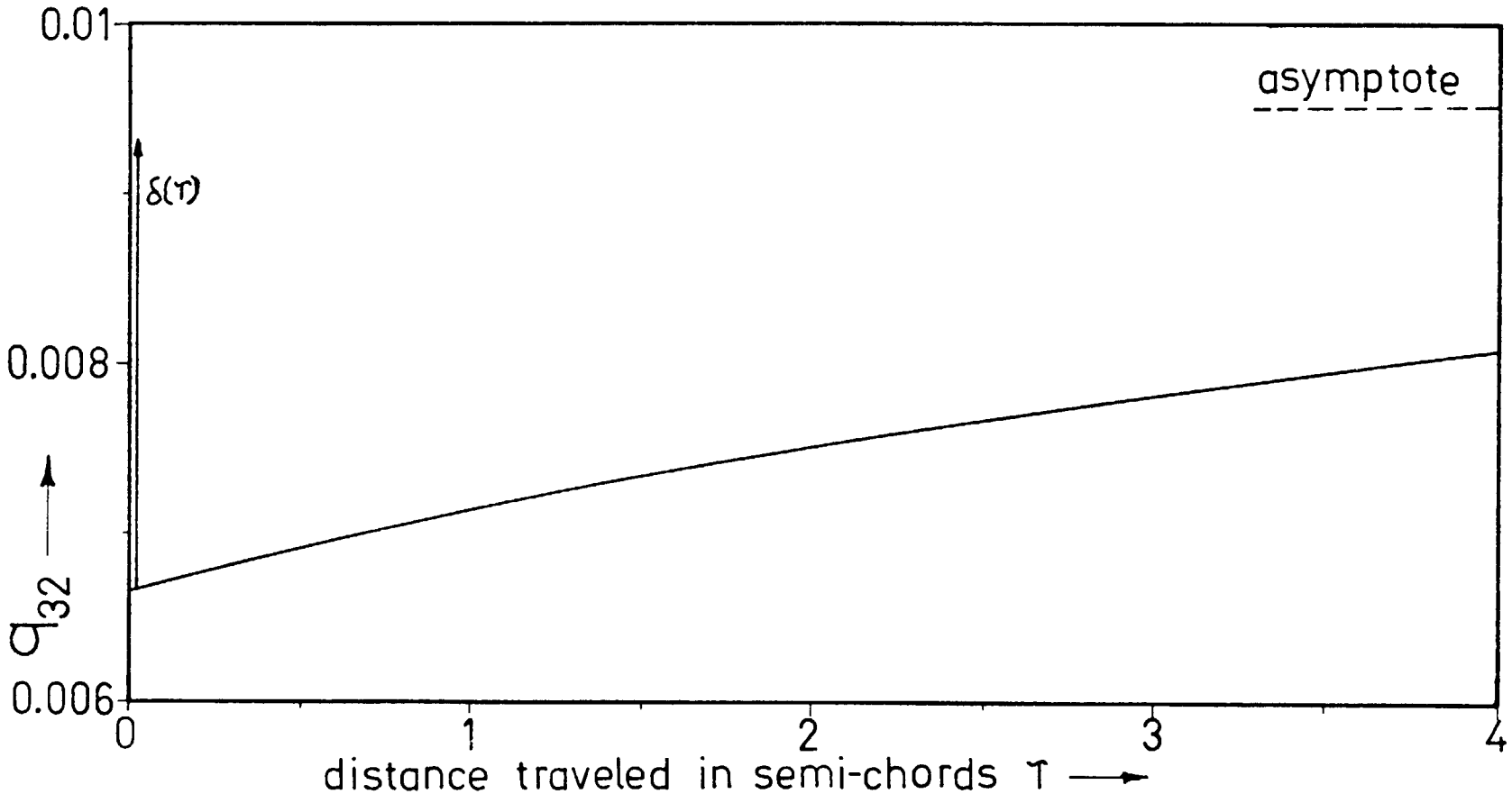

Fig. 45. Indicial function for q_{32}.

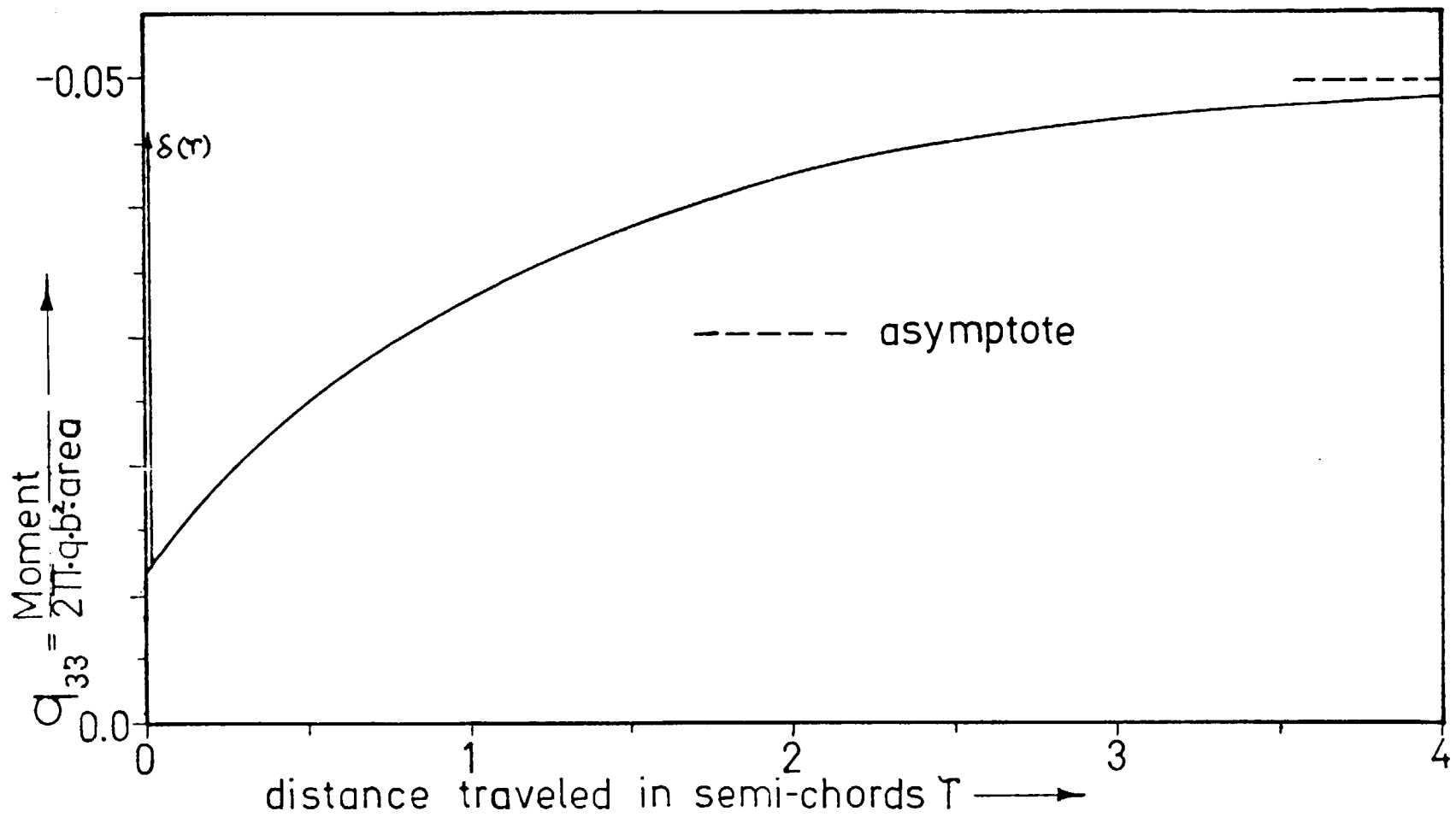

Fig. 46. Indicial function for q_{33} .

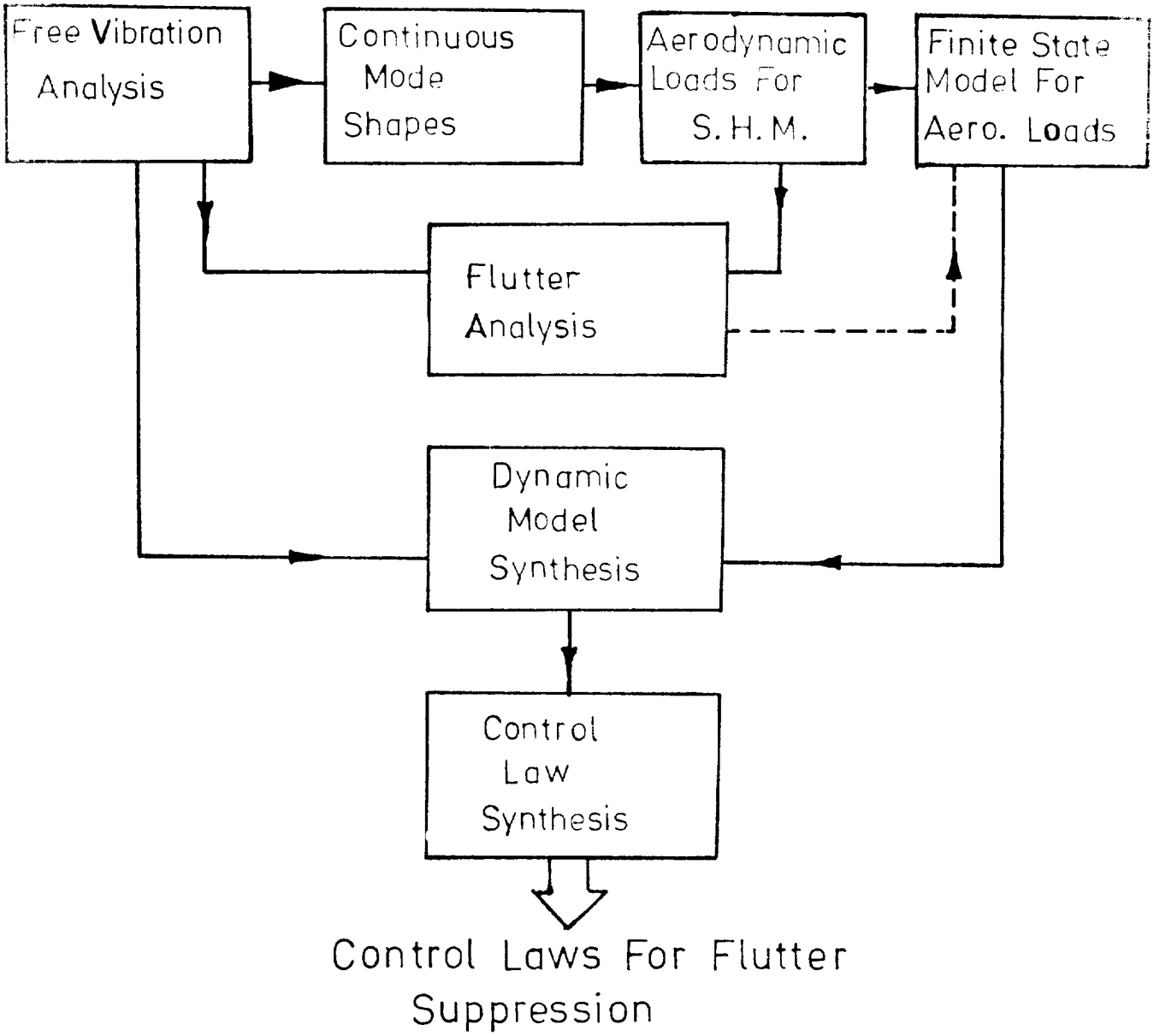

Fig. 47. Block diagram for control law synthesis procedure.

*U.S. GOVERNMENT PRINTING OFFICE: 1977 - 735-004/31